

TABLE OF CONTENTS

INTRODUCTION 1

CHAPTER 1 LITERATURE REVIEW 5

1.1 Introduction..... 5

1.2 Importance of Material Removal..... 5

1.3 Metal cutting..... 5

 1.3.1 Milling Operation..... 6

 1.3.2 Turning Operations 6

1.4 Cutting mechanics..... 6

 1.4.1 Heat in metal cutting..... 8

1.5 Machinability 9

 1.5.1 Machinability Criteria, Tests, and Indices 9

 1.5.2 Work piece material properties..... 10

 1.5.3 Hardness and Strength 10

 1.5.4 Ductility 11

 1.5.5 Effect of deformation and heat treatment processes..... 12

 1.5.6 Surface roughness 13

 1.5.7 Cutting Forces..... 16

 1.5.8 The chip formation..... 18

 1.5.9 The burr..... 20

1.6 Types of Stainless steels 21

 1.6.1 Ferritic..... 22

 1.6.2 Martensitic 22

 1.6.3 Austenitic 22

 1.6.4 Duplex..... 22

 1.6.5 Machining of stainless steels 23

 1.6.6 The machinability of stainless steel 24

1.7 Tool wear 26

 1.7.1 Load factors 26

 1.7.2 Tool wear mechanisms 28

 1.7.3 Types of tool wear 29

1.8 The tool life..... 34

1.9 Conclusion 35

CHAPTER 2 METHODOLOGY 37

2.1 Introduction..... 37

2.2 The test materials 37

2.3 Experimental plan 41

2.4 Error calculation..... 45

2.5 Equipment..... 46

2.5.1	Machine tool	46
2.5.2	Microscope.....	47
2.5.3	Leit microscope for measuring Microstructure.....	48
2.5.4	Mitutoyo SJ 410 for measuring Surface Quality	49
2.5.5	Dynamometer for force measurement	49
2.5.6	Mitutoyo Rockwell hardness testing machine	51
CHAPTER 3 RESULTS AND DISCUSSION.....		53
3.1	Introduction.....	53
3.2	Surface roughness analysis	54
3.2.1	Statistical analysis.....	54
3.2.2	Analysis of variance (ANOVA).....	63
3.2.3	Surface quality (μm)	71
3.3	Cutting force analysis	75
3.3.1	Identification of dynamic cutting force:	75
3.3.2	The analysis impact of cutting speed and feed rate on cutting force of 409 Ferritic:.....	76
3.3.3	The analysis impact of cutting speed and feed rate on cutting force of 304L Austenitic:.....	78
3.3.4	The analysis impact of cutting speed and feed rate on cutting force of 410 Martensitic:	80
3.3.5	Comparison between three different alloys on dry milling operation ...	81
3.4	Chip forming analysis	83
3.4.1	The chip forming of stainless steel materials 409 Ferritic	83
3.4.1	The chip forming of stainless steel materials 304L Austenitic.....	85
3.4.2	The chip forming of stainless steel materials 410 Martensitic	86
3.4.3	The Comparison of chip geometry for three different grades of stainless steel.....	88
3.4.4	The burr:.....	89
3.5	Machinability Comparison.....	91
CONCLUSION		93
RECOMMENDATIONS.....		97
BIBLIOGRAPHY		99

LIST OF TABLES

	Page
Table 1.1 General impact of increasing values of different properties on machinability.....	11
Table 2.1 Hardness of Test Materials	38
Table 2.2 Chemical composition (weight %) of test materials (as supplied by the manufacturers)	38
Table 2.3 Experiments parameters data	41
Table 2.4 The Cutting Data Parameters of the Stainless Steel Alloys.....	42
Table 2.5 Tool specifications	43
Table 2.6 Data of Machine Taken from 2014 Yamazaki.....	46
Table 3.1 Data of surface roughness dependence on cutting speed and feed rate for the 409	54
Table 3.2 Data of surface roughness on cutting speed and feed rate for the 304L.....	57
Table 3.3 Data of surface roughness on cutting speed and feed rate for the 410	59
Table 3.4 Shows cutting tool for experiments 7, 8 and 9 for material 410 shows minimum and maximum tool wear for each tool, and the volume of material removed 1800mm^3	62
Table 3.5 ANOVA result for Ra (μm) with 95% confidence level	63
Table 3.6 ANOVA result for Rq (μm) with 95% confidence level	63
Table 3.7 ANOVA result for Ra (μm) with 95% confidence level	66
Table 3.8 ANOVA result for Rq (μm) with 95% confidence level	66
Table 3.9 ANOVA result for R a (μm) with 95% confidence level	69
Table 3.10 ANOVA result for Rq (μm) with 95% confidence level	69
Table 3.11 Data of average (Ra) and (Rq) of different grades of stainless steels tested	71
Table 3.12 Cutting force data based on cutting speed and feed rate for 409 Ferritic	77
Table 3.13 Cutting force data based on cutting speed and feed rate for 304L Austenitic	78
Table 3.14 Cutting force data based on cutting speed and feed rate for 410 Martensitic.....	80

Table 3.15 Data of arithmetic cutting force of three diverse grades of stainless steel	82
Table 3.16 Comparison of the chip form for the tests of 409 Ferritic	84
Table 3.17 Comparison of the chip form for the tests of 304L Austenitic	85
Table 3.18 Comparison of s the chip form for the tests of 410Martensitic	87
Table 3.19 Comparison of the from chip geometry for three tests of three materials	88
Table 3. 20 Comparison of burr formation for the three stainless steel materials tested (feed rate 0.1mm/ tooth)	90

LIST OF FIGURES

	Page
Figure 1.1 Shear plane and chip forming factors	7
Figure 1.2 Chip contact areas Take from (Black et al., 1996	8
Figure 1.3 Heat distribution in metal cutting	9
Figure 1.4 Diagram change of mechanical properties with carbon content	10
Figure 1.5: Ductility (D) Hardness (HB)	11
Figure 1.6 Definition of the arithmetic average height (Ra).....	13
Figure 1.7 The ten-point height parameter (Rz)	15
Figure 1.8 Definitions of the parameters Rp, Rv, Rt	15
Figure 1.9 Relationship between cutting force and cutting speed	16
Figure 1.10 The three components of the cutting force	17
Figure 1.11 The relationship between cutting force and chip thickness.....	17
Figure 1.12 Relationship between cutting force and rake angle.....	18
Figure 1.13 The ways to break a chip	19
Figure 1.14The types of chip formation	20
Figure 1.15 The burr	21
Figure 1.16 Typical wear zones	27
Figure 1.17 Typical wear zones	27
Figure 1.18 Data of wear mechanisms.....	29
Figure 1.19 Places of wear on insert.....	29
Figure 1.20 Flank wear	30
Figure 1.21 Crater wear	30
Figure 1.22 Plastic deformation	31

Figure 1.23 Notch wear on the trailing edge.....31

Figure 1.24 Thermal cracking.....32

Figure 1.25 Mechanical fatigue cracking.....32

Figure 1.26 Chipping of the cutting edge33

Figure 1.27 Fracture.....33

Figure 1.28 The built-up edge (BUE).....34

Figure 2.1 Microstructure of.....39

Figure 2.2 Microstructure of.....40

Figure 2.3 Microstructure of.....40

Figure 2.4: The TOOL43

Figure 2.5 The tests layout during experiment44

Figure 2.6 Mazatrol MATRIX NEXUS CNC47

Figure 2.7 Digital microscope KEYENCE, VHX-500F.....47

Figure 2.8 The LEXT OLS4100 laser scanning digital microscope.....48

Figure 2.9 Mitutoyo measured Surface Quality testing machine49

Figure 2.10 Cutting efforts at milling and Kistler 9255B Torque Acquisition System50

Figure 2.11 Mitutoyo Rockwell hardness machine51

Figure 3.1 Curves showing mean Ra as a function of different speeds
and feed of 409 Ferritic.....55

Figure 3.2 Average Ra and Rq of 409 Ferritic.....55

Figure 3.3 Curves showing mean Ra as function of different speeds
and feed of 304L Austenitic.....57

Figure 3.4 Average Ra and Rq of the 304L Austenitic.....58

Figure 3.5 Curves showing mean Ra as the function of different speeds
and feed of the 410 Martensitic60

Figure 3.6 Average Ra and Rq of the 410 Martensitic60

Figure 3.7 Main impact plot for Ra (μm) on 409 Ferritic.....	64
Figure 3.8 Main impact plot for Rq (μm).....	65
Figure 3.9 Main impact plot for Ra (μm)	67
Figure 3.10 Main impact plot for Rq (μm)	68
Figure 3.11 Main impact plot for Ra(μm)	70
Figure 3.12 Main impact plot for Rq(μm)	71
Figure 3.13 Average Ra and Rq of three different grades of stainless steels	71
Figure 3.14 Image of tool wear when cutting 410 (50 \times) Cutting Speed at 150m/min and feed rate at 0.1 mm/tooth	72
Figure 3.15 Data of profile surface roughness parameters dependence on cutting speed 150m/min and feed rate 0.1mm/tooth, for the 409 Ferritic.....	73
Figure 3.16 Data of profile surface roughness parameters dependence on cutting speed 150m/min and feed rate 0.1mm/tooth, for the 304L Austenitic	74
Figure 3.17 Data of profile surface roughness parameters dependence on cutting speed 150m/min and feed rate 0.1mm/tooth, for the 410- Martensitic.....	75
Figure 3.18 Cutting force vs Time.....	76
Figure 3.19 Curves showing mean cutting force of different cutting speeds and feed rates of the 409 Austenitic.....	77
Figure 3.20 Curves showing mean cutting force of different cutting speeds and feed rates of the 304L Austenitic	79
Figure 3.21 Curves showing mean cutting force of different cutting speeds and feed rates the 410 Martensitic	81
Figure 3.22 Cutting Forces of three different grades of stainless steel.....	82
Figure 3.23 comparative machinability related to Surface finish	91
Figure 3.24 comparative machinability related to cutting force	92

LIST OF ABBREVIATIONS

ANN: Artificial neural network

ANOVA: Analysis of variance.

AISI: the American Iron and Steel Institute.

BUE: Built-Up Edge.

ISO: International standard organizations.

SEM: Scanning electron microscopy.

.

LIST OF SYMBOLS

- X_i : Values determined from a series of n measurements
- \bar{x} : The average value of a series of n measurements
- n : The total number of measurements
- a : Axial depth of cut
- dz : Differential height of the chip segment
- dF_r, dF_t, dF_a : Differential tangential, radial and axial forces
- D, R, R_r, R_2 : Parametric radial dimensions of the end mill
- F_x, F_y, F_z : Force components in the X, Y and Z directions
- h : Valid cutting edge height from the tool tip
- K_{tc}, K_{rc}, K_{ac} : *Cutting* force coefficients in tangential, radial and axial directions
- K_{te}, K_{re}, K_{ae} : *Edge* force coefficients in tangential, radial and axial directions
- CI: Clearance angle
- a_p : Depth of cut
- N : Rotational speed(rpm)
- V_c : Cutting speed (m/min)
- R_a : The arithmetic average height
- R_q : Root mean square roughness
- R_t : The maximum height of the profile
- R_z : Ten-point height
- R_p : The maximum height of peaks

INTRODUCTION

Some metals are more difficult to machine, or cut than others. Metal cutting processes involve removing unwanted material from metallic parts with harder shaped tools. These tools plunge into the metal and plastically deform some portion to remove them from the main part. These operations are explained by using basic orthogonal and oblique cutting models (Stephenson et Agapiou, 2005).

In the present study, we experimentally investigate the cutting tool and work material interactions during the machining of hardened materials (stainless steels) used in industry. The materials under consideration are three stainless steel alloys namely; the AISI 409-grade Ferritic stainless steel, the AISI 304L- grade Austenitic stainless steel, and the AISI 410 -grade Martensitic stainless steel, whose features include high mechanical strength and heavy-weight.

These three metal alloys are low alloy stainless steel characterized by high tensile strength and toughness and used in the manufacture of several structural components for the automotive and aerospace industries. These materials were selected in an attempt to provide a comprehensive study of the machining of large range of metals. The next paragraphs will enumerate the steps taken during the investigation.

Firstly, experimental tests will be carried out on a high precision CNC (Computer Numerical Control) machine, under dry milling conditions by varying cutting parameters like cutting velocity, feed rate and the depth of cut. Thereafter, surface quality testers will be used to measure the surface quality of the workpiece. In addition, the digital microscope will also be used to measure chip and chip formation mechanism during the milling process to better understand the chip formation process.

Afterwards, standards will be selected with various criteria aiming at finding the best possible range of values for machining and equipment safety.

Lastly, a three components dynamometer with data acquisition system is used to determine the cutting forces component F_Y , feed force component F_X and radial or thrust force component F_Z .

The machinability criterion of materials is usually evaluated using indicators such as surface roughness, chip formation, tool wear, and cutting forces. However tool wear and surface roughness are the most often used. Since the tool wear is not considered in the present work, only surface roughness, chip formation and cutting forces results are considered. Previous research works on the surface roughness of machined stainless steels alloys and hardened stainless steels are also reported in this chapter.

The purposes and objectives of the study

The purpose of this research is to gain a deep understanding of the fundamental machining of stainless steel alloys: The AISI 409-grade Ferritic stainless steels, the AISI 304L- grade Austenitic stainless steels, and the AISI 410 -grade Martensitic stainless steels.

The specific objectives of the study are:

- 1) To establish and measure the surface roughness after machining the workpieces using calibrated digital microscopes.
- 2) To determine the cutting forces component F_Y , feed force component F_X and radial or thrust force component F_Z by using three components dynamometer with data acquisition system.
- 3) To construct new cutting force model using particular cutting force in various parameters to gain the best result in milling process in terms of measure, standard, size and impact on tool wear origin and surface quality process.
- 4) To investigate chip morphology, burr development, and assess the chip formation mechanism during milling to better understand its formation process.
- 5) To measure the tool wear for each experiment by Optical Microscopy, and study the tool wear improvement and related parameter in order to represent tool wear in various cases.

Structure of thesis

The theses consists of four parts: It begins with introduction followed by the first chapter that presents the literature review, the second chapter explaining the methodology the third chapter containing a summary of the results linked to the proposed research goals. In the last chapter, conclusion, recommendation and outline for the future work will be discussed.

The experimental cases and situations with all parameters used in this research project will be given at the beginning of each chapter. A brief discussion on each chapter is structured as following:

Chapter 1: Displays a detailed outline on metal cutting tools and typical cutting operations. Also, types of stainless steels and the machinability of stainless steel are summarized. Tool wear, and types of tool wears are presented. Therefore, this chapter reviews previous research works in areas relevant to the machinability and surface roughness characteristics of machined parts made of stainless steels alloys.

Finally, the tool-life decreasing and removal are reviewed. Specific focus is paid to milling. This chapter furthermore presents a review of burr, the surface roughness, and chip formation. A general review or summary of optimization technique is displayed, after which epilogue of the state of the art literature review is presented.

Chapter 2: Shows and presents a set of experimental works to realize and comprehend the variation condition of the surface integrity. The experimental plan has been prepared according to a factorial design. The experiment of milling tool against austenitic stainless steel dry cutting test will be conducted. The cutting test will be carried out using CNC Milling tool and Mazak (Vertical Center, NEXUS 410A). The work piece will fixed by means of the vice. The radius of the cutting tool is 6 mm. Another objective of the chapter is also to comprehend and realize the formation mechanism and dominant process parameters on visible and big burrs during end milling of three stainless steel alloys (409 Ferritic , 304L Austenitic, and 410Martensitic 410). The factors scrupulous include the cutting tool, the machining parameters, geometry tool, and the workpiece material.

Chapter 3: It consists of an analytical model of the final milling in materials based on of the choice of the geometry of the formation of optimal levels of setting process parameters for the optimization of multiple responses.

Besides, a study of the effects of cutting conditions on surface roughness parameters is presented with a discussion of the results. In addition, an analysis of the impact on chip formation, burr, and cutting force. The recorded optimal cutting parameters were studied to

generate an experimental model that recommends optimal cutting parameters for different tools with a prediction of arithmetic surface roughness value. In addition, we treated the damage or defects that appear on the different functional faces of the cutting tool.

Finally, the conclusion: It consists in presenting the most significant summaries and conclusions of the research work presented in Chapter 3. This allows the reader to link the results of this study and previous studies and assists to explain, some aspects and shortcomings that have been specified for research problem and purposes of the study. The discussion also displays the accomplishments of this research work on the improvement of certain aspects of science related to the minimization of the dimensions of burrs in the face milling of stainless steel alloys. In addition, recommendations will be offered.

CHAPTER 1

LITERATURE REVIEW

1.1 Introduction

Nowadays, most manufacturing industries, including aerospace industries and particularly the machining sector are looking to produce parts with improved functional performance. The functional performance and in-service life of mechanical components are known to be significantly influenced by the machined surface roughness. Milling is probably one of the most frequently used operations in industry.

1.2 Importance of Material Removal

The significance of materials removal operations in the scheme of things can be understood by taking into account the over-all costs associated with this activity, including the cost of the expendable instrument, the cost of labor and the cost of capital investments. The importance of the cutting process can be further assessed by the observation that almost all the devices used in our complex society have one or more treated surfaces or holes. There are many factors for developing a rational method to material removal:

- 1) To improve cutting methods - even minor improvements in productivity is of great importance in the production of large volumes.
- 2) Produce products with greater accuracy and greater useful lifespan.
- 3) Increase production rates and increase the number and variety of products with the help of available tools (Jasni, 2013; Shaw, 2005).

1.3 Metal cutting

Machining operations have been divided into two main categories: cutting processes and grinding processes. The most common cutting operations are milling, drilling, turning and boring, as well as special operations such as pulling, forging, shaping and cutting shapes.

All metal cutting operations have the same principles of mechanics, but their geometry and kinematics can differ from each other (Altintas, 2012).

1.3.1 Milling Operation

Milling is one of the most commonly used processes for cutting metals and it is specially utilised in finishing an operations. According to the cutting models, the cutting force depends on the area of the chip (feed and depth of cutting), the tool path (width of the cut), the properties of the material and the cutting tool, and some experimentally specified constants.

1.3.2 Turning Operations

Turning process is the metal removal from the outer diameter of a rotating cylindrical workpiece to a specified dimension. One of the most important feature of this operation is producing a smooth finish on the metal. In turning process, the workpiece will be turned so that adjacent sections have different diameters. Normally, a workpiece is generally machined on a lathe for two main reasons: 1) To cut it to determined size. 2) To produce a true diameter.

1.4 Cutting mechanics

Today, most metal cutting operations are aimed at investigating the process of chip formation. Although the process is directed at cutting metals to design, shape and size, this is done by producing chips.

Metal cutting produces a lot of chips and controlled chip formation is a prerequisite for any operation, whatever the volume of metal removed. The comprehension of the metal cutting method is much about the behaviour of different types of metal as chips are formed, along with predicting deformation, temperatures, and forces as these have a dominant role in the quality of the process. Temperatures affect the process itself and, if high enough, can

negatively affect the cutting tool material. Forces impact the power and strength wanted to do the process. Designing the cutting edge means to have control of the temperature, forces and the chip formation during certain machining conditions. The influence of the work process on tool life and edge safety is a very important factor in the design of the cutting geometry.

The boundary-line between the work pieces, which divides the deformed/undeformed metal, is defined as the shear plane. It has an angle to the work piece defined as the shear plane angle (ϕ) as shown in Figure 1.1. The metal to the right of the plane is the deformed chip, with thickness (h_c), and the metal to the left is undeformed chip, with thickness (h). The chip deformation is related mainly to the thickness of undeformed chip, the rake angle (R) between the chip face and the normal to the work piece surface as well as the work piece-material mechanical properties. These factors also impact the shear plan angle and forces in the cutting process. Decreasing shear plane angle makes the shearing force high. In practice factors such as that angular angle and cutting data impact the shear case too (Modern metal cutting : a practical handbook, 1996).

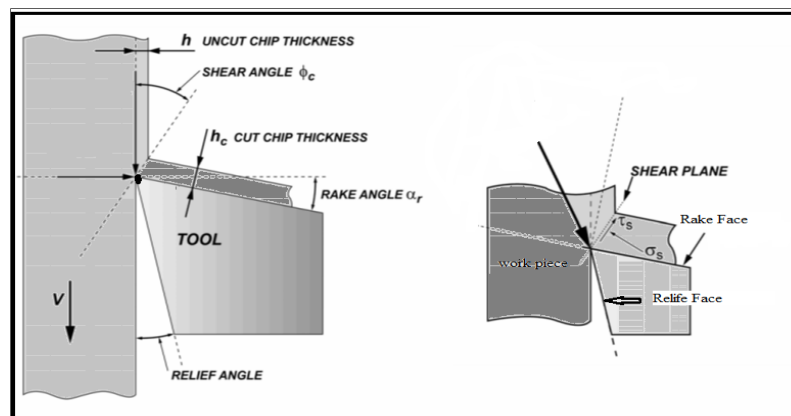


Figure 1.1 Shear plane and chip forming factors
Taken from (Modern metal cutting: a practical handbook, 1996)

The rake face where contact length is made between the chip and the tool along is split into three distinct areas, with various responses during cutting process, these responses are:

- 1) Sticking (A);
- 2) Adhesion and diffusion (B);
- and 3) Adhesion (C).

Where with higher temperatures, the spread, and adhesion growing, as shown in Figure 1.2. The flow area is one of molten metal at high temperatures. For different types of materials, various levels of stress are required to achieve shear in the machining process. The thin flow zone plays an important part in metal cutting at certain conditions and materials, successive layers of flow area of material is built up and hardened on the tool face (Black et al., 1996).

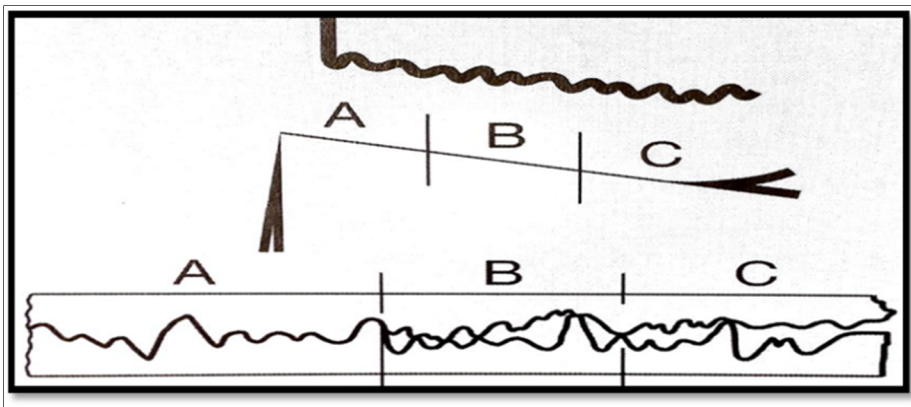


Figure 1.2 Chip contact areas Take from (Black et al., 1996)

1.4.1 Heat in metal cutting

Most of the mechanical energy derived from cutting forces applied to metal cutting is transformed into heat. The next important factor in the cutting process is therefore the heat generation and temperatures in the cutting zone. This obviously has consequences on as the tool performance and the work piece quality.

Excessive temperatures are the primary cause of unsatisfactory tool-life and limitations on high cutting speed. Most of heat generated in the process is ideally removed from the cutting zone by the chip as shown in Figure 1.3. Heat in the chip will mostly affect the cutting tool as long as there is contact between the two. Small shear angles, which may be a result of smaller rake angles, can raise heat flow into the work piece (1996; Saglam, Unsacar et Yaldiz, 2006).

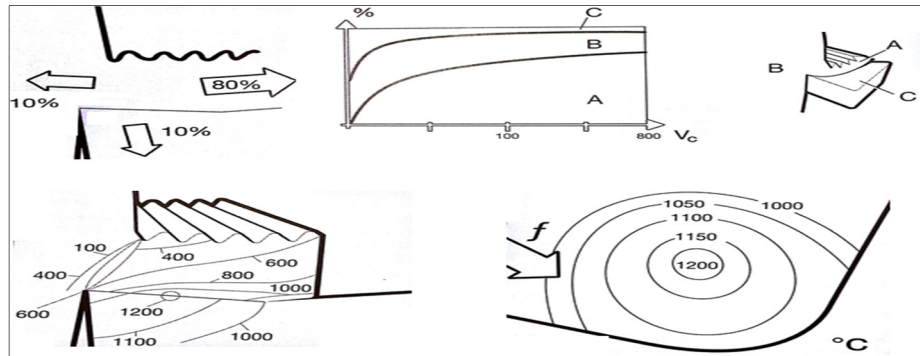


Figure 1.3 Heat distribution in metal cutting
 Take from (Modern metal cutting : a practical handbook, 1996)

1.5 Machinability

Machinability is the ability of a work piece material to machine or be machined. In other words, it indicates how easy or demanding it is to shape a work piece with a cutting tool. Improving machinability may entail, for instance, improving the quality of castings to a free machining material and changing the tool material, tool geometry, the condition of the fixture or the cutting fluid, etc.

1.5.1 Machinability Criteria, Tests, and Indices

The most commonly used standard for assessing and determining machinability are:

- 1) Achievable surface finish;
- 2) Cutting force or power consumption;
- 3) Chip form;
- 4) Tool life or tools wear rates;
- 5) Achievable tolerance;
- 6) Functional or surface integrity;
- 7) Cutting temperature;
- 8) Mechanical properties.

The most commonly used formula to measure and determine the machinability rating or index, I_m , is given by:

$$I_m = \frac{100 \times (V_{60})_{mat}}{100 \times (V_{60})_{ref}} \times 100 \quad (1.1)$$

Ref: Reference material; SAE B111. Recently SAE 1045, 1018, 1212.

Where $(V_{60})_{mat}$ is cutting speed that yields a 60 minute tool life for specified cutting situation and material.

$(V_{60})_{ref}$ is cutting velocity that yields a 60 minute tool life for a reference material with a determined machinability rating of 100 under the same situation (Stephenson et Agapiou, 2016).

Workpiece material properties

Figure 1.4 shows the general trends of four mechanical properties (A: tensile strength, B: hardness, C: impact strength, D: elongation) with varying carbon content.

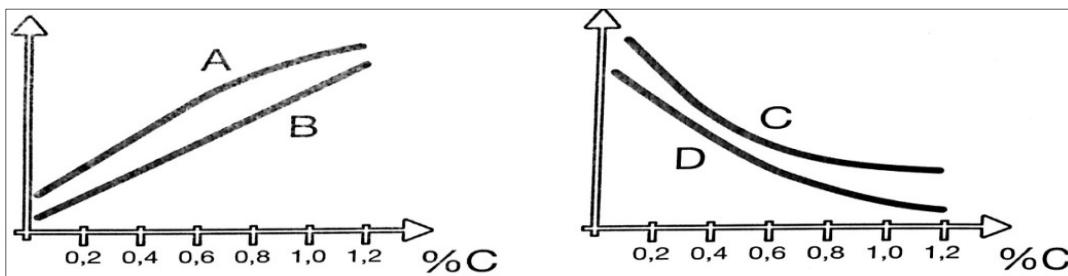


Figure 1.4 Diagram change of mechanical properties with carbon content
Taken from (Modern metal cutting: a practical handbook, 1996)

1.5.2 Hardness and Strength

Usually low values of hardness and strength are favourable but, some exceptions exist. For example, there are very ductile materials which create problems including the formation of built-up edges in the form of poor surface texture, short tool-life as well as burr formation.

1.5.3 Ductility

Low ductility values are generally beneficial. In fact, the best machinability is always a compromise between the material ductility and the material hardness as show in Figure1.5.

In the diagram (A), Ductility (D) and Hardness (HB) are plotted against tensile strength (TS).

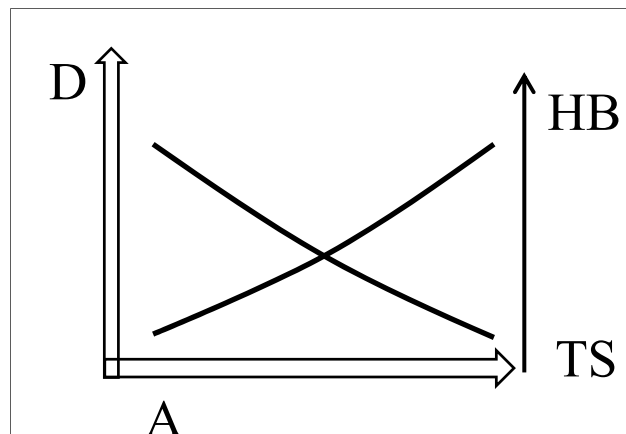


Figure 1.5: Ductility (D) Hardness (HB)
Plotted against (TS) tensile strength.

The high hardening average denotes a rapid rise in strength in relation to the increasing deformation rate. High hardening work rates denote that a lot of energy is required for chip formation (high specified cutting force). Work hardening can also be an advantage in a sense that it reduces the tendency for edge built up (BUE)(Coromant, 1996) .

The main properties that affect machinability are: Hardness, Strength, shear, Ductility, Thermal conductivity, and free machining additive properties of stainless steel which have been determined to affect machinability.

Table 1.1 General impact of increasing values of different properties on machinability

Hardness and Strength	negative
Ductility	negative
Thermal conductivity	positive
Work hardening	negative
Free machining additive	positive

Other properties that affect machinability are material structure, work piece conditions, alloying elements, surface integrity (1996; El-Sonbaty, Khashaba et Machaly, 2004).

1.5.4 Effect of deformation and heat treatment processes

Heat treatment of metals is used to modify properties by controlling the heating and cooling of the process. The choice of the selected heat treatment process used depends upon the type of material and the properties required. Using a hot rolled treatment condition has in many cases produced an inhomogeneous and coarse structure. In respect to machinability, an inhomogeneous structure may result in deviations/voids, depending on the amount of uniformity in the material. During the normalization process, the material is heated within the austenite area and, after full transformation into austenite the material is immediately cooled down to room temperature. This is done in order to achieve a finer and more homogeneous structure. In hot rolled condition, normalization mainly aims at improving the toughness behaviour of the material and as such an improved machinability level is achieved (Coromant, 1996).

Cold working is mostly performed on comparatively small size blanks or work pieces. Cold working will increase strength – how much depends on the reduction. The cold working in itself can be favourable from machining point of view in that it may mean: improved surface texture, reduced formation of the built up edges (BUE) and reduced burr-formation. The hardness of the work piece affects the amount of tool wear. Considerably softer material may lead to tendencies of built up edges while considerably harder, affects machinability negative. The alloying elements in material have a profound impact on its properties. In steel, carbon is the dominating element that determines much of the mechanical and machinability properties.

General machinability effect of alloying elements: Mn, Ni, Co, Cr, V, Mo, Nb, W, C < 0.3% & C > 0.6% have a marked negative effect on machinability, while Pb, S, P and C 0.3-0.6% have a marked positive effect on machinability (AKIN, 2012).

1.5.5 Surface roughness

Determination of surface quality is a measurement of the experimental roughness, regularity and quality of products and a factor that significantly affects the cost of production. It characterizes the geometry of the machined surface and in combination with the surface texture, which depends on the process can have a very important impact on the performance characteristics of the workpiece material (e.g. appearance of too much friction and/or too much wear) (Benardos et Vosniakos, 2002; Gadelmawla et al., 2002).

1.5.5.1 The arithmetic average height (Ra)

Ra is the most vastly used parameter to evaluate the overall roughness for quality insurance. It is named as the average absolute perversion of the roughness that is in other words irregularities from the midline along the length of one specimen, as shown in Figure1-6. The parameter is perfect to determine measure and define or describe, a general characterization of the altitude difference, but it does not define or describe any information about the wavelength and it does not define or describe the potential small changes in the profile (Gadelmawla et al., 2002).

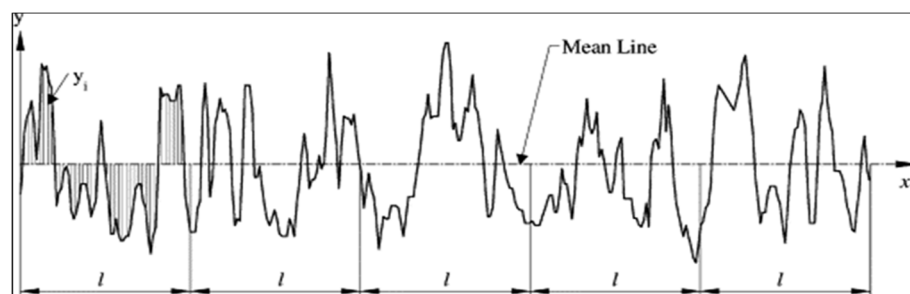


Figure 1.6 Definition of the arithmetic average height (Ra)
Taken from (Gadelmawla et al., 2002)

1.5.5.2 Root mean square roughness (Rq)

Rq: This parameter displays the standard deviation of the distribution of surface elevations. This parameter is also called RMS. It is one of the most significant parameters to characterize

the surface quality by statistical methods. It is more important and susceptible than (Ra) to a large variation or perversion, from the mean line.

The digital implementation and the mathematical determination of this parameter are obtained from the following equations:

$$R_q = \sqrt{\frac{1}{\tau} \int_0^1 \{y(x)\}^2 dx} \quad (1.2)$$

$$R_q = \sqrt{\frac{1}{n} \sum_{i=1}^n y_i^2} \quad (1.3)$$

The R_q is the line that divides the profile so that the total of the squares of the perversion, and variation of the height profile from it outcome to Zero (Gadelmawla et al., 2002).

1.5.5.3 Ten-point height (Rz)

This parameter determined in two ways. The International ISO system determines this parameter as the variation in top between the average of the five towering peaks and the five most down valleys along the assessment length of the profile. The German DIN system determines (Rz) as the medium of the summation of the five towering peaks and the five most down valleys along the assessment length of the profile. Figure 1.7 shows the determination of the ten-point height parameter.

The mathematical determinations of the two kinds of Rz are as follows: z (ISO) and z (DIN)

Where n denotes the number of samples along the assessment length (Gadelmawla, Koura et al. 2002). It has been found this parameter to be more oversensitive to occasional high tops or profound valleys than Ra (Gadelmawla et al., 2002).

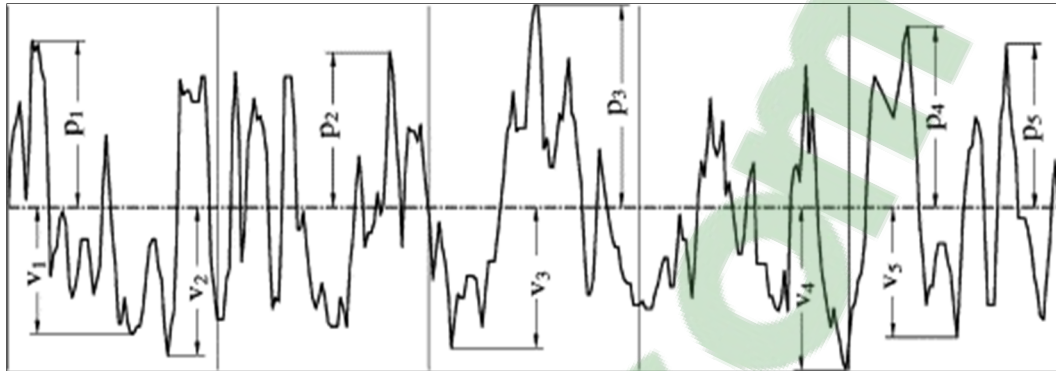


Figure 1.7 The ten-point height parameter (R_z)
Taken from (Gadelmawla, Koura et al. 2002)

1.5.5.4 The maximum height of the profile (R_t)

It is one of the most oversensitive parameters to high tops or profound scratches. R_t or R_{max} is determined as the perpendicular space between the most elevated, top and the most down valley along the estimated length of the profile. Figure 1.8 can be seen that (Gadelmawla, Koura et al. 2002).

$$R_t = R_p + R_v \quad (1.4)$$

1.5.5.5 The maximum height of peaks (R_p)

R_p is determined as the top height of the profile above the average line within an estimation extent as in Figure 1.18.

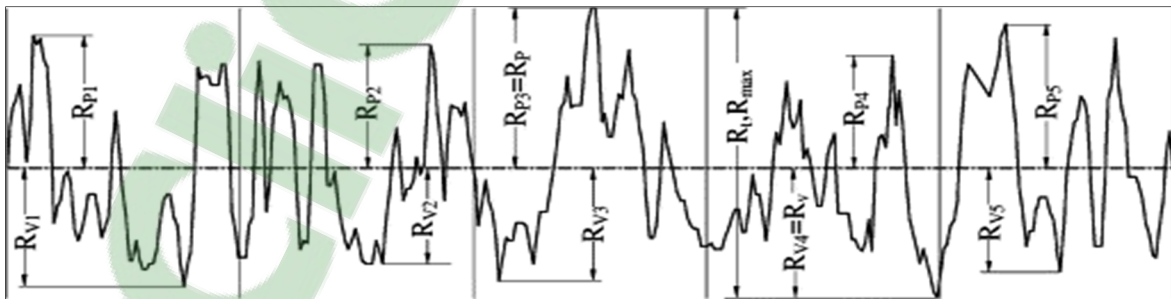


Figure 1.8 Definitions of the parameters R_p , R_v , R_t
Taken from (Gadelmawla, Koura et al. 2002)

1.5.6 Cutting Forces

Metal cutting needs a lot of power to separate the chip from the workpiece. There is a relationship between the power needed for the cutting process and the cutting forces involved. Cutting forces can be calculated theoretically and/or be measured with a dynamometer. These are mainly made up of chip removal and chip breaking forces. The stress applied on a cutting edge, through the cutting process, is mainly compressive but there is also usually some shear stress. For most work piece material, increasing cutting speed leads to lower cutting force as shown in figure 1.9. Higher temperature in the flow-area and reduced contact area contribute to this impact. The reduction in force varies with the type and condition of material (Trent et Wright, 2000).

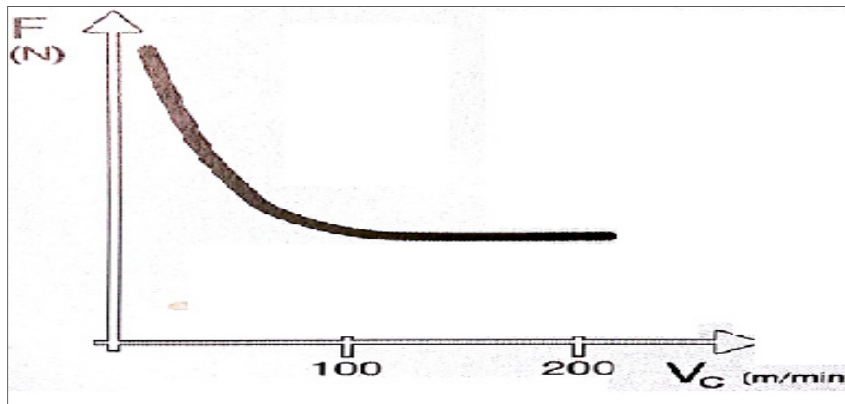


Figure 1.9 Relationship between cutting force and cutting speed
Taken from (Coromant 1996)

The cutting force can be divided into three components: the tangential force (F_c), radial force (F_{CN}), and axial force (F_p) as shown in Figure 1.10. The tangential force is to a great extent not only dependent on the contact and friction between, on the work piece and on the tool, but also on the condition of the contact between chip and rake face of the cutting edge. The amplitude of the tangential cutting force contributes to the torque that arises and in so doing influences the power requirement for the cut in question. In principle, the product of the tangential force and the cutting speed represents the power needed (Modern metal cutting : a practical handbook, 1996).

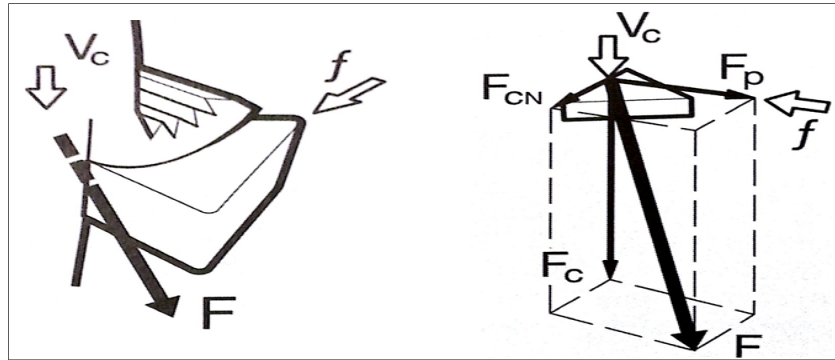


Figure 1.10 The three components of the cutting force
Taken from (Coromant 1996)

The equation of cutting power as following:

$$P = (F_c) (V_c) \quad (1.4)$$

$$K_c = \frac{F_c}{A} \quad (1.5)$$

$$P = K_c * A * V_c = K_c * f * a_p * V_c \quad (1.6)$$

Where P is power, K_c is specific cutting force (N/mm^2), a_p is cutting depth (mm), f is feed (mm), V_c is cutting speed (m/min), F_c is cutting force.

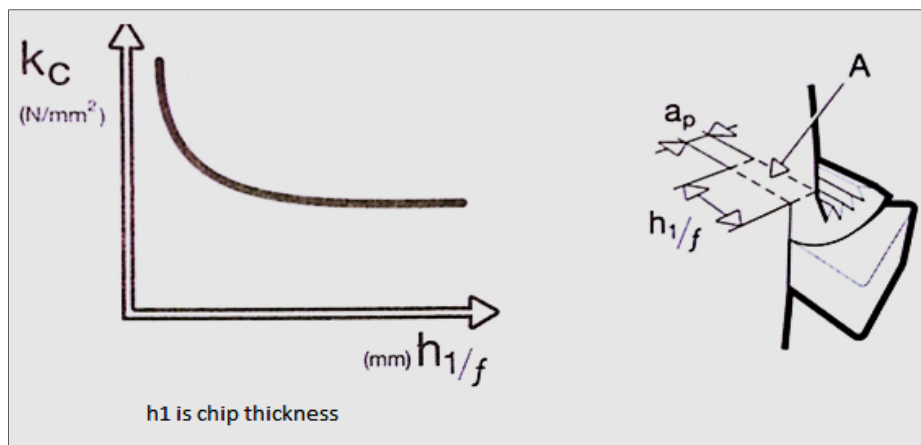


Figure 1.11 The relationship between cutting force and chip thickness
Taken from (Coromant 1996)

All three components increase in amplitude with an increase in the cross-section of the chip, which is the most tangential. The vibration trend is one of the consequences of cutting forces. Like the deviation of the tool or workpiece, cutting force can be impacted by changes in the cutting process, such as changing the workload or material conditions, and forming a built-up edge. Along with the importance of the design of the cutting geometry, to provide smooth chip breaking, and the use of a positive rake angle, as shown in Figure 1.12, higher cutting speed generally have a favourable influence on the cutting force/ vibrations. Stability of complete system that is formed by the factors in the machining process is important to be achieved. The quality of the tool holder and its ability to reliably hold the indexable inclusion are among the most important factors (Coromant, 1996).

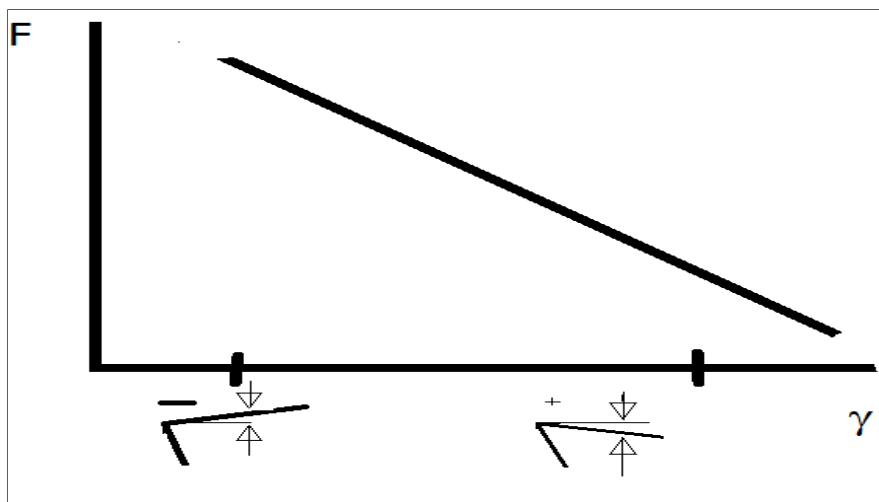


Figure 1.12 Relationship between cutting force and rake angle
Taken from (Coromant 1996)

1.5.7 The chip formation

The workpiece materials, which are being cut, have highly impacted the chip morphology, The deformed chip may have various segmental forms, commonly held with each other in ductile materials. The chip formation is beginning with the first arch also it is impacted by the collection of cutting information, especially the feed rate and depth of cut, rake, the kind and case of the workpiece material and also the measurement of nose radius. When the chip

curve is minimal for a thicker chip formation, the chip/tool contact-length becomes longer together more greater deformation and pressure as an outcome(Black et al., 1996). The high thickness makes a negative effect on the machining process. Comma helical chips shaped up to a limited length are ordinarily found to be most suitable and formed by a carefully designed cutting edge. Figure 1.13 below shows some of the methods of chip breakage:

- (A) Self-breaking.
- (B) The tool stop.
- (C) The work piece stop.

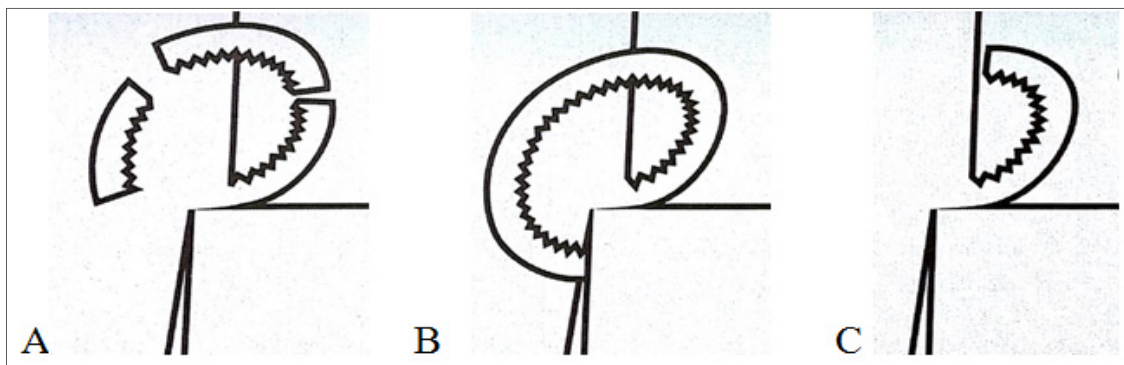


Figure 1.13 The ways to break a chip Taken from (Coromant 1996)

During chip self-breaking, achieving an appropriate direction of chip is one of the most significant factors to consider.

Breaking against the tool could be detrimental if the chip hammering takes place against the insert edge. Likewise chip breakage against the workpiece may also be detrimental if the chip impacts work piece quality or lands up in the cutting area again (Black et al., 1996).

There are several factors that influence the formation of chips such as the work piece shape, material, hardness, structure, strength and size. All these have impact on chip formation. The size of the chips and shape of the chips, particularly feed rate and cutting depth and to some extent cutting speed are impacted by the cutting data directly. The chip formation is also affected by cutting fluid application and the geometry of the tool. The result of the interaction affects the length, width and direction of the chip. The impact of the nose radius on the chip largely depends on the depth of the cut. The rake face of the cutting edge influences chip

formation considerably. It is through the design of this face that chip control can be built into the cutting edge. The rake angle and the amount of negative land are the primary factors to consider. They affect the amount of chip deformation in the process and the initial curving of chips generated (Black et al., 1996).

The types of materials related to the chip formation are:

- 1) Continuous, long chipping, such as most steels
- 2) Lamellar chipping, such as most stainless steel
- 3) Short chipping, such as most cast-iron
- 4) Varying, high force chipping, such as most super alloy
- 5) Soft, low force chipping, such as aluminium.
- 6) High pressure/temperature chipping, such as hard materials.
- 7) Segmental chipping, such as titanium(Black et al., 1996).

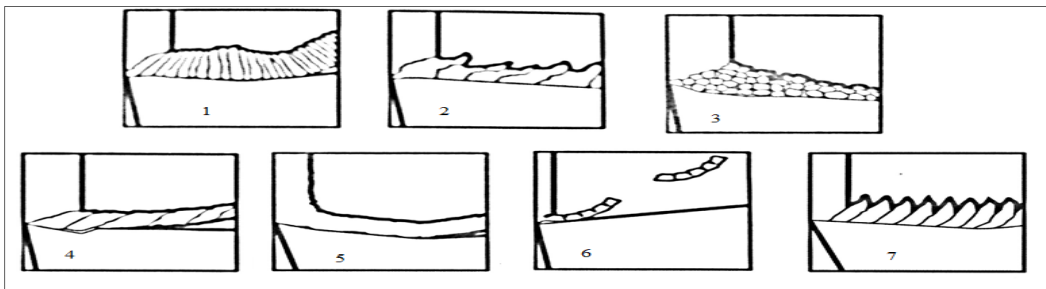


Figure 1.14 The types of chip formation
Taken from (Black et al., 1996).

1.5.8 The burr

A burr is the rough residue of the material outside the ideal geometric shape of an outer edge, machining residue or an unwanted (ISO 2000). ISO 13715 [ISO] defines the edge of a workpiece as a burr if it has a surplus greater than zero. (Schäfer et al., 1975), give one of the first technical descriptions of a burr. They describe a burr as the part of a part that is produced by manufacturing processes on an edge or surface and that is outside the desired geometry.

Gillespie's definition of burr is limited to cutting and shearing processes. A burr produced by these operations includes all materials extending beyond the theoretical intersection of the two surfaces surrounding the burr. The reference in this case is the theoretical intersection of the two surfaces and not the desired surface. In addition, Gillespie's definition includes the burrs that lie within the theoretical intersection as shown in Figure 1.15 (Aurich et al., 2009; Gillespie, 1999).

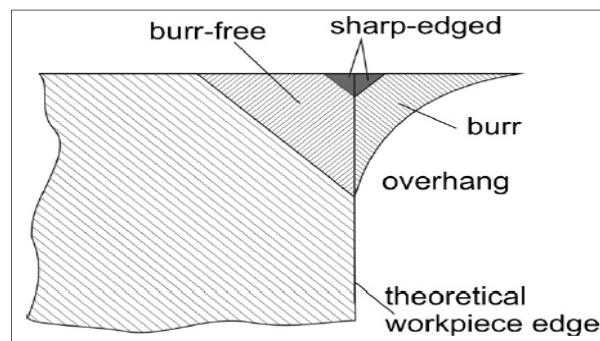


Figure 1.15 The burr
Taken from (Aurich et al., 2009)

1.6 Types of Stainless steels

The stainless steels alloys contain elevated proportions of chromium and are difficult to machine because their high strength, elevated ductility, elevated work hardening average, low thermal conductivity, and abrasive character. The main alloying element is Chromium (Cr) with content over 12%. Chromium is an essential part of stainless steel. In fact, it forms an oxide film on the surface. It resists to corrosion as well as the oxidation of the metal etc, in line with the increasing chromium content. Molybdenum has the same effect as chromium on the structure and generally increases the strength and corrosion resistance. These alloyed steels belong often to the acid-proof type. According to their structure, stainless steels can be systemized into four main groups. These are the ferrite, martensitic, austenite and duplex steel group. The mechanical properties joined with superior resistance to corrosion makes stainless steel one of the most versatile material to use (Callister Jr et Rethwisch, 2012).

1.6.1 Ferritic

Ferritic stainless steel (16-30% Cr, Ni, No, max 0.2% C): The most common ferrite steel is the 17% Cr, which has a fairly low carbon content of below 0.10%. In order to improve corrosion properties, molybdenum alloyed ferrite steels where the contents vary from 0.5 to 2 % have been created. Free machining types are available in the low-chromium range where the most of common free machining additives is sulphur. Higher-chromium alloyed types are selected in the case where corrosion resistance properties are more important and the adverse influence of sulphur cannot be accepted (Coromant, 1996).

1.6.2 Martensitic

There are Martensitic with 0.2-1.0 % C and 13-18% Cr. The low Chromium/ low Carbon types are available in free machining conditions. Martensitic is often available in an annealed condition consisting of a ferritic matrix with chromium carbides. Normally it is machined in this condition and hardening operation is done after machining (Coromant, 1996)

1.6.3 Austenitic

The most common type of austenitic stainless steel is the 18/8-type (ex: AISI304) corresponding to 18%Cr and 8% Ni. If improved corrosion properties are required, Mo can be added (18/8+2% Mo), thereby obtaining the acid resistant stainless steel. In several situations, the machining problems with austenitic alloys are correlating with built up edge formation, burr formation, poor surfaces and bad chip formation (Coromant, 1996).

1.6.4 Duplex

It is a mixture between ferritic and austenitic and 22-25% Cr, 4-7% Ni, No, N, and little carbon (Coromant 1996).

1.6.5 Machining of stainless steels

The general guidelines for machining stainless steels are:

- 1) Using lower metal removal rates than for carbon steels and lower cutting speeds.
- 2) Using rigid tooling and fixtures for averting chatter.
- 3) For averting bad surface roughness, we have to maintain feed above a minimum level.
- 4) For averting BUE formation, we have to use sharp tools with a fine finish.
- 5) Using appropriate cutting fluids with adequate flow rates for heat removal, (Stephenson et Agapiou, 2005) Altintas, 2012).

For machining of most stainless steels, there is normally a low and a high-speed range. The higher the alloys content of a stainless steel is, the more demanding and costly the machining. Demands for material properties such corrosion resistance limit the amount of free-machining additives for some applications.

The following characteristics are typically observed for stainless steel machining:

- 1) Marked tendency for deformation hardening (notching problems).
- 2) Toughness and strength (high cutting forces and demanding chip breaking).
- 3) Smearing tendency (BUE formation) (1996).

There are some general points and recommendations for machining that are especially useful for machining stainless steel (Coromant, 1996):

- 1) Select machine tools having a stable construction. The stiffness of the machine base and the quality of spindle are important. Sufficient support should be provided when turning long bars. Tool clamping and work piece fixtures should be as stable as possible.
- 2) Select the nose radius for the application. An excessively large radius causes vibrations. A smaller, but sufficiently strong one often gives better chip control and lower forces.
- 3) Use a cutting geometry that combines high edge sharpness with sufficient edge strength.
- 4) Select grade and geometry together to suit the operation in question.
- 5) To avoid plastic deformation of the cutting edge, use a larger nose radius.
- 6) Employ a sufficiently large positive rake angle and plenty of clearance. Smaller edge rounding may be useful for increased sharpness.

- 7) For roughing operations, cutting edges should have the smallest possible reinforcement land on edge.
- 8) The right cutting fluid can be used in large volume for turning to facilitate heat removal from the cutting zone.
- 9) Select an insert geometry that gives minimum friction contact between chip and chip face.
- 10) For roughing, employ larger cutting depths and feed rates in combination with lower cutting speed, rather than lower depths and feeds with higher speeds.
- 11) Roughing or semi-finishing should leave sufficient working allowance for finishing to allow the tool to go beyond the deformation-hardening zone.
- 12) Do not allow flank wear to develop excessively. A dull cutting edge cuts heavily and gives rise to more rapid hardening. Hardness up to 500 HB is not uncommon in such cases, and leaves the finishing tool with poor machining conditions.
- 13) Cermets should be considered a useful option for turning and milling stainless steel.
- 14) Climb milling is recommended since conventional milling has a longer contact time in the deformation-hardened layer and gives rise to higher cutting forces.
- 15) Avoid interruptions in feed movement during machining, as this may lead to extra local deformation hardening. If unavoidable, exit and enter with reduced table feed. The milling cutter position in relation to the work piece and the cutter diameter relationship to the radial cutting depth are especially important factors to get right for successful milling of stainless steel.
- 16) Cutting fluid in milling should only be used for low cutting speeds and for form-milling.
- 17) A larger lead angle is beneficial. A d thick, hard burr may form with a large entering angle which can then lead to rapid, mechanical notch wear.

1.6.6 The machinability of stainless steel

The machinability of stainless steel alloys differs considerably, however there are other requirements for stainless steels in addition to machinability, such as corrosion resistance and tensile strength, occasionally contrary to the best machinability (Altintas, 2012). The

stainless steels containing 12% Cr are among the most hard to cut materials because of their high tendency for hardening and high resistance to heat.

Research conducted by Shao, Liu and Qu found that cutting tools with inserts with an angular angle of 17° have a longer service life than a doctor blade angle of 28° . SEM and EDX were used to analyze the mechanism of wear and tear of the tool. In the experiment, it was found that the progression of tool wear follows a three-stage wear structure, while abrasion, adhesion and diffusion wear are manifested at various stages. Correlations between cutting conditions, surface roughness and tool wear were also explored. The cited authors found that:

- 1) The stability of the machining system could be a serious problem when processing 3% Co- 12% Cr stainless steel and the best surface roughness, by choosing good tool geometry and good cutting conditions.
- 2) During the machining of experimental materials, three stages of tool wear are found: Initial wear, Uniform wear and Accelerating wear. The main modes of tool wear are abrasive wear and adhesive wear at the initial and stable stage of wear. Diffusion occurs at the stage of final wear.
- 3) The basic mode of failure of cutting tools can be trimming and breaking.
- 4) A smaller angle of inclination has a longer tool life, and a higher inclination angle tends to a more stable machining surface.
- 5) A smaller angle of inclination may also make the processing operation more talkative, subject to certain combinations of cutting conditions (Shao, Liu et al., 2007).

Chien and Chou (Chien et Chou, 2001) wrote paper about the development of a predictive model for machinability of stainless steel. In this model, the theory of (ANN) was used to predict the roughness of the workpiece surface, the cutting force and the tool life. It is displayed that the errors of the surface roughness are due to the cutting force and tool life. They selected process parameters: feed rate and cutting speed. The predictive model contains three networks, which are a network of surface quality, a network of cutting force and a tool life support network. After entering the experimental data for the training samples, the average comparison errors between the predicted values and the measured values are 4.4% for the surface roughness, 5.4% for the cutting force and 4.2% for the tool life, respectively. It seems that all three networks have coped well with the task. In addition, by adopting GA

with neural networks, you can find optimal cutting conditions with MMR based on surface roughness and tool life limitations.

It is found that the maximum metal removal rate (MMRR) increases with the expected surface roughness, which is named the single restriction. When the expected surface roughness is selected to be $2.0\mu\text{m}$, and the tool life is used as the second limitation, the MMRR is reduced due to the limitation of the upper cutting speed limit. In addition, the corresponding optimal cutting conditions were found, which were the main goal of this research (Chien et Chou, 2001).

1.7 Tool wear

Tool wear is losing material with time. Every cutting tool wears out during machining and continues to do so until it reaches the end of the tool life. The life of the cutting edge is counted in minutes, and today's tools lives are often smaller than the old, fixed mark of fifteen minutes, but often a little more. Nowadays, the usual parameters are surface quality, chip formation, tool wear model, accuracy and predictable reliable tool life. The method used depends on the kind of operation (quality, roughing, and finishing). In the process of finishing, the tool is worn out when it can no longer generate a specific surface texture. When working with roughing, wear develops along a much longer part of the edge, and much more wear can be carried, as there are no surface texture limitations. The choice of the right cutting tool is critical and sensitive to acquire the maximum processing performance. Especially the choice of tool material and cutting geometry is very significant. The tool wear is the result of a combination of load factors on the cutting edge. Depreciation is the result of the interaction between the tool and the material of the workpiece as well as the processing conditions.

1.7.1 Load factors

The main factors that affect wear zones are:

- A) mechanical
- B) Thermal

C) chemical

D) abrasive as shown below (Jackson et al., 2013).

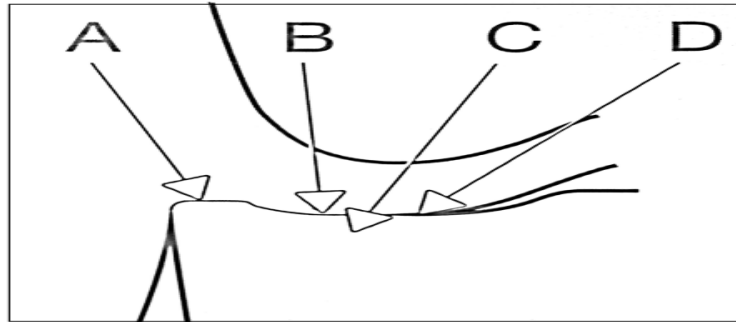


Figure 1.16 Typical wear zones
Taken from (Jackson et al., 2013)

The consequences of load factors apply on the cutting edge through machining. Few basic wear mechanisms dominate the cutting of metal. By inspecting and measuring, we can determine and define the tool wear. It develops in relation to cutting time which elapses before a certain stage of wear is reached. The flank wear is measured from the original edge. If the flank wear is relatively uniformly spread over the three zones as shown in Figure 1.17, the mean flank wear is recorded as VB_{a-c} over the cutting part of the edge (Coromant, 1996).

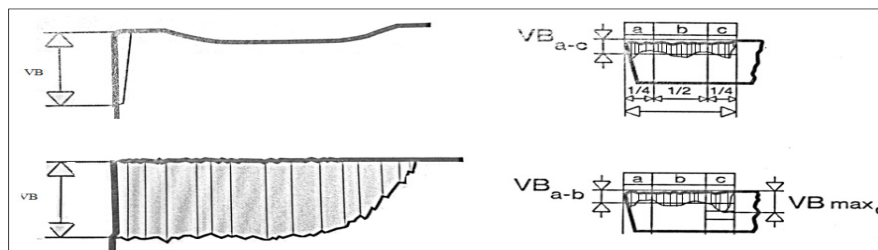


Figure 1.17 Typical wear zones
Taken from (Coromant, 1996)

Tool wear studies done by Kumar A Senthil have been conducted on martensitic stainless steel (60 HRC) using alumina-based ceramic cutting tools. Different kinds of wear were observed. (Senthil Kumar, Raja Durai et Sornakumar, 2006)

1.7.2 Tool wear mechanisms

There are several wear mechanisms that may occur simultaneously, or one of them may dominate the process.

- A) Abrasion wear: is very popular and increased mainly, but not entirely, by the hard particles of the work piece material. The ability of the cutting edge to resist abrasive wear is to a large extent connected to its hardness (Black et al., 1996) (Coromant, 1996).
- B) Diffusion wear: is high and strongly affected by the chemical load through the cutting process. The chemical characteristics of the tool-material and the affinity of the tool-material to the work piece material will determine the expansion and the diffusion of wear mechanism. The metallurgical relationship between the materials will define the measure of the wear mechanism (KABAKLI, 2009).
- C) Oxidation wear: High temperature and the existence of air oxidation for most metals.
- D) Fatigue wear: is predominantly a thermo-mechanical combination. Temperature fluctuations and the loading and un-loading of cutting forces can lead to cutting edges cracking and smashing (KABAKLI, 2009).
- E) Adhesion wear: appears fundamentally at minimum machining temperatures on the chip face of the tool. The mechanism predominantly induces the formation of a built up edge, between the chip and edge (*Modern metal cutting : a practical handbook*, 1996).

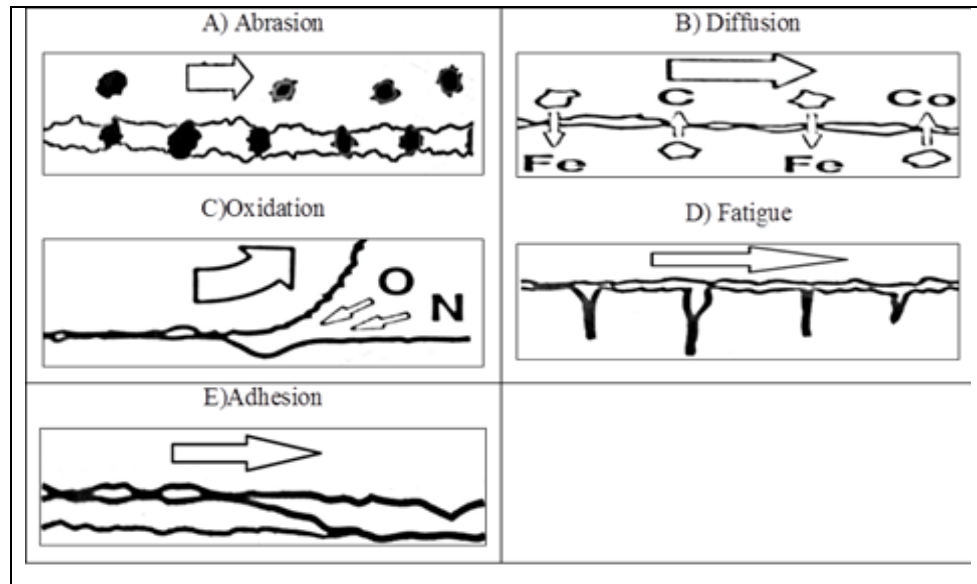


Figure 1.18 Data of wear mechanisms
Taken from (Coromant, 1996)

The main areas of tool wear on the cutting edge are the (A) chip face, the (B) flank of the leading clearance face and (C) flank of the trailing clearance face as well as the actual nose radius or parallel land area (D) as shown in Figure 1.19 (Coromant, 1996).

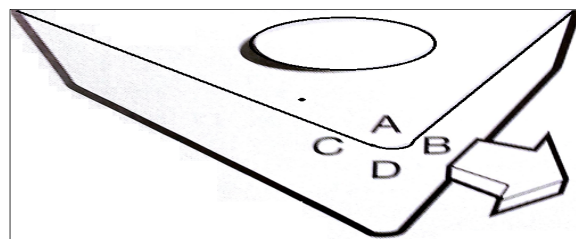


Figure 1.19 Places of wear on insert
Taken from (Coromant, 1996)

1.7.3 Types of tool wear

- 1) Flank wear: picks place on the flanks of cutting edge, fundamentally from the abrasive wear mechanism. It will lead to bad surface texture, accuracy and rising friction as the edge modifies and changes shape as shown in Figure 1.20 (Faraz, Biermann et Weinert, 2009; KABAKLI, 2009).

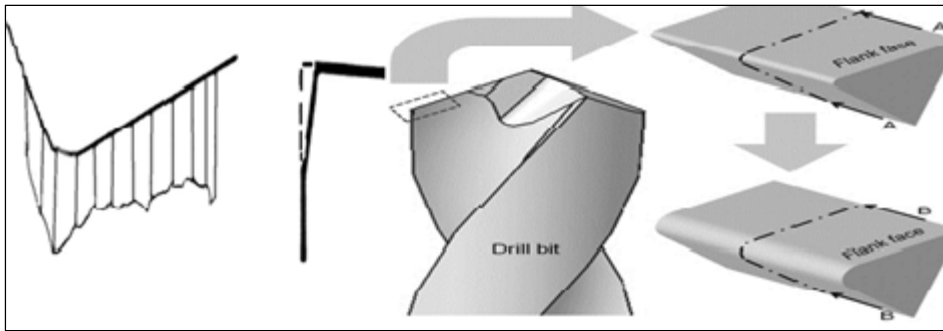


Figure 1.20 Flank wear
Taken from (Faraz, Biermann et Weinert, 2009)

- 2) Crater wear: It occurs on the chip face and it can be caused by the mechanism of abrasive and diffusion wear. The crater is formed out from the tool material being removed from the chip face or by the grinding action of solid particles, or in the hottest section of the chip surface through the diffusion action between the tool material and the chip. Excessive wear of the crater changes the geometry of the edge and can worsen the formation of chips, change the direction of cutting force and weaken the edge as shown in Figure 1.21 (Black et al., 1996; Stephenson et Agapiou, 2016).

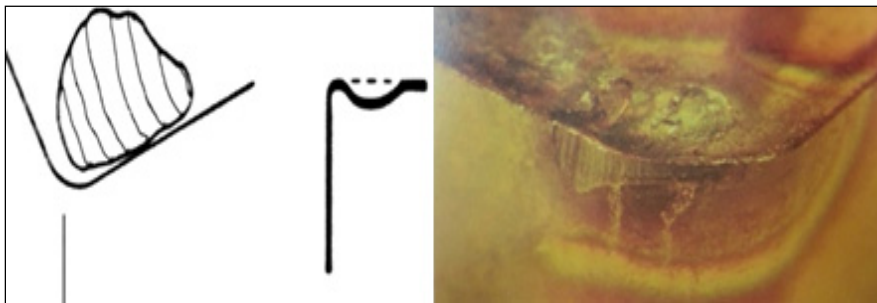


Figure 1.21 Crater wear
Taken from (Stephenson et Agapiou, 2016)

- 3) Plastic deformation: takes place as a result of combined high temperatures (high speeds & feeds) and high pressure (hard workpiece materials) on the cutting edge as shown in Figure 1.22 (KABAKLI, 2009; Stephenson et Agapiou, 2016).

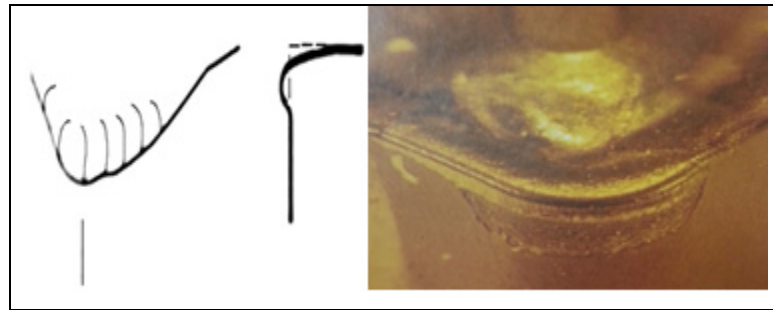


Figure 1.22 Plastic deformation
Taken from (Stephenson et Agapiou, 2016)

- 4) Notch wear: It occurs at the trailing edge, typically, but it can occur also to some extent during the oxidation wear mechanism. The cut out will be formed where the cutting edge and part of the material. Excessive notch wear impacts the surface texture when finishing and ultimately weakens the cutting edge, as shown in Figure1.23(KABAKLI, 2009; Stephenson et Agapiou, 2016).

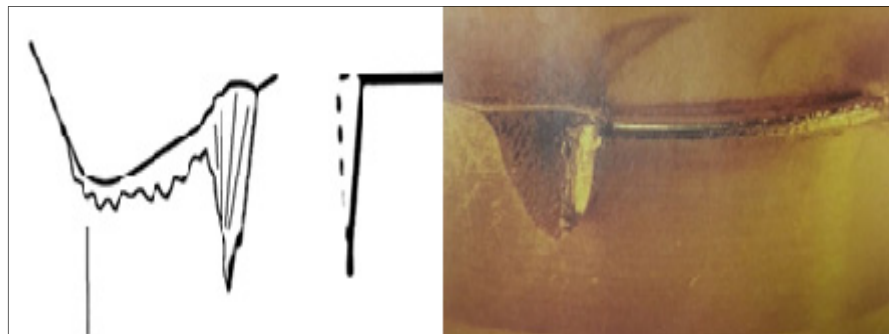


Figure 1.23 Notch wear on the trailing edge
Taken from (Stephenson et Agapiou, 2016)

- 5) Thermal cracking: This is mainly due to fatigue because of thermal cycling. It happens in milling processes. The cracks formed are perpendicular to the cutting edge and pieces of tool material between the cracks can be pulled out of the edge as shown in Figure1.24 (KABAKLI, 2009; Stephenson et Agapiou, 2016).

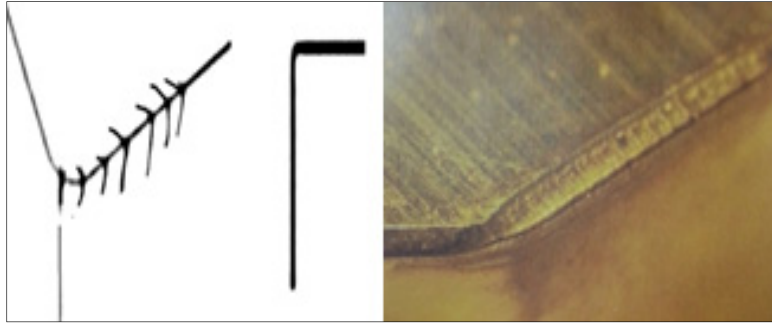


Figure 1.24 Thermal cracking
Taken from (Stephenson et Agapiou, 2016)

- 6) **Mechanical fatigue cracking:** it can occupy place when the cutting force shocks are so excessive. It leads to fracture because of continual differences and changes in load even if the load in itself is not so great enough to cause fracture. These cracks are basically parallel to the cutting edge, as shown in Figure1.25 (KABAKLI, 2009; Stephenson et Agapiou, 2016).



Figure 1.25 Mechanical fatigue cracking
Taken from (Stephenson et Agapiou, 2016)

- 7) **Chipping of the cutting edge:** It occurs, when the edge line breaks, and does not wear out. Intermittent cutting is a common cause of this kind of wear as shown in Figure1.26 (KABAKLI, 2009; Stephenson et Agapiou, 2016).

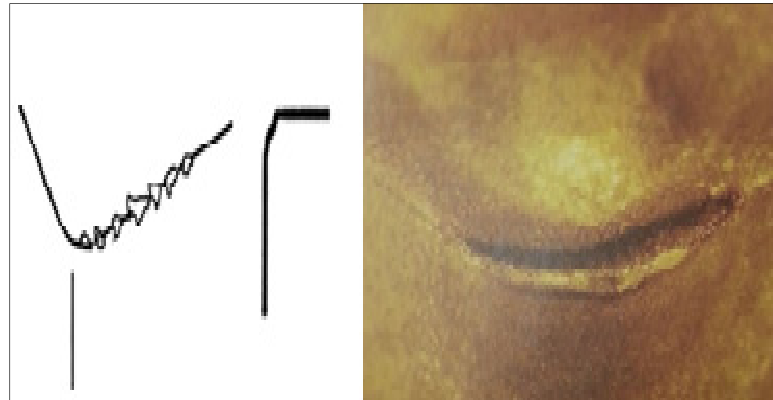


Figure 1.26 Chipping of the cutting edge
Taken from (Stephenson et Agapiou, 2016)

- 8) Fracture: The bulk breakage is the main harm. Fracture of the edge is also often the end of the line for other kinds of wear. Changing the geometry, weakening the edge and raising the temperature and forces will eventually lead to some serious destruction of the edge, as shown in .Figure1.27 (KABAKLI, 2009; Stephenson et Agapiou, 2016).

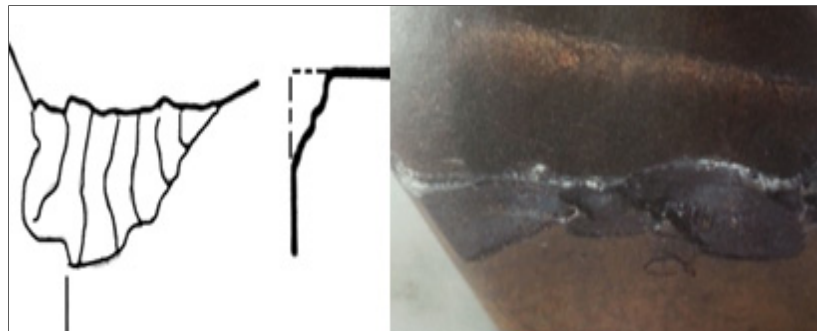


Figure 1.27 Fracture
Taken from (Stephenson et Agapiou, 2016)

- 9) The built-up edge formation: It occurs because of high temperatures, and therefore the cutting speed associated with this phenomenon, but it can also be the result of edge flagging and other wear, as shown in Figure 1.28. BUE is negative for the cutting edge when the geometry changes and the particles from the tool material can come off the welded material that forms the BUE. Surface texture is often the first to suffer with the growth of BUE, but if it is allowed to continue, there is a risk of rapid

destruction of the edge and even fracture (KABAKLI, 2009),(Gómez-Parra et al., 2013).

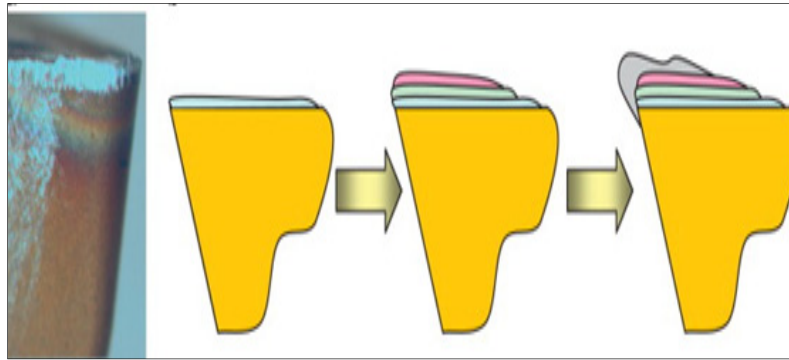


Figure 1.28 The built-up edge (BUE)
Taken from (Gómez-Parra et al., 2013)

1.8 The tool life

Tool life is one of the most substantial parameters in evaluating and estimating the performance of the cutting tools. Tool wear impacts dimensions, surface roughness and type of the work piece and also, it is one of the most essential standards in defining tool life. It has also been described as when the tool reaches the cutting edge damage and can no longer be used (Kumar, Durai et al. 2006).

The cutting parameters result in a small amplitude of the cutting force, but experiments and results of machining show that the wear of the machine during milling is significant and can seriously worsen the accuracy of processing and the quality of the surface. Tool wear is also a major factor in the formation of burrs, which adversely impacts the operation of micro particles. For a small batch production of a single part, the quality of the machining can be controlled by replacing a worn tool, however, for the processing of hundreds of structured surfaces with a massive structure, monitoring tool wear is of great importance for maintaining the precision of processing and its consistency. Important and effective processes of online monitoring of the deterioration of equipment are quite necessary (Jiao 2015).

Krolczyk, Gajek, and Legutko, presented a paper that examines the impact of cutting parameters on developing the possibility of the tool life in the machining process of duplex stainless steel. The required parameter of tool life in the process of dry machining is an important part of the process. Also, the Factorial design of an experiment can be successfully employed using coated carbide cutting tools in duplex stainless steel. It was established that the cutting speed was the main effective factor on the tool life. (Krolczyk, Gajek et Legutko, 2013).

1.9 Conclusion

In this chapter, we have identified the context and the problematic of our research topic that tackles the problems of the machine, machining tool, and surface roughness during the machining of stainless steels alloys. In particular, we conducted a review of the literature regarding the problem. After setting the objectives, we elucidated the methodology of our work.

Given the complexity of the analysis to determine and optimize the relationship between independent variables and yield, some researchers have used the experimental design method to control tool contact, surface finish and surface contact problems. This method makes it possible to more effectively control variables that influence performance with a minimum of experience. Most researchers were interested in working only on cutting speed, feed rate as well as axial and radial pass depth, while others were interested in tool life and problems with establishing their models. We propose in the next chapters to study the surface integrity which includes the roughness the microstructural defects and the cutting forces and to determine the existing relations between them as well as the optimum cutting conditions.

CHAPTER 2

METHODOLOGY

2.1 Introduction

The development of stainless steel alloys is often conditioned by Industry requirements, but alloys are significant for many applications in other sectors. Depending on the cutting conditions of these alloys, the alloys can be classified according to its machinability, recyclability, etc. In this work, the machinability performance (force, surface roughness, hardness and chip form) of three commercially available stainless steel alloys were investigated. For one of these applications, many different materials by their chemical composition and each having different mechanical properties are available on the market. However, their differences are so far unknown. Characterization between these stainless steel alloys. The study of the samples and the experimental protocol were developed in the school laboratories research centers. The goal in the modern industry is to manufacture low cost, high-quality products in a short time and Conservation of the environment. During the entire milling process, Hardness of material is one of the most important issues and an efficient and precise Hardness model is thus crucial for the selection of machining parameters, such as cutting force, feed rate and Depth of cut (Wu et al., 2013). In this chapter, we checked and verified the effect of the shaping or manufacturing process on the properties of the material. The sample identification process is divided into two parts: hardness and microstructure analysis. It will then compare our results with databases of literature to characterize the materials studied.

2.2 The test materials

The tasted materials are Stainless steel alloys, 409 Ferritic stainless steels, 410 Martensitic stainless steels, and 304L Austenitic stainless steels. Alloys were manufactured by AK Steel

Company a special manufacturing process, and a very severe heat treatment, to act on the microstructure of this alloy and therefore on the mechanical characteristics.

The hardness of the test samples before the experiment was evaluated using a Mitutoyo Rockwell HR-430MR hardness test machine. Customer No. 963-240-10Ao-hardness tester Table 2.1 presents typical hardness data for three alloys in sampling, which were measured using Rockwell hardness testing machines in the ÉTS laboratory. Each Hardness value of the material was checked 5 times, and the average value was used as the main result. This sample allowed accurate tracking of cutting.

Table 2.1 Hardness of Test Materials

Materials	AISI 304 L	AISI 410	AISI 409
Hardness (measured)	81.3HRB	44.6 HRC	83.1HRB
Hardness as supplied by the manufacturer	84 HRB	45 HRC	83. HRB

The materials

The materials used in this investigation were the 409 grade Ferritic stainless steels, the 410 grade Martensitic stainless steels and the 304L grade Austenitic stainless steels. The sizes of the workpieces used for experimentations (i.e. test samples) are of dimension 25 mm diameter and 150 × 150mm (length × width).

The chemical composition is shown in Table 2.2, and the initial microstructure is presented in Figures 2.1, 2.2, and 2.3.

Table 2.2 Chemical composition (weight %) of test materials (as supplied by the manufacturers)

Elements	Fe	Ni	Cr	Cu	N	Si	Mn	Co	C	P	S	Ti
304L	Bal. ¹	9.00	19.00	0.35		0.75	2.00	0.11	0.03	0.030	0.02	
409	Bal.	0.82	11.09	0.00	0.085	0.40	0.53	0.0	0.0102	0.022	0.0022	0.20
410	Bal.	0.20	12.50	0.10		0.30	0.1	0.00	0.08	0.04	0.03	

¹: Balance

For a better understanding of the microstructure evolution in the workpieces during the process, samples were prepared and the microstructures of the workpieces materials are presented in Figures 2.1, 2.2, and 2.3.

Microstructure of 410, 304L, and 409 stainless steels

Samples of 3mm dimension cut from a row material for each grade and Grinding (sanding) with using different sandpaper gradient. Polishing with diamond paste (0.3 μm) was used and as finishing step (0.1 μm). Electrolytic Etching is used with HCL- H_2O to reveal the microstructure features; the microstructure was investigated by an Optical microscope The Olympus LEXT OLS4100 laser scanning digital microscope. Figure 2.1 shows the microstructure of 409 layer obtained. Other slight difference is that the overall aspect of the layer is typical of all samples. The 409 samples were then examined to determine microstructure of the compound layer. The phase constituents on the sample surface consisted of mainly Ferrite (black color) + Austenite (grey color).

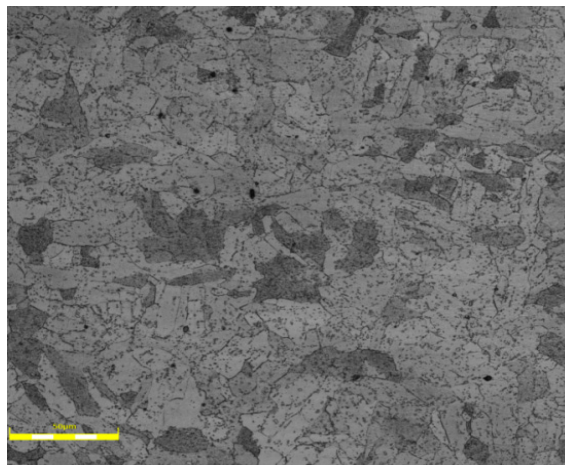


Figure 2.1 Microstructure of 409 Ferritic (ferrite + austenite)

Figure 2.2 represents the microstructure of the 304L row material. The phase constituents on the sample surface consisted of mainly 100 % Austenite (grey color). The microstructures are described by equiaxed grains with grain sizes in a range of 40–100 μm . In addition, there are

some annealing twins with orientations varying from grain to grain. Inclusions with sizes and of some micrometers can only be revealed sometimes.

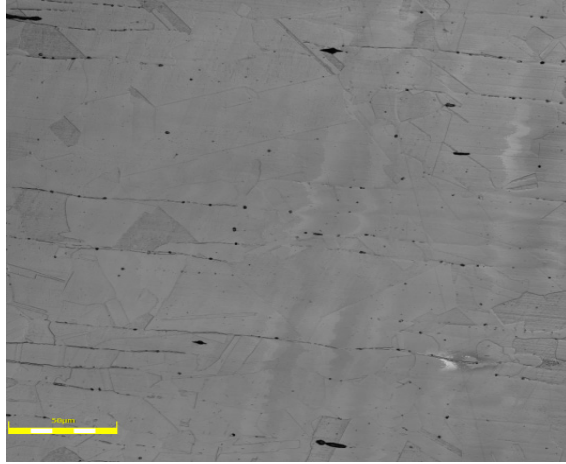


Figure 2.2 Microstructure of 304L Austenitic (austenite 100%)

Figure 2.3 represents the microstructure of the 410 row material. The phase constituents on the sample surface consisted of mainly Martensitic (black color) + Austenite (grey color). However, it has been frequently found that micro-twins exist within the martensitic laths as shown in Figure 2.3 in this stainless steel.

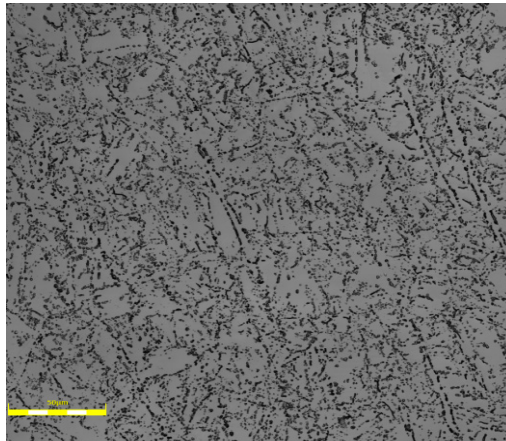


Figure 2.3 Microstructure of 410 Martensitic (martensitic + austenite)

All three alloys undergo commercial cycles of homogenization:

The 304L Austenitic was a typical commercial version of Austenitic steel, and high strength 304L contains higher levels of the base alloy. The 410 Martensitic was based on martensitic and use in barrels, cutlery, and jet engine parts. The 409 Ferritic is usually supplied in the fully annealed and desensitized condition. Final annealing is performed at temperatures below the (normally between 700 C and 750 C) after air cooling or cold rolling. Though the modified 12.5% Cr ferritic are having better weldability than conventionally used Ferritic. The 409 is widely used for the manufacture of coal wagons for transporting iron ore. In addition, it used for box body, vertical side stanchions. Also, it used in automotive exhaust components, tanks for agricultural sprays.

2.3 Experimental plan

investigation to check for machinability consisted of milling details and recording the following machinability indices: surface roughness, the average values of the cutting force when milling, and the chip shape and chip formation mechanism during milling, as well as the burr. All these information is necessary for better processing material traits. Indeed, to understand the condition for changing the integrity of the surface, an experiment will be conducted with a milling tool against stainless steel were the 409 Ferritic, the 304L Austenitic, and the 410 Martensitic.

Table 2.3 Experiments parameters data

Factors	Materials	cutting speed (m/min)	Feed rate (mm/tooth)	Depth of cut (mm)
Low Level	Ferritic 409	50	0.1	1
Mid-Level	Austenitic 304L	100	0.2	
High Level	410 Martensitic	150	0.3	

A total of 9 tests have been performed for each work-piece material. Pre-machining of face milling is needed for each work-piece to ensure same depth of cut for all experiments. Each

tool needs to continuously used till wear occur. It was decided that the maximum wear of the flange is 0.30 mm, according to the ISO standard.

The test conditions are given in Table2.4. In this way set of data, groups were generated, for rule generation (learning) and for estimation tests.

Table 2.4 The Cutting Data Parameters of the Stainless Steel Alloys

Materials	Test	Cutting speed (m/min)	Rotating Speed (rpm)	Depth of cut (mm)	Feed rate (mm/tooth)	Cutting time (seconds)
Ferritic 409	1	50	1326	1	0.1	17.04
	2	100	2653		0.1	8.52
	3	150	3979		0.1	5.7
	4	50	1326		0.2	8.46
	5	100	2653		0.2	4.26
	6	150	3979		0.2	2.82
	7	50	1326		0.3	5.64
	8	100	2653		0.3	2.82
	9	150	3979		0.3	1.86
Austenitic 304L	10	50	1326		0.1	17.04
	11	100	2653		0.1	8.52
	12	150	3979		0.1	5.7
	13	50	1326		0.2	8.46
	14	100	2653		0.2	4.26
	15	150	3979		0.2	2.82
	16	50	1326		0.3	5.64
	17	100	2653		0.3	2.82
	18	150	3979		0.3	1.86
Martensitic 410	19	50	1326		0.1	17.04
	20	100	2653		0.1	8.52
	21	150	3979		0.1	5.7
	22	50	1326		0.2	8.46
	23	100	2653		0.2	4.26
	24	150	3979		0.2	2.82
	25	50	1326		0.3	5.64
	26	100	2653		0.3	2.82
	27	150	3979		0.3	1.86

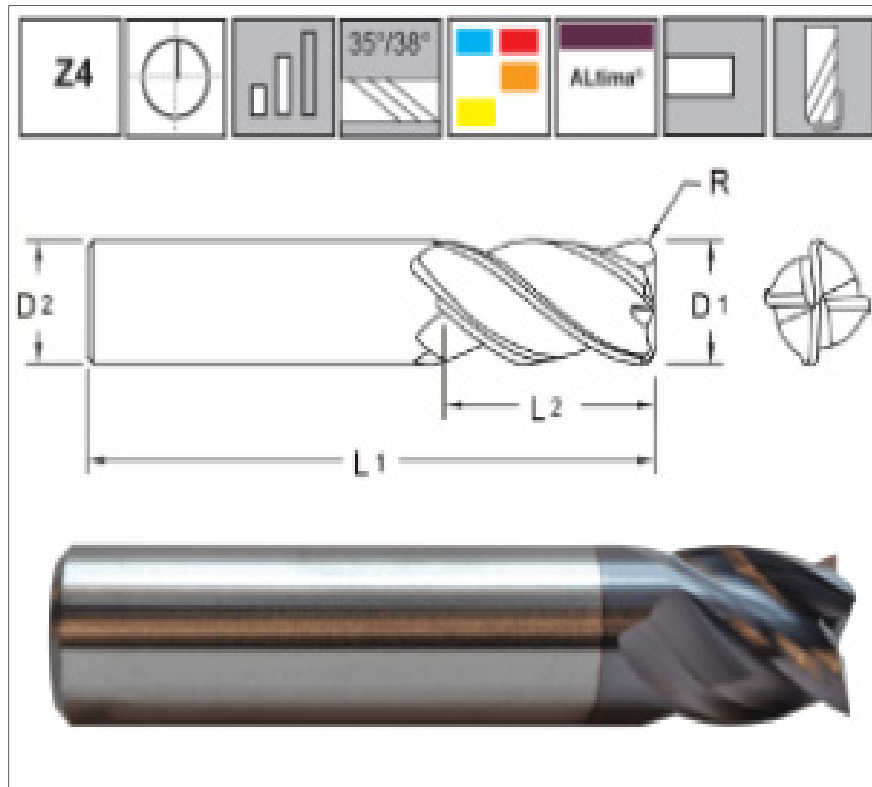


Figure 2.4: The TOOL
Taken from M.A. Ford (2010)

Table 2.5 Tool specifications
Taken from M.A. Ford (2010)

Tool	EDP	Metric	Size	O.A.L.	Flute Length	Shank Diam.
17747200A	17943	177 1200A	12mm	83	26	12

Each tool needs to be continuously used till wear occur. It was decided that the maximum wear of the flange is 0.30 mm, according to the ISO standard.

The machined material, the geometry of the tool, the conditions and parameters of the cut are the variables that have a major influence on the variation of the cutting forces. In this project the cutting parameters targeted as variables.

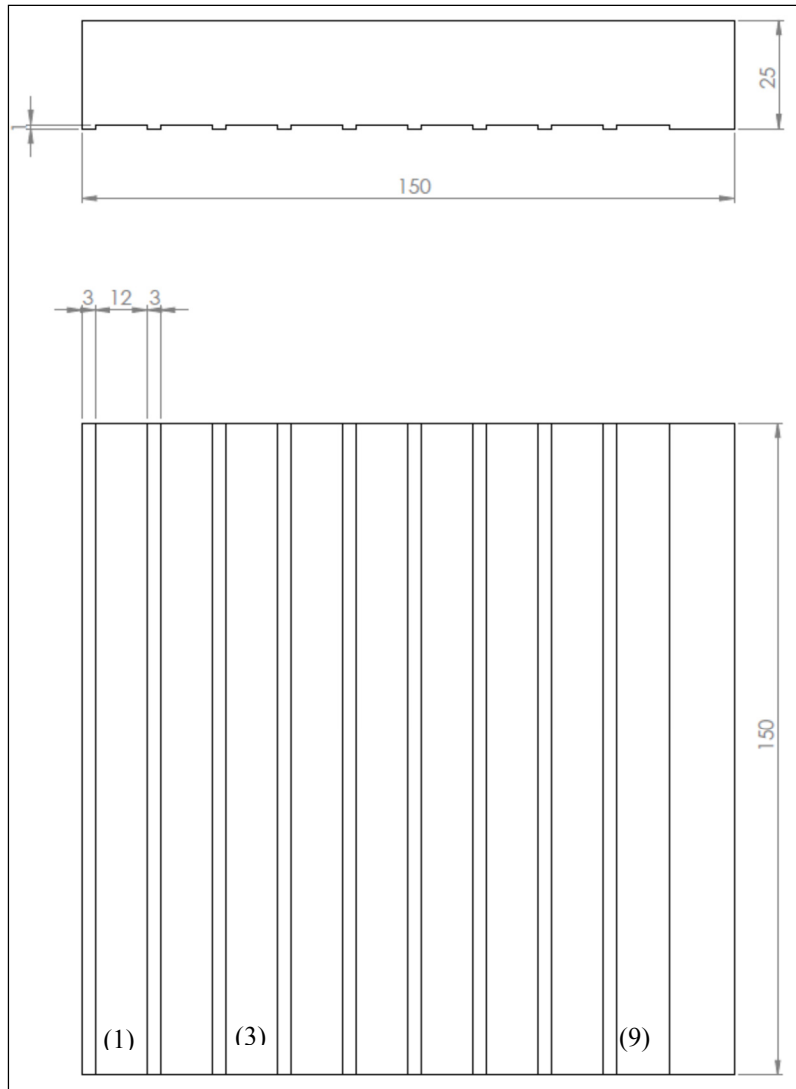


Figure 2.5 The tests layout during experiment

To understand the condition for changing the integrity of the surface, an experiment will be conducted with a milling tool against three stainless steel alloys the 409 Ferritic, the 304L Austenitic, and the 410 Martensitic. The cutting test will be carried out using a CNC Milling machine. The workpiece will be fixed by means of the vice. The designation of the used tool holder is (9930-C3-S12-074) and the designation of the cutting tool is (TUFFCUT XR 4 FL EM). For tool specification see Table 2.5. The tests will be conducted on a high-precision

CNC machine (computer numerically controlled), Mazak milling, in dry milling conditions by changing cutting parameters such as cutting speed, and feed rate .

The Number of experiments calculated is as follows: $(3)^3=9$ for each specimen for 3 different materials = 27 experiments. The number three represents the number of cutting parameters. After machining, the surface roughness tester will be used to measure the surface roughness of the workpiece. Each roughness value of the surface will be checked 5 times, and the average value will be used as the main result. The length of the path of the milling tool will be about 150 mm as shows Figure 2.5, and each time the wear and cut forces of the tool will be measured.

The factor levels in Table 2.3 were chosen with different criteria for each factor aimed at the widest possible range of values and equipment safety. It is important to note that the recommended values of the tool manufacturer have been taken into account. Feed per tooth: 0.1, 0.2, and 0.3mm/tooth, the Cutting speeds: 50 m/min to 150 m/min. The cutting forces components (F_x , F_y , and F_z) were measured using a 3 axis table dynamometer (Kistler 9255B) the average values of force were used for analysis.

2.4 Error calculation

The standard deviation allows us to have an estimate of the reproducibility of the measurements:

$$e = \sqrt{\frac{\sum_1^n (x_i - \bar{x})^2}{n-1}} \quad (2.1)$$

x_i : Values determined from a series of n measurements.

\bar{x} : The average value of a series of n measurements.

n : the total number of measurements. For each of our measurements, a statistical analysis was made. For example, for hardness measurements, machinability as well as for other parts, we applied the same strategy for roughness measurements.

2.5 Equipment

The machines used in this study are shown in the figures 2.7 to 2.11. They consisted of milling machines, microscopes, dynamometers and hardness testers:

2.5.1 Machine tool.

The machine-tool used is The VERTICAL CENTER NEXUS 410A-II Vertical Machining Center combines advanced technology, productivity, and value for a wide variety of applications. Equipped with the Mazatrol MATRIX NEXUS CNC, this control provides conversational or EIA programming, giving the capability and productivity necessary for today's technology-driven shops. *(Taken from 2014 Yamazaki Mazak Singapore Pet).*

Table 2.6 Data of Machine Taken from 2014 Yamazaki

Machine type:	3-axis CNC milling machine
Maker :	Mazak
Controller:	Mazatrol 640M
Number of pins:	1 milling (12 000 TPM).
Number of tools:	30
Displacements:	560 x 409 x 510 mm - [22 x 16.1 x 20.08 in]
Capacity:	500 kg - [1100 lbs]
Max. :	36m / min. - [1417 in./min.]
Optional equipment:	System of table changer (2 tables) - [pallet change]



Figure 2.6 Mazatrol MATRIX NEXUS CNC
Taken from 2014 Yamazaki Mazak Singapore Pte

2.5.2 Microscope

To check and measure wear of the tool, an optical microscope (digital microscope KEYENCE, VHX-500F) equipped with a digital camera was used. The optical microscope includes many complex designs that are aimed at improving the resolution and contrast of the sample. The combination of a digital camera and software provides optimized workflows and flexible solutions for image acquisition, measurement. The optical microscope also provides a non-contact geometric measurement of tool wear, shaping of chips, burrs and machined parts by means of high-precision measurement (Li et al., 2013).



Figure 2.7 Digital microscope KEYENCE, VHX-500F

2.5.3 Lext microscope for measuring Microstructure.

The Olympus LEXT OLS4100 laser scanning digital microscope non-contact 3D, can easily measure the microstructure with high resolution. The OLS4100 industrial microscope has distinctive features for fast image acquisition and high-resolution microscope images over a wider area. The OLS4100 digital microscope employs a dual confocal system, incorporating two confocal optical light paths. In combination with a high sensitivity detector for precise 3D microscope images from a sample consisting of materials with different reflectance characteristics. Since conventional 3D scanning requires complicated settings that are difficult for novice users, Smart Scan mode lets first-time users quickly acquire 3D roughness images with one click. Taken from 2018 Leica Microsystems (Kaplonek et Nadolny, 2012)

In addition to upper and lower limit settings, the appropriate brightness level is automatically set up by the system based on the image to be captured. All of these functions speed the imaging, measuring and reporting processes, besides making them reliable with same use by all operators Surface finish analysis with this microscope requires very specific information and parameters found in (Aidibe et al., 2016) and that can ensure good results for this study.



Figure 2.8 The LEXT OLS4100 laser scanning digital microscope
Taken from (Kaplonek et Nadolny, 2012)

2.5.4 Mitutoyo SJ 410 for measuring surface quality

Mitutoyo SJ 410 measurement equipment was used to measure surface relative to the drive unit reference surface. This equipment measures waviness and finely stepped features accurately, in addition to surface roughness, but its range is limited to the stylus travel available. The SJ-410 series supports a variety of surface feature measurements simply by replacing the stylus. Equipment measurement, surface features are measured with reference to a skid following close behind the stylus. This cannot measure waviness and stepped features exactly but the range of movement within which measurement can be made is greater accuracy because the skid tracks of the workpiece surface contour (Zucuni et al., 2017).



Figure 2.9 Mitutoyo measured Surface Quality testing machine

2.5.5 Dynamometer for force measurement

The energy consumption during machining varies enormously depending on the cutting forces. This allows us to have a reasonable idea of the machining and machinability performance. So, it is essential to study the influence and the variation of the cutting forces. During machining, the tool removes the chip from plastic deformation and this contact generates cutting forces that greatly affect the tool life and the workpiece. Figure 2.11 shows

a decomposition of the cutting forces generated at the time of orthogonal machining. it has been used in the Kistler dynamometer which able to directly measure the forces in three directions X, Y and Z (F_x ; F_y ; F_z) in practice. To study the milling processes, the workpiece was fixed on a vise mounted on the table of dynamometer.

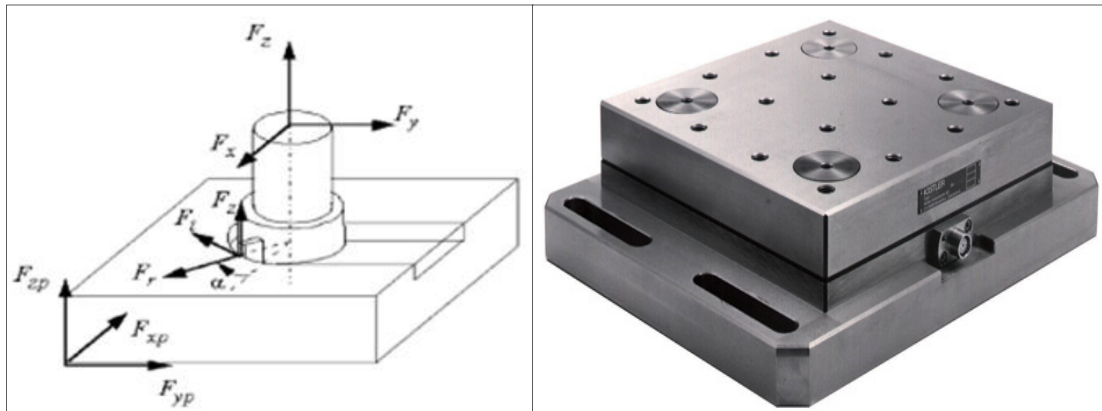


Figure 2.10 Cutting efforts at milling and Kistler 9255B Torque Acquisition System
Take from (Balazinski, 2009)

The Kistler 9255B three-axis dynamometric acquisition system, Figure 2.11, allows us to acquire the forces generated by the cutting tool. This dynamometer can measure forces ranging from -20 KN to 200 KN in the cutting plane and from -10 KN to 40 KN on the vertical axis. According to our objectives, to know the cutting forces according to the three axes that can be determined by the following formula (2.2):

$$F_c = \sqrt{(f_x^2 + f_y^2 + f_z^2)} \quad (2.2)$$

The machined material, the geometry of the tool, the conditions and parameters of the cut, etc. are the variables that have a major influence on the variation of the cutting forces. In our project, it has been targeted the cutting parameters as variables, and had set those of the tool except the diameter, the geometry of the tool, the conditions and parameters of the cutting are already chosen by the parent company of the manufactured tool.

2.5.6 Mitutoyo Rockwell hardness testing machine

Rockwell Hardness Testing Machine: HR430 models feature automatic brake and automatic start function that prevents overloading and begins test cycle. The HR430 model also includes the dial a weight system for easier load selection. The model is complete with Flat and VEE anvils, diamond and 1/6" carbide ball indenters, 2 HRC and 1 HRBW Rockwell blocks (MR models) sor 3 Rockwell blocks and an HR30N and HR30TW for MS testers. The machine is used to measure hardness of workpiece material before and after the experiment.



Figure 2.11 Mitutoyo Rockwell hardness machine

CHAPTER 3

RESULTS AND DISCUSSION

3.1 Introduction

End milling of surfaces is very often during the finishing process, and thus requires the lower surface roughness of the machined surface. However, the variation of the end mill versus the workpiece significantly affects cutting forces and thus the surface texture (Antoniadis et al., 2003). In end milling, there are several parameters such as the tool geometry, feed rate, and cutting speed that affecting the surface roughness. When the tool changes with a new one then after each run is a noted as very inefficient and costly operation. Therefore, estimating the observed effects of overall variables in this research (project) emerge to be a more meaningful direction from practical and as well economic points of view (Wojciechowski, 2015), KyunBaek, Jo Ko et Sool Kim, 1997).

In order to optimize such machining operations, it is important to understand the chip forming mechanics of these cyclic chips in fundamental terms. Before discussing experimental results related to end milling of stainless steels, it is useful to review chip formation from a broad point of view (Shaw et Vyas, 1998). This chapter treats the chip formation of three kinds of stainless steel alloys at different cutting speeds, between 50 m/min and 150 m/min and different feed rates between 0.1 and 0.3 mm/tooth, respectively. Dry machining is more famous in the manufacturing sectors in reducing the overhead expenses and preventing the environmental pollution (Haron, Gintinget Arshad, 2007). It has great significance on both economical and the environmental factors (Nouariet Ginting, 2006). The cutting forces are proportional to the cross-sectional area of cut and so-called specific cutting force coefficients (Kline, DeVor et Lindberg, 1982)(Wojciechowski, 2015).

3.2 Surface roughness analysis

3.2.1 Statistical analysis

3.2.1.1 The analysis of results for the 409 Ferritic:

The surface roughness analysis of results presented in Figures 3.1, and 3.2 as well as in Table 3.1, supports the hypothesis which claims that feed rate has significant impact on surface.

Table 3.1 presents results of surface roughness with different parameters cutting speed and feed rate for the 409 Ferritic as a function of the following parameters for three cutting speeds of 50, 100 and 150 m/min, and three feed rates of 0.1, 0.2 and 0.3 mm/tooth.

Table 3.1 Data of surface roughness dependence on cutting speed and feed rate for the 409

Material	Test number	Feed Rate (mm/tooth)	Cutting speed (m/min)	Ra (μm)	Rq (μm)	Rp (μm)	Rz (μm)	Rt (μm)
Ferritic 409	1	0.1	50	1.463	1.744	4.306	7.803	8.425
	2		100	0.924	1.203	3.018	5.865	6.954
	3		150	0.893	1.183	3.749	6.506	9.175
	4	0.2	50	2.238	2.894	8.215	15.543	21.332
	5		100	2.076	2.644	5.680	12.819	14.562
	6		150	1.947	2.29	4.326	8.671	9.229
	7	0.3	50	4.706	5.691	11.858	23.074	26.511
	8		100	4.167	4.872	9.722	18.900	19.662
	9		150	4.021	4.809	10.271	19.584	22.714

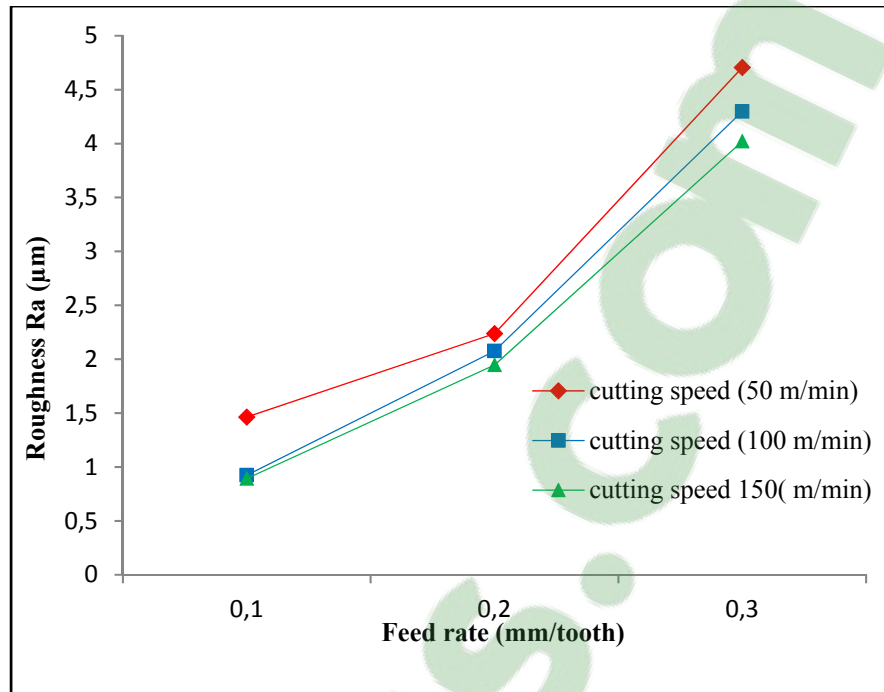


Figure 3.1 Curves showing mean Ra as a function of different speeds and feed of 409 Ferritic

As it can be seen from Figure 3.2 the average Ra and Rq of the 409 Ferritic are increasing with increasing feed rate and cutting speed.

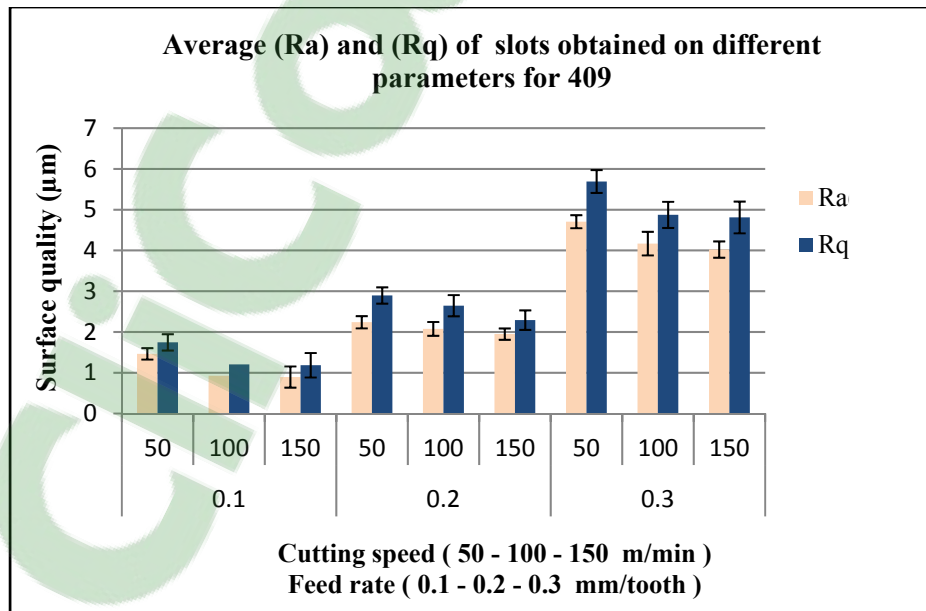


Figure 3.2 Average Ra and Rq of 409 Ferritic

Furthermore, according to Figure 3.2, the feed rate seems to have a significant impact on the surface finish of the tested samples. However, cutting speed showed less remarkable impact on this parameter. In fact, when feed rate is equal to 0.1 mm/tooth, a relatively good surface finish was obtained. When the feed rate was increased to 0.2 mm/tooth, we noticed that the mean surface roughness almost doubled, especially for high speeds (100 and 150 m/min). However, it is worth mentioning that according to the literature, this increase still fits in the acceptable range (Xavior et Adithan, 2009) and (Lin, Lee et Wu, 2001). Finally, when the feed rate achieves the last step of 0.3 mm/tooth, the surface roughness continued increasing and exceeded $4\mu\text{m}$. The analysis of the data was carried out to study the influence of cutting parameters on the surface roughness and to analyse the relationship between the surface and the Interaction effects Table 9. Overall, there is a satisfying surface quality $R_a = 0.893\mu\text{m}$.

Another aspect is worth to be considered, the surface roughness values were found to decrease with increasing cutting speed. This finding was also reported in literature (Risbood, Dixit et Sahasrabudhe, 2003). As a side point, it can be mentioned that the type of chip produced during the machining process can seemingly have an effect on the surface finish (Ezugwu et Tang, 1995). Some experiments were applied to two other materials, which are 304L Austenitic and 410Martensitic, respectively.

3.2.1.2 The analysis of results for the 304L Austenitic:

Table 3.2 and Figure 3.4, and Figure 3.3 show the effect of feed rate and cutting speed on the surface roughness, for all different parameters and insert forms. In general, according to table 3, the best case corresponds to R_a value equal to $1.176\mu\text{m}$, which is lowest value, It was obtained when the feed rate was equal to 0.1(mm/tooth) and the cutting speed equal to 150 (m/min). In another hand the highest value of R_a , equal to $6.591\mu\text{m}$, was obtained when the feed rate was equal to 0.3(mm/tooth) and cutting speed was equal to 150 (m/min). The wear effect might also contribute to this behavior. The other interesting results are the lower values of R_a obtained when the modified cutting speed was used, compared to the case when the feed rate was equal to 0.1mm/tooth and cutting speed was equal to 50 (m/min). (Selvaraj,

Chandramohan et Mohanraj, 2014; Xavior et Adithan, 2009). This conclusion/observation is valid except under conditions where tool wear was comparatively height, which adversely affected the surface roughness (Bh, Ch et Vinay, 2014; Coelho et al., 2004).

Table 3.2 Data of surface roughness on cutting speed and feed rate for the 304L

Material	Test number	Feed Rate (mm/tooth)	Cutting speed (m/min)	Ra (μm)	Rq (μm)	Rp (μm)	Rz (μm)	Rt (μm)
Austenitic 304L	1	0.1	50	1.571	1.817	5.483	8.783	9.971
	2		100	1.463	1.744	4.306	7.803	8.425
	3		150	1.176	1.463	3.992	7.061	8.441
	4	0.2	50	2.394	2.896	7.775	13.481	15.494
	5		100	2.140	2.611	6.112	11.233	12.842
	6		150	1.979	2.445	6.156	11.290	13.151
	7	0.3	50	4.936	5.449	9.474	17.724	19.140
	8		100	4.434	5.121	10.545	17.505	21.240
	9		150	6.591	7.609	13.847	28.172	29.684

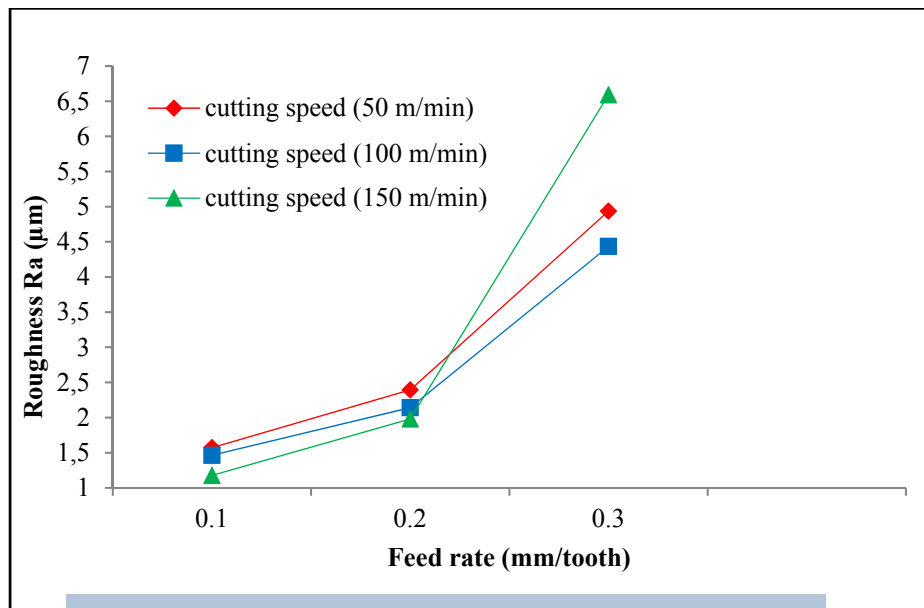


Figure 3.3 Curves showing mean Ra as function of different speeds and feed of 304L Austenitic

Table 3.2 and Figures 3.4 and 3.3 show the influence of feed rate and cutting speed on the surface roughness, for all different parameters and insert forms. In general, according to Table 3, the best case corresponds to Ra value equal to $1.176\mu\text{m}$, which is the lowest value. It was obtained when the feed rate was equal to 0.1 mm/tooth and the cutting speed equal to 150 m/min . In another hand the highest value of Ra, equal to $6.591\mu\text{m}$, was obtained when the feed rate was equal to 0.3 mm/tooth and cutting speed was equal to 150 m/min . The wear effect might also contribute to this behavior. The other interesting results are the lower values of Ra obtained when the modified cutting speed was used, compared to the case when the feed rate was equal to 0.1 mm/tooth and cutting speed was equal to 50 m/min (Selvaraj, Chandramohan et Mohanraj, 2014; Xavier et Adithan, 2009). This conclusion/observation is valid except under conditions where tool wear was comparatively high, which adversely impacted the surface roughness (Bh, Ch et Vinay, 2014).

The differences in roughness between average Ra and Rq of the 304L Austenitic are not significant as shown in Figure 3.4.

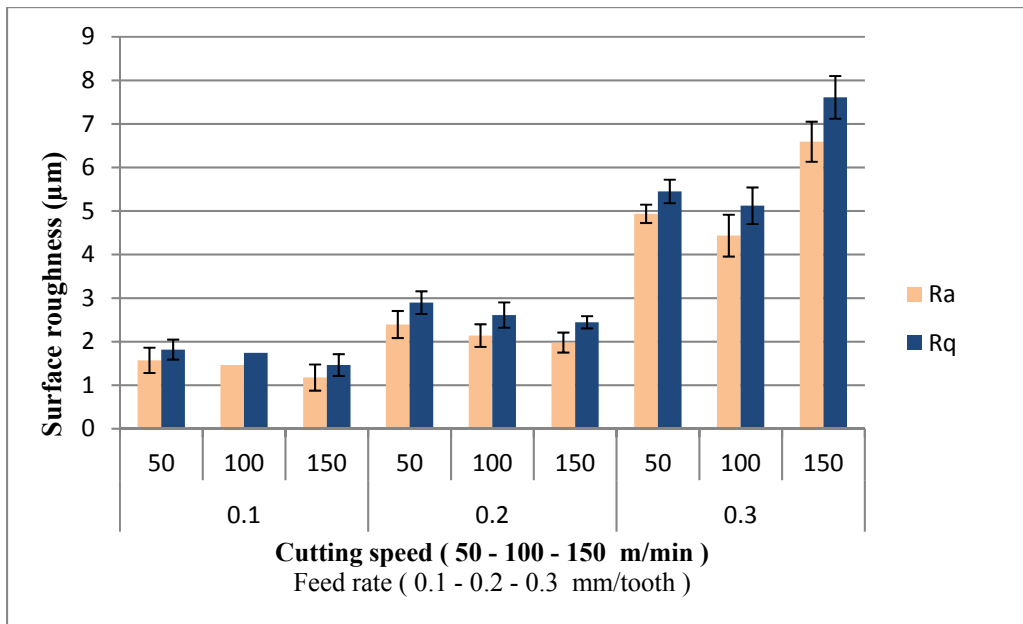


Figure 3.4 Average Ra and Rq of the 304L Austenitic

Values on Figure 3.4 are the mean of several measurements for Ra and Rq and vertical bars are the confidence intervals for the mean, and the graph shows Ra and Rq have the same trend.

3.2.1.3 The analysis of results for the 410 Martensitic stainless steel

Table 3.3 and Figure 3.5 present experimental results of criteria Ra for various parameters of feed rate and cutting speed for full factorial design. Minimal value of criteria Ra=2.018 μ m was obtained at feed rate = 0.1 mm/tooth and cutting speed =150 m/min. That means that a decrease in the feed rate and an increase of cutting speed lead to a decrease of surface roughness. It was found that feed rate has the most significant effect on Surface quality, more than cutting speed. The maximum value of Ra =7.477 μ m was registered at a feed rate = 0.3 mm/tooth and cutting speed =150 m/min (test No. 9).

Table 3.3 Data of surface roughness on cutting speed and feed rate for the 410

Material	Test number	Feed Rate (mm/tooth)	Cutting speed (m/min)	Ra (μ m)	Rq (μ m)	Rp (μ m)	Rz (μ m)	Rt (μ m)
Martensitic 410	1	0.01	50	2.341	2.990	7.483	13.582	15.688
	2		100	2.255	2.873	7.153	13.380	14.818
	3		150	2.018	2.618	4.860	14.585	15.146
	4	0.2	50	2.755	3.204	5.099	14.024	15.038
	5		100	2.664	3.216	7.445	16.213	17.853
	6		150	2.644	3.048	4.833	12.920	14.152
	7	0.3	50	5.077	6.159	12.241	26.509	30.976
	8		100	6.828	8.392	22.345	34.535	36.346
	9		150	7.477	9.503	29.490	40.105	40.541

In order to achieve better surface finish, the highest level of cutting speed, and the lowest level of feed rate should be recommended.

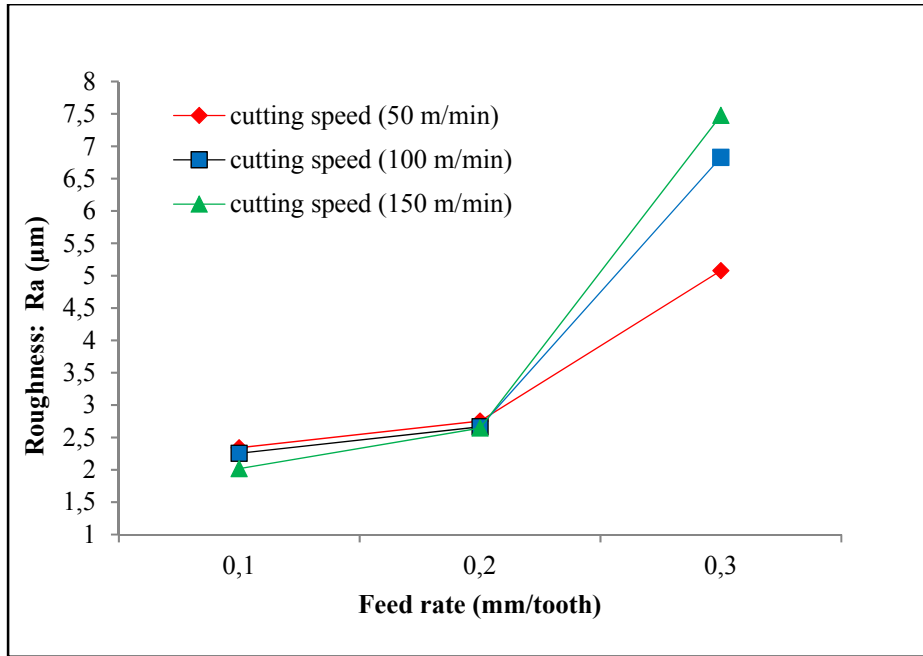


Figure 3.5 Curves showing mean Ra as the function of different speeds and feed of the 410 Martensitic

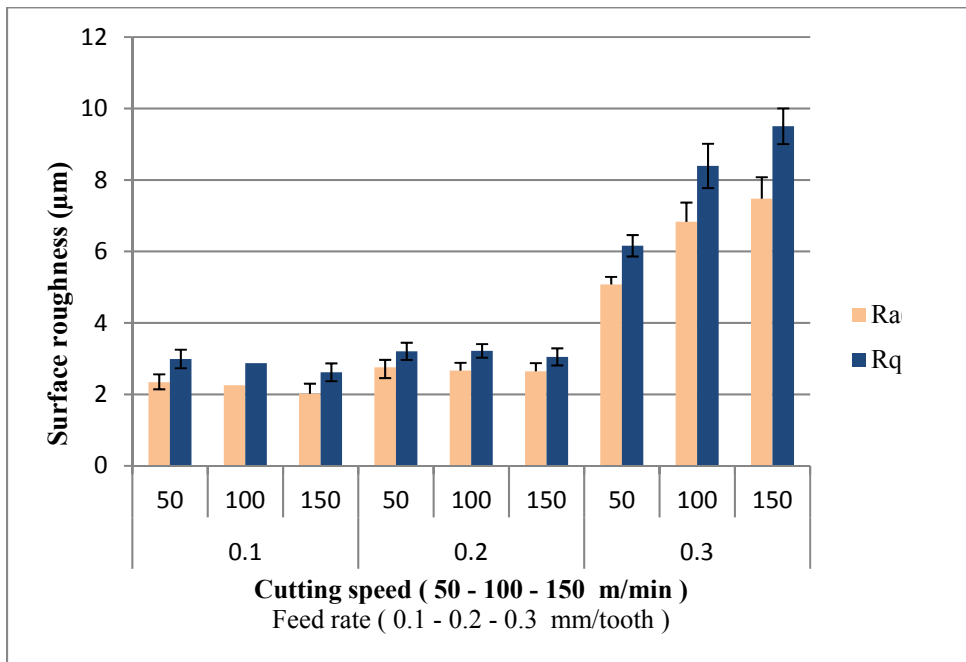


Figure 3.6 Average Ra and Rq of the 410 Martensitic

The effect of feed rate is significant on the surface roughness. In the cutting tests, a new tool was used for each feed rate and the surface measurements were carried out at the beginning

using a feed rate 0.1 mm/tooth) in order to eliminate the possibility of tool wear. Besides, the average surface roughness measurements were also carried out at a feed rate equal to 0.3 mm/tooth. It can be seen from Figure 3.6, that there is an unstable situation for cutting tools. The surface roughness value is equal to 5.077 μm at a feed rate equal to 0.3 mm/tooth and a cutting speed of 50 m/min and increased to 7.477 μm at a feed rate of 0.3 mm/ tooth and a cutting speed of 150 m/min. Also, it can be seen from Figure 3.6 that the surface roughness value is minimum at the feed rate of 0.1 μm for all cutting speeds.

The pictures for experimental 7, 8 and 9 shown in Table 11 may be due to tool wear. The divergence or waviness in surface roughness is due to tool wear and chip effects (Dhar, Kamruzzaman et Ahmed, 2006) .In addition to the results shown in Figure3.5, it can be said that the surface roughness obtained was high due to tool wear. However, in this study, the difference between the effects of cutting speeds is very small. Another factor influencing the surface roughness might be the tool wear formation. As it is known, tool wear has a negative effect on the surface roughness (Bh, Ch et Vinay, 2014; Ucun, Aslantas et Bedir, 2015a).

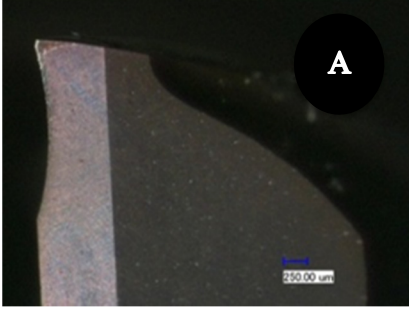
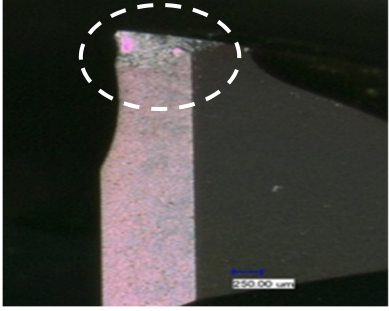
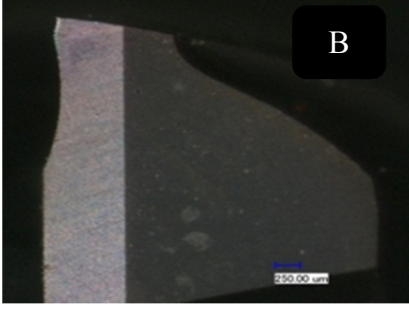
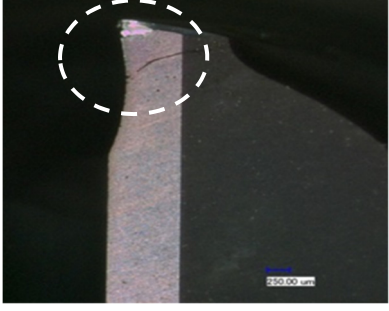
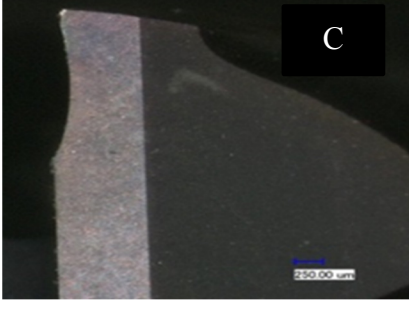
Therefore, it is difficult to make a comparison between the cutting speeds when feed rate is at 0.3 mm/tooth, due to the effect of tool wear. Another interesting result is that the surface roughness values obtained at cutting speed 50 are lower than ones at cutting speed 150. On the one hand, the diameter of cutting tool decreases with increasing cutting speed due to abrasive wear and chipping (Ucun, Aslantas et Bedir, 2015a).On the other hand, severe abrasive wear results in the increase of the tool corner radius, which influences the surface roughness (Ucun, Aslantas et Bedir, 2015a).

Images of the cutting tool end-mill, for experiments 7,8 and 9 showing the minimum tool wear and the maximum tool wear after milling the slots using the cutting conditions that are indicated in images reported in Table 3.4. These micrographs were taken using an Olympus optical microscope. Also, a micrograph of the sharp cutting edge is shown in Table 3.4. Comparing the images of the cutting edges in Images of The minimum tool wear with the image of the sharp edge in Images of the maximum tool wear, it is evident that regardless of the type of experiment, cutting edges develop a larger edge radius due to abrasive tool wear (Jomaa, Songmene et Bocher, 2014; Ucun, Aslantas et Bedir, 2015a). Considering the increase in the edge radius as a measure of the tool wear, one can see that the tool wear is

significantly higher in dry cutting; It is known that fracture wear is usually the reason for the deterioration of the machined part surface roughness. But, the bulk breakage is the most harmful. Edge fracture is often also the end of the line for other wear types. The change of geometry, weakening of the edge and rise of temperatures and forces will eventually lead to some major failure of the edge similar to what was shown for tool.

To present a quantitative comparison of the tool wear progression, tool wear is characterized by the reduction in the surface area of the cutting edge as it is observed under the microscope. All those reasons have affected the surface roughness negatively.

Table 3.4 Shows cutting tool for experiments 7, 8 and 9 for material 410 shows minimum and maximum tool wear for each tool, and the volume of material removed 1800mm³

TEST NO	The minimum tool wear	The maximum tool wear
7		
8		
9		

3.2.2 Analysis of variance (ANOVA)

3.2.2.1 Analysis of variance (ANOVA) for the 409 Ferritic:

The performance results were examined using the analysis of variance (ANOVA) for perfectly recognizing the significant components that impacting the performance measurements. The results of ANOVA for Ra, and Rq are shown in Tables 3.5 and 3.6 respectively. This analysis was taken out to a valuable level of $\alpha = 0.05$ (i.e., confidence level of about 95%). Tables 3.5 and 3.6 show the determined essential levels connected with the F tests for the origin of variation separately. In the given tables, the last columns show the percentage of contribution the significant source to overall variation, showing the level of impact on the results.

Table 3.5 ANOVA result for Ra (μm) with 95% confidence level

Source	Sum of Square	Df	Mean Square	F-Ratio	P-Value	C%
A:Cutting speed	0.398353	1	0.398353	2.81	0.1448	2.39
B:Feed rate	15.4048	1	15.4048	108.62	0.0000	92.49
Total error	0.850934	6	0.141822	-	-	5.1
Total (corr)	16.6541	8	-	-	-	100

R-squared = 94.890%, and R-squared (adjusted for d.f.) = 93.1874

Table 3.6 ANOVA result for Rq (μm) with 95% confidence level

Source	Sum of Square	Df	Mean Square	F-Ratio	P-Value	C%
A:Cutting speed	0.698368	1	0.698368	4.18	0.1448	2.98
B:Feed rate	21.717	1	21.717	130.02	0.0000	92.73
Total error	1.0022	6	0.167033	-	-	4.27
Total(corr)	23.4176	8	-	-	-	100

R-squared = 95.7203%, and R-squared (adjusted for d.f.) = 94.2938%

The F test is standardized as that greater the F amount for a specific parameter, larger the impact directly on the characteristics of computed performance because of the modification

in operation of parameter. In Tables 3.5 and 3.6, the results of ANOVA present that the F amount for the factor feed rate (factor B) is greater comparing to the other parameters, i.e., the main target to the workpiece roughness parameters (R_a , and R_q) is because of the Feed rate. The total difference of the portion examined in the experiment referred to each important element that is considered by the percent contribution given in the tables (last column), the Feed rate (the main factor, that is most important) contributed 92.49% for R_a , and 92.73% in the case of R_q .

3.2.2.2 Main impact plot for R_a and R_q

The main impact plot for the tow various surface roughness parameters R_a and R_q displayed in Figures 3.7 and 3.8.

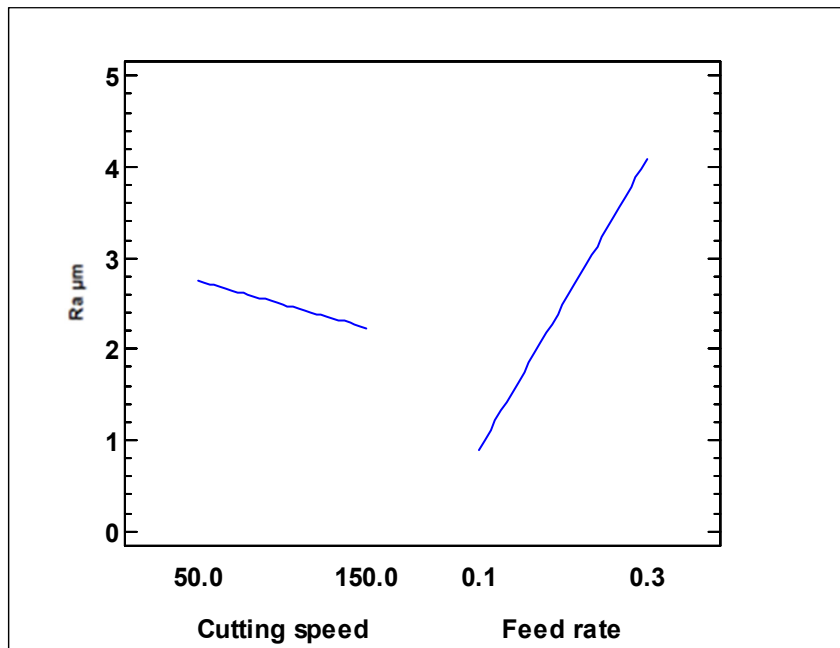


Figure 3.7 Main impact plot for R_a (μm) on 409 Ferritic

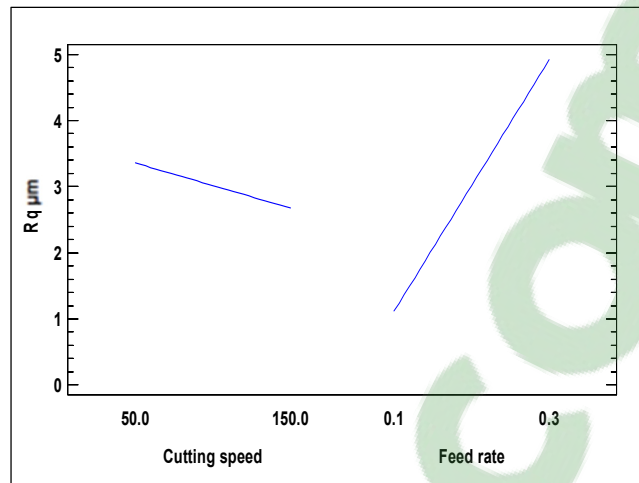


Figure 3.8 Main impact plot for R_q (μm)

Figures 3.7 and 3.8 show the main impact plot. The plots display the difference of individual responsibility with parameters, i.e. cutting speed, feed rate alone. In the plots, the x-axis presents the amount of each parameter at three levels and y-axis the response amount. Horizontal line in the plot presents the mean amount of the responses. Figure 3.7 displays the main impact plot for workpiece roughness R_a for cutting speed, and feed rate. The results display that with the increase in feed rate there is a continuous increase in surface roughness amount. The feed rate at 0.3 mm/tooth produces the coarse surface roughness and 0.1 mm/tooth shows the fine surface roughness one, i.e. the greatest surface roughness. In the Figure 3.8 the nearly flat line difference reference that there is a very small impact, or there is no impact because cutting speed. Figure 3.8 presents the main impact plot for R_q roughness parameter, R_q . Here also, the main impact plot presents the reduction in roughness with increased feed rate. At 0.3 mm/tooth the maximum R_q roughness was observed whereas feed rate of 0.1 mm/tooth displays the minimum roughness. The cutting speed again show very small impact on the R_q roughness, which has displayed by nearly a simple deviation line.

3.2.2.3 Analysis of variance (ANOVA) for the 304L Austenitic:

The performance results were examined using the analysis of variance (ANOVA) for perfectly recognizing the significant components that impacts the performance

measurements. The results of ANOVA for Ra, and Rq are shown in Tables 3.7 and 3.8 respectively. This analysis was taken out to a valuable level of $\alpha = 0.05$ (i.e., confidence level of about 95%).

Table 3.7 ANOVA result for Ra (μm) with 95% confidence level

Source	Sum of Square	Df	Mean Square	F-Ratio	P-Value	C%
A:Cutting speed	0.0193802	1	0.0193802	0.03	0.8621	0.06
B:Feed rate	24.5349	1	24.5349	41.63	0.0007	87.34
Total error	3.53654	6	0.589424	-	-	12.58
Total(corr)	28.0909	8	-	-	-	100

R-squared = 87.4103%, and R-squared (adjusted for d.f.) = 83.2138 %.

The principle of the F test is that the higher the F amount for a particular parameter, the greater the influence on the performance characteristic because the change in that process parameter.

In Tables 3.7 and 3.8, the ANOVA result displays that the F amount for the factor feed rate (factor B) is higher than that of the other parameters, i.e., the main contribution to the workpiece surface roughness parameters (Ra, and Rq) is because the feed rate.

Table 3.8 ANOVA result for Rq (μm) with 95% confidence level

Source	Sum of Square	Df	Mean Square	F-Ratio	P-Value	C%
A:Cutting speed	0.306004	1	0.306004	0.28	0.6137	0.85
B:Feed rate	28.8423	1	28.8423	26.70	0.0021	80.94
Total error	6.48211	6	1.08035	-	-	18.19
Total (corr.)	35.6305	8	-	-	-	100

R-squared = 81.8074%, and R-squared (adjusted for d.f.) = 75.7432%.

The portion of the total difference observed in the test attributed to each important element is directly reflected due to the percent contribution in the last column of the tables. The feed rate (the most important factor) contributed 87.34% for Ra, and 80.94% in Rq.

3.2.2.4 Main impact plot for Ra and Rq:

The main impact plots for the two diverse Ra and Rq is displayed in Figures 3.9 and 3.10.

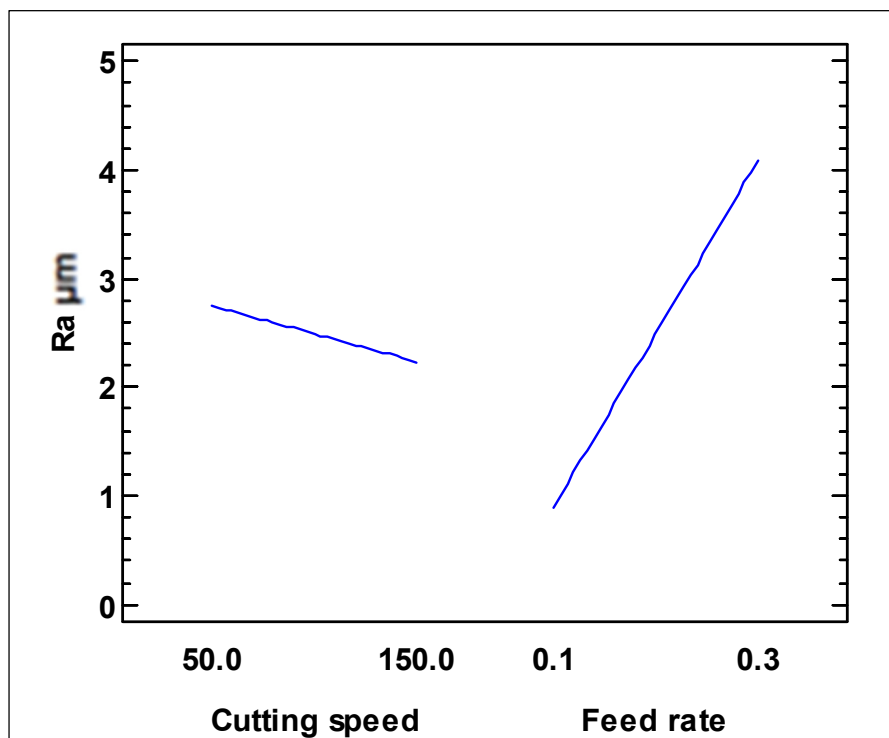


Figure 3.9 Main impact plot for Ra (μm)

Figures 9 and 10 display the main effect plot for the plots display the difference of individual responsibility with parameters, the cutting speed, and feed rate separately.

Figure 9 displays the main impact plot for workpiece surface finish parameter Ra. The results show that the feed rate is more influence on Ra than cutting speed. The feed rate at 0.3 mm/tooth produces the highest roughness and 0.1mm/tooth presents the minimum one, i.e. the greatest surface roughness this was expected as Ra known to be proportional to feed rate.

In the figure the nearly flat line difference indicates that there is a small, or there is no impact because cutting speed.

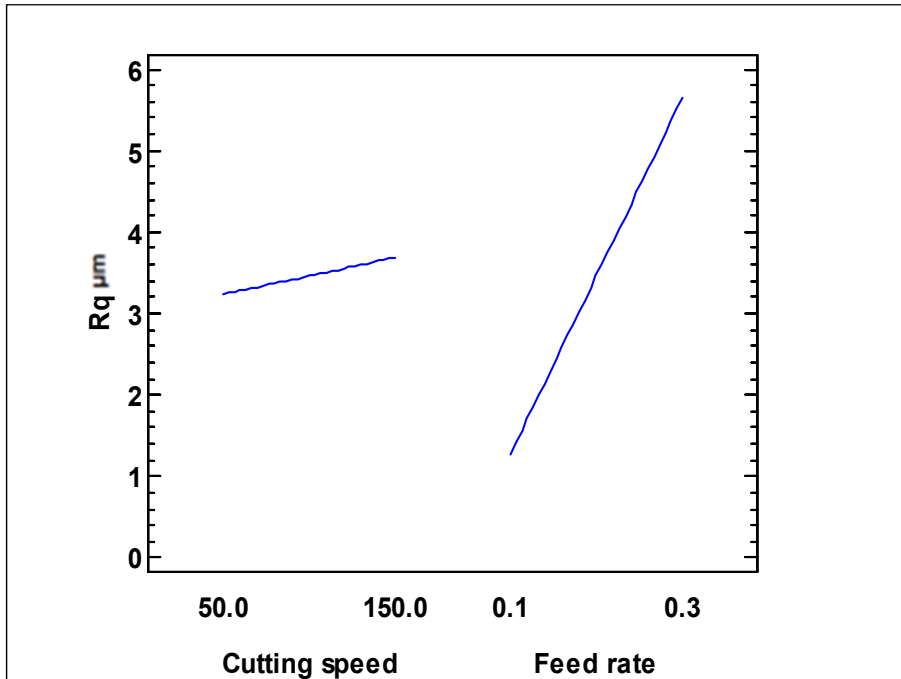


Figure 3.10 Main impact plot for Rq (μm)

Figure 3.10 presents the highest influence plot for Rq roughness parameter, the main impact plot presents the decrease in roughness with increased feed rate. At 0.3 mm/tooth the maximum Rq roughness was observed whereas feed rate of 0.1mm/tooth displays the minimum roughness. The cutting speed show the small impact on the Rq which has displayed by nearly a simple deviation line.

3.2.2.5 Analysis of variance (ANOVA) for the 410 Martensitic:

The performance results were examined using the analysis of variance (ANOVA) for perfectly recognizing the significant components that impacting the performance measurements. The results of ANOVA for Ra, and Rq are shown in Tables 3.9 and 3.10, respectively. This analysis was taken out to a valuable level of $\alpha = 0.05$ (i.e., confidence level of about 95%).

Table 3.9 ANOVA result for R a (μm) with 95% confidence level

Source	Sum of Square	Df	Mean Square	F-Ratio	P-Value	C%
A:Cutting speed	0.0108375	1	0.0108375	0.01	0.9343	0.028
B:Feed rate	29.0444	1	29.0444	19.80	0.0043	76.72
Total error	8.80241	6	1.46707	-	-	23.25
Total(corr)	37.8576	8	-	-	-	100

R-squared = 76.74 %, and R-squared (adjusted for d.f.) = 68.99 % .

Tables 3.9 and 3.10 show the determined essential levels connected with the F-tests for the origin of variation separately. In the given tables, the last columns show the percentage of contribution the significant source to overall variation, showing the level of impact on the results.

The principle of the F-test is that the higher the F-amount for a particular parameter, the bigger the impact on the performance characteristic because the change in that process parameter. In Tables 16 and 17, the ANOVA result displays that the F amount for the factor feed rate (factor B) is higher than that of the other parameters, i.e., the largest contribution to the workpiece surface roughness parameters (R_a , and R_q) is because the Feed rate. The portion of the total difference observed in the experiment attributed to each important factor is reflected by the percent contribution in the last column of the tables the Feed rate (the most important factor) contributed 76.72% for R_a , and 71.43% for R_q . In addition, there is a small effect in cutting speed.

Table 3.10 ANOVA result for R_q (μm) with 95% confidence level

Source	Sum of Square	Df	Mean Square	F-Ratio	P-Value	C%
A:Cutting speed	1.32164	1	1.32164	0.53	0.4924	2.33
B:Feed rate	40.4197	1	40.4197	16.34	0.0068	71.43
Total error	14.8433	6	2.47389	-	-	26.23
Total(corr)	56.5847	8	-	-	-	100

R-squared = 73.7 %, and R-squared (adjusted for d.f.) = 65.02 % .

3.2.2.6 Main impact plot for Ra and Rq:

The main impact plot for the two diverse parameters Ra and Rq have been displayed in Figures 3.11, and 3.12.

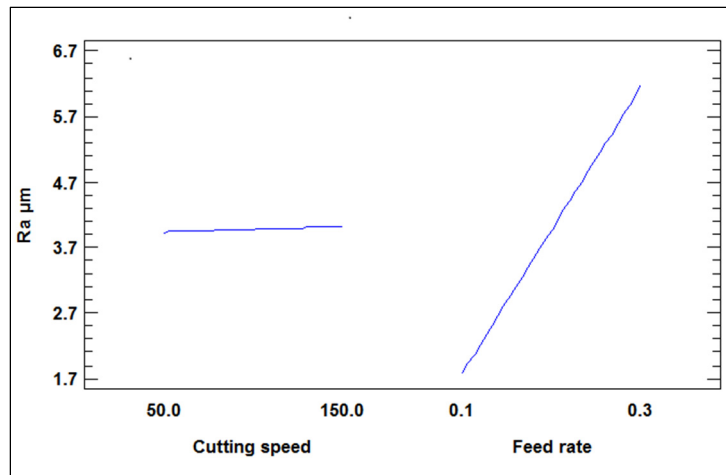


Figure 3.11 Main impact plot for Ra(μm)

Figures 3.11 and 3.12 display the main impact plot for Ra. The plots display the difference of individual responsibility with parameters, the cutting speed, feed rate separately.

Figure 3.11 displays that with the increase in feed rate there is a continuous increase in surface roughness amount. The feed rate at 0.3 mm/tooth produces the highest roughness and 0.1 mm/tooth displays the minimum one, i.e. the greatest surface roughness. In the figure the nearly flat line difference indicates that there is a small or no impact because cutting speed.

Figure 3.12 displays the main impact plot for Rq roughness parameter. The main impact plot displays the decrease in roughness with increased feed rate. At 0.3 mm/tooth the maximum Rq roughness was observed whereas feed rate of 0.1 mm/tooth shows the minimum roughness. The cutting speed and doc again show the very small impact on the Rq which is displayed by nearly a simple deviation line.

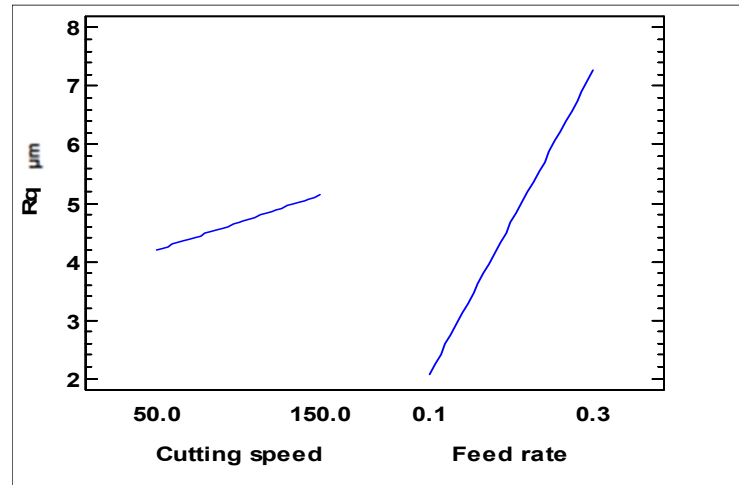


Figure 3.12 Main impact plot for Rq(μm)

3.2.3 Surface quality (μm)

Table 3.11 Data of average (Ra) and (Rq) of different grades of stainless steels tested

Materials	Feed Rate (mm/tooth)	Cutting speed (m/min)	Ra(μm)	Rq(μm)
Ferritic 409	0.1	150	0.893	1.183
Austenitic 304L			1.176	1.463
Martensitic 410			2.018	2.618

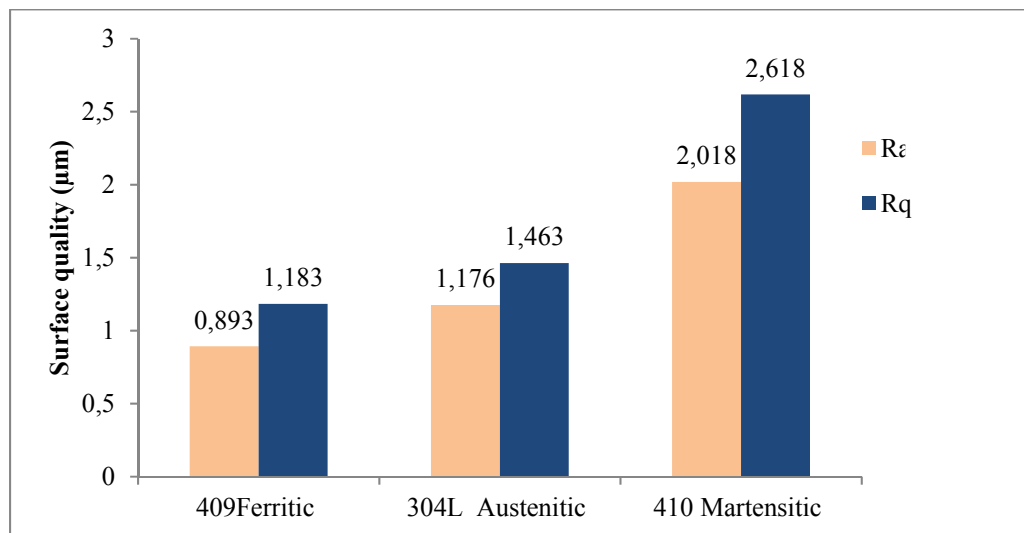


Figure 3.13 Average Ra and Rq of different grades of stainless steels

Figure 3.13 illustrates the mean average Ra and Rq on slot milling for the previously described materials machined under the same parameters; feed rate of 0.1 mm/tooth, cutting speed of 150 m/min, and depth of cut of 1 mm. A statistical analysis confirmed that the roughness of the three tested alloys was different.

The best surface roughness Ra and Rq was obtained for the 409 which also exhibited the lowest hardness while the highest values of these parameters were obtained for the 410 Martensitic.



Figure 3.14 Image of tool wear when cutting 410 (50×) Cutting Speed at 150m/min and feed rate at 0.1 mm/tooth

The performance of the 410 Martensitic could be related to tool wear (Notch wear), (See the Figure 3.14 and 1.23). This result is in agreement with those obtained when machining using standard cutting operations. (Jomaa, Songmene et Bocher, 2014). It is known that Notch wear: it occurs at the trailing edge, typical wear, but to some extent also can be during the oxidation wear mechanism. The cut out will be formed where the cutting edge and part of the material. Excessive notch wear impacts the surface texture when finishing and ultimately weakens the cutting edge, as shown in Figure 1.23 (*Modern metal cutting : a practical handbook*, 1996).

However, the obtained values of surface roughness for all the three materials are within acceptable ranges. For a milling operation, a value between 2.018 μm and 0.893 μm is considered acceptable for general applications. There is a good agreement between these results and other reported results. (Aslantas et al., 2016; Axinte et Dewes, 2002; Bh, Ch et Vinay, 2014; Elgnemi et al., 2017; Ezugwu et Tang, 1995; Mantle et Aspinwall, 2001;

Nalbant, Gökkaya et Sur, 2007; Philip Selvaraj, Chandramohan et Mohanraj, 2014; Selvaraj, Chandramohan et Mohanraj, 2014; Senthil Kumar, Raja Durai et Sornakumar, 2006; Suresh Kumar Reddy et Venkateswara Rao, 2006; Suresh et Basavarajappa, 2014; Ucu, Aslantas et Bedir, 2015b; Wang et Chang, 2004; Xavier et Adithan, 2009; Zhang, Chen et Kirby, 2007).

The more demanding applications require Ra values close to $2.018\mu\text{m}$ and $0.893\mu\text{m}$.

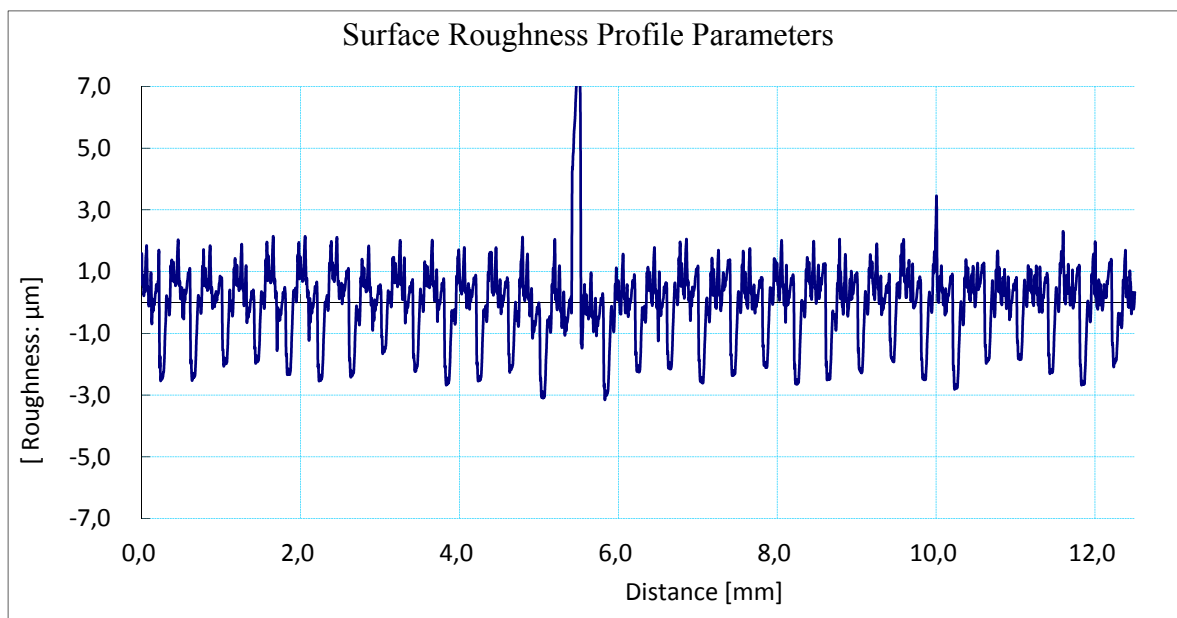


Figure 3.15 Data of profile surface roughness parameters dependence on cutting speed 150m/min and feed rate 0.1mm/tooth, for the 409 Ferritic

The axial roughness profile showed each these roughness parameters describe one or more of the machined surface characteristics. such as the peak-to-valley height (R_t), the mean peak to valley height (R_z), and the Arithmetical mean height (R_a).The surface profile consists of mostly sharp peaks and rounded valleys as shown in Figure 15.The Figure 15 shows the Arithmetical mean height which indicates the average of the absolute value along the sampling length. It is reflected by the two quantities: R_a equal to $0.893\mu\text{m}$ and R_q equal to $1.183\mu\text{m}$. The Maximum profile peak height measured R_p is $3.749\mu\text{m}$.The maximum height of the profile which indicates the absolute vertical distance between the maximum profile peak height and the maximum profile valley depth along the sampling length is R_z

and is equal to $6.506 \mu\text{m}$. It is referred to as the maximum roughness. Finally, the total height of profile R_t is $9.175 \mu\text{m}$ and refers to the vertical distance between the maximum profile peak height and the maximum profile valley depth along the evaluation length.

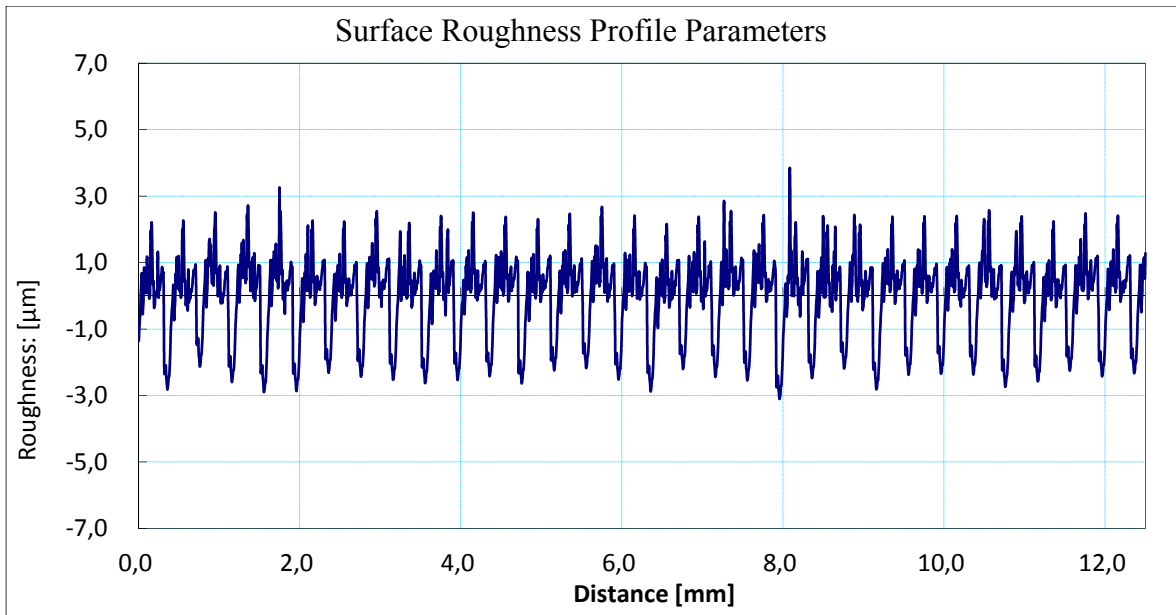


Figure 3.16 Data of profile surface roughness parameters dependence on cutting speed 150m/min and feed rate 0.1mm/tooth, for the 304L Austenitic

The surface profile consists of mostly sharp peaks and rounded valleys as shown in Figure 3.17. The Figure 3.16 shows that the Arithmetical mean height is: R_a equal to 1.176 and R_q equal to $1.463 \mu\text{m}$. The Maximum profile peak height R_p is $3.992 \mu\text{m}$. The maximum height of the profile R_z is $7.061 \mu\text{m}$ and The total height of profile R_t is $8.441 \mu\text{m}$. The differences between the profiles of the two grades, 409 and 304L are not significant, as shown in Figure 3.15 and 3.16 For both grades, the profile consists of mostly sharp peaks, and rounded valleys as However, there are significant differences between 409 and 410.

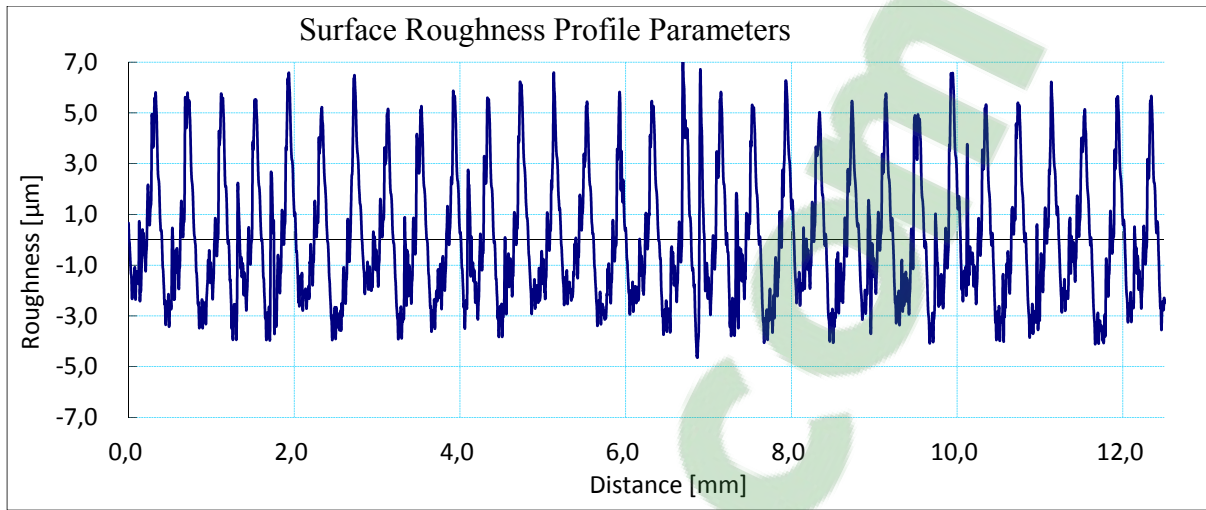


Figure 3.17 Data of profile surface roughness parameters dependence on cutting speed 150m/min and feed rate 0.1mm/tooth, for the 410- Martensitic

In fact, for the latter, the surface profile consists of mostly oscillating but irregular wave as shown in Figure 17. The Arithmetical mean height is R_a equal to $2.018 \mu\text{m}$ and R_q equal to $2.618 \mu\text{m}$. The Maximum profile peak height R_p is $4.860 \mu\text{m}$. The maximum height of the profile R_z is $14.585 \mu\text{m}$, and the total height of profile R_t is $15.146 \mu\text{m}$. Figures. 3.16 and 3.17 show the simulated and the measured roughness profiles generated under Condition I and Condition II, respectively.

3.3 Cutting force analysis

3.3.1 Identification of dynamic cutting force:

The steady state a main part of the cutting forces was considered due to reliability in average force. Typically 15 percent at the beginning and further 15 percent of ending part, the cutting force was totally neglected during the measurements (Figure 3.18). Additionally, the cutting tests were carried out at nearly the same ambient temperature because of the high sensitivity of the dynamometer.

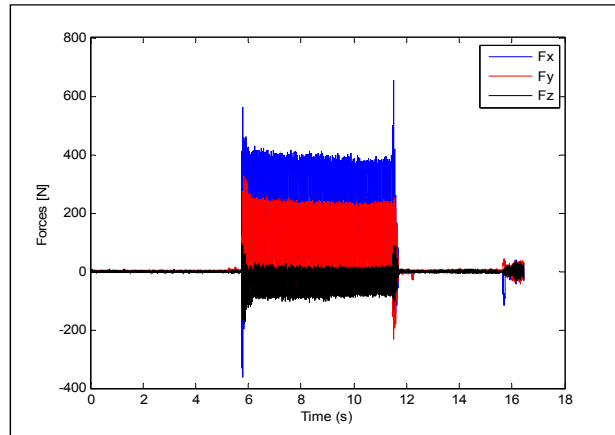


Figure 3.18 Cutting force vs Time
(test 3) 410 Martensitic

3.3.2 The analysis impact of cutting speed and feed rate on cutting force of 409 Ferritic:

The influence of feed rate on the cutting force of 409 Ferritic is shown in Table 3.12 and Figure 3.19. As observed, the cutting force is increased with the increasing of feeding rate at all the cutting speeds. Therefore increasing of the feed, the amount of material used in associating with the tool as increases. This indicates an increased tool-work contact length. Because, the estimated value of cutting force also increases. Moreover to increased the contact length, the force withstand deflection is quite high, which is because of the higher amount of material contacting with the tool. At higher cutting speeds, the temperature generation rate is higher which creates the material soft at the cutting zone, which helps in eliminating the material at lower cutting forces. Alongside, the cutting speed increases, the chip starting thinner and then there is a reduction in cutting forces. The decrease in cutting force is because of the reduction in the contact environment and slightly because of the drop in shear strength in the flow region due to the temperature increases with an increase in cutting speed. It contributes also to an increase in cutting forces. The minimal cutting force is therefore gets by using the incorporation of the lower level feed rate 0.1mm/tooth with higher level cutting speed 150 m/min.

Table 3.12 Cutting force data based on cutting speed and feed rate for 409 Ferritic

Test	Feed rate (mm/tooth)	cutting speed (m/min	Cutting force (N)			
			Fx	Fy	Fz	F= $\sqrt{(fx^2 + fy^2 + fz^2)}$
1	0.1	50	260	147	17	298.67
2		100	232	123	30	262.58
3		150	207	97	42	228.60
4	0.2	50	508.6	205	28	548.36
5		100	377.4	138.8	57	402.11
6		150	304	101.5	66	320.49
7	0.3	50	602	227	32	643.37
8		100	449.5	118.5	76.1	464.85
9		150	423.	91.3	91	432.81

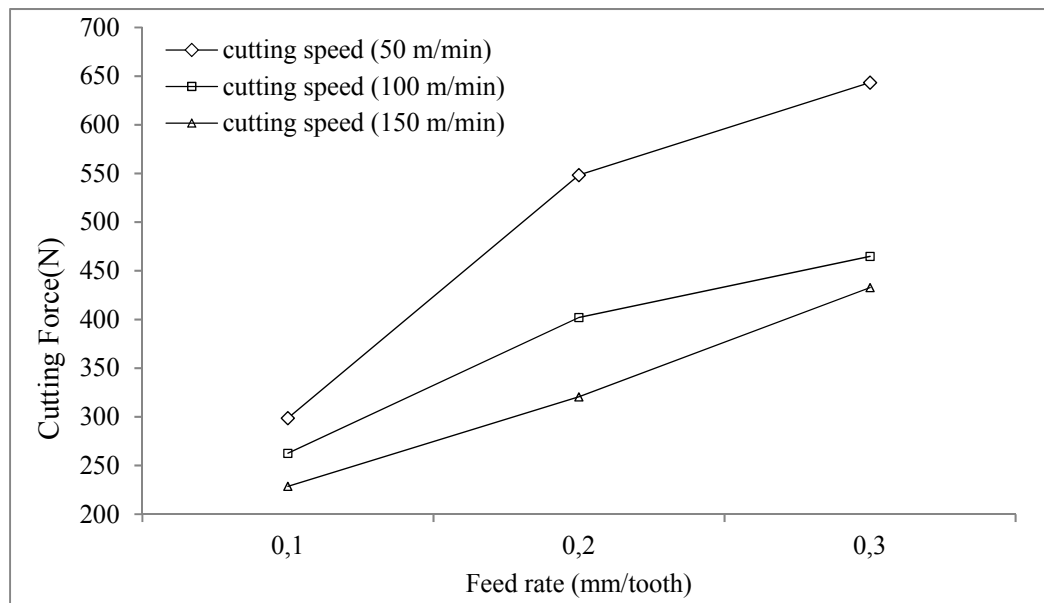


Figure 3.19 Curves showing mean cutting force of different cutting speeds and feed rates of the 409 Austenitic

For all the tested alloys, the cutting force followed a linear trend with feed rate. This observation confirms the work with the experimental data reported by other researchers under similar cutting conditions. For instance, such as, (Qian et Hossan, 2007) (Korkut et Donertas, 2007) (Abrão et al., 2008; Sun, Brandt et Dargusch, 2009).

3.3.3 The analysis impact of cutting speed and feed rate on cutting force of 304L Austenitic:

The influence of feed rate on the cutting force of 304L Austenitic is shown in Table 3.13 and in Figure 3.20, for three different cutting speeds. The cutting force is increased with increasing feed rate at all the selected cutting speeds. As the feed rate is increased, the amount of material in contact with the tool also increases. This implies an increased tool-work contact length. Due to this, the value of cutting force also increases. In addition to increased contact length, the force resisting deflection is high, which is due to the higher amount of material in contact with the tool. This also contributes to an increase in cutting forces.

Table 3.13 Cutting force data based on cutting speed and feed rate for 304L Austenitic

TEST	Feed rate (mm/tooth)	cutting speed (m/min)	Cutting force (N)			
			F _x	F _y	F _z	F= $\sqrt{(fx^2 + fy^2 + fz^2)}$
1	0.1	50	260	147	17	304.84
2		100	232	123	30	254.46
3		150	207	97	42	221.92
4	0.2	50	508.6	205	28	539.05
5		100	377.4	138.8	57	465.36
6		150	304	101.5	66	428.61
7	0.3	50	602	227	32	729.53
8		100	449.5	118.5	76.1	621.69
9		150	423.	91.3	91	571.45

However the increase on cutting speed proportional reverse proportionality with cutting force. At higher cutting speeds, the temperature generation rate is higher which makes the material soft at the cutting zone, which helps in removing the material at lower cutting forces. As the cutting speed increases cutting forces reduced. The minimum cutting force can be obtained by employing the combination of lower level feed rate (0.1mm/tooth) with higher level cutting speed (150 m/min). For all the tested alloys, the cutting force followed a linear trend with feed rate. This observation confirms the work with the experimental data reported by other researchers under similar cutting conditions. For instance, such as, (Qian et Hossan, 2007) (Korkut et Donertas, 2007)(Abrão et al., 2008)(Sun, Brandt et Dargusch, 2009).

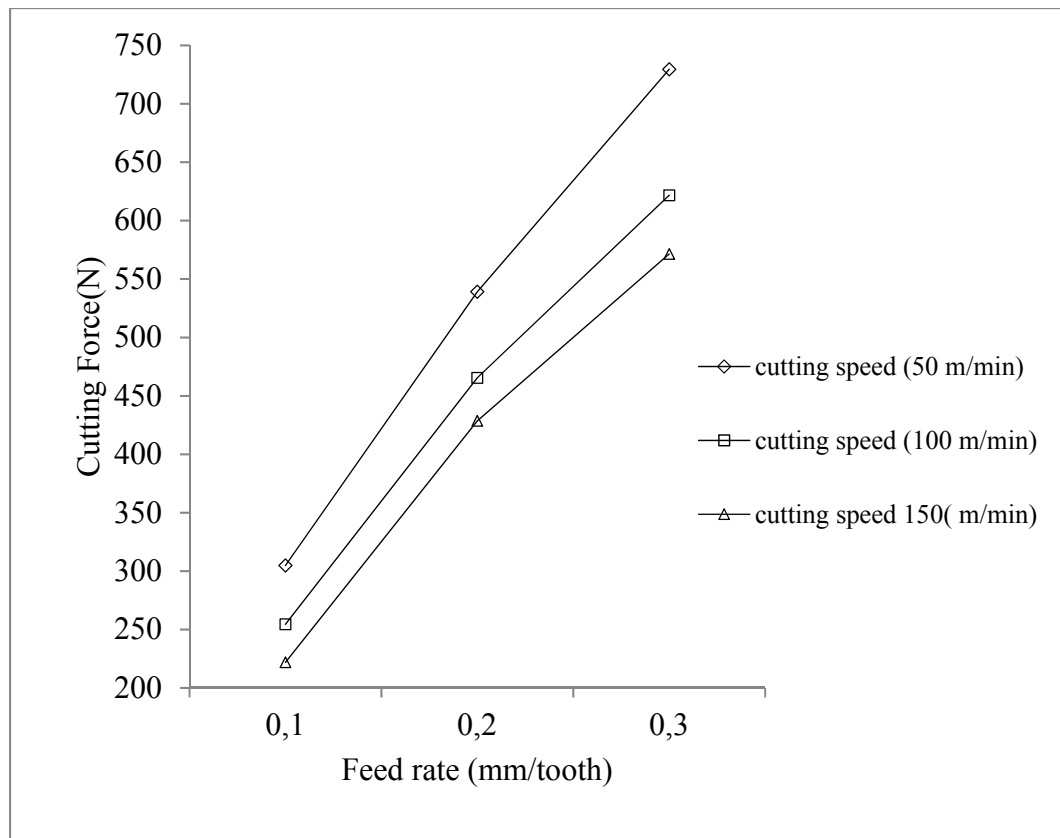


Figure 3.20 Curves showing mean cutting force of different cutting speeds and feed rates of the 304L Austenitic

3.3.4 The analysis impact of cutting speed and feed rate on cutting force of 410

Martensitic:

The peak-to-peak values of the measured cutting forces in the conducted experiments are shown in Figure 3.21. Each diagram in Table 3.14 and Figure 3.21 shows the peak-to-peak magnitudes of the resultant forces during the machining of nine slots using a specific feed rate and cutting speed. Regardless of the depth of cut, two important observations are consistently made in all of the experiments. The first observation is that the cutting forces are the higher value when the feed rate 0.3, and the second observation reduce to the lowest value when the cutting speed 150 is used means that the higher the cutting speed the less the value of force.

Table 3.14 Cutting force data based on cutting speed and feed rate for 410 Martensitic

TEST	Feed rate (mm/tooth)	cutting speed (m/min)	Cutting force (N)			
			F _x	F _y	F _z	F= $\sqrt{(f_x^2 + f_y^2 + f_z^2)}$
1	0.1	50	260	147	17	326.06
2		100	232	123	30	253.12
3		150	207	97	42	212.11
4	0.2	50	508.6	205	28	529.46
5		100	377.4	138.8	57	428.63
6		150	304	101.5	66	366.65
7	0.3	50	602	227	32	732.95
8		100	449.5	118.5	76.1	562.02
9		150	423.3	91.3	91	513.93

This observation may be attributed to the reduction in the friction between the chip and the rake face of the tool. The second observation is that under identical cutting conditions, with the increase feed rate, the cutting forces increase as we move from the 0.1 tooth/mm to the 0.3 tooth/mm. The feed rate at which the forces increase is the fastest in dry cutting. This observation can be explained due to the higher rate of the tool wear in dry cutting.

Our observation of the tool wear progression is described in Section 3 which confirms the correlation between the increase in the tool wear and the cutting forces. For all the results alloys, the cutting force followed a linear trend with feed rate. This observation confirms the work by other authors, such as (Korkut et Donertas, 2007; Wu et al., 2013)

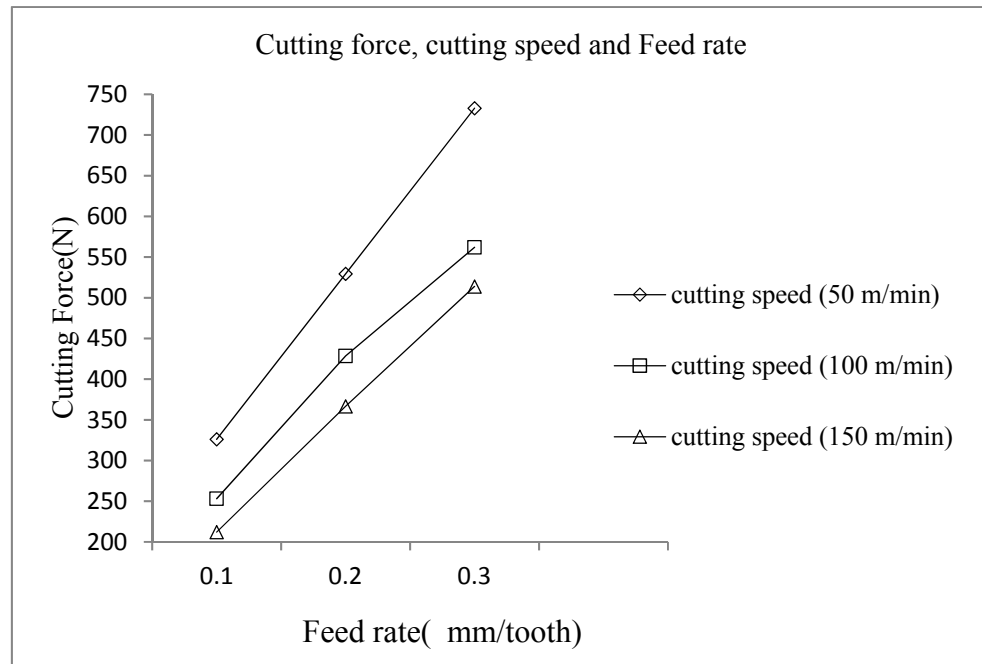


Figure 3.21 Curves showing mean cutting force of different cutting speeds and feed rates the 410 Martensitic

3.3.5 Comparison between three different alloys on dry milling operation

The comparison of cutting force values of dry machined workpiece of 409, 304L and 410 stainless steel are depicted in Figures. 3.19, 3.20, and 2.21 respectively. The result reveals that the cutting force values are reduced by about 2–5% compared to the low hardness materials. The cutting force reduced in the low hardness material and chip friction during milling. Moreover, low friction at the tool-chip interface will reduce the tool-chip contact length which in turn decreases the cutting force.

Table 3.15 and Figure 3.22, illustrate the cutting force on slot milling for the previously described materials machined under the same parameters; feed rate of 0.1 mm/tooth, and with two different cutting speed 50 and 150 m/min respectively.

Table 3.15 Data of arithmetic cutting force of three diverse grades of stainless steel

Materials	Feed rate (mm/tooth)	cutting speed (m/min)	Cutting force (N)
Ferritic409	0.1	50	298.67
		150	228.60
Austenitic304L	0.1	50	304.84
		150	221.92
Martensitic410	0.1	50	326.06
		150	212.11

A statistical analysis confirmed that the cutting force of the three tested alloys was different. 409 Ferritic, which has the lowest hardness, exhibited the highest values of cutting force, but for the . 410 Martensitic shown the lowest values of cutting force.

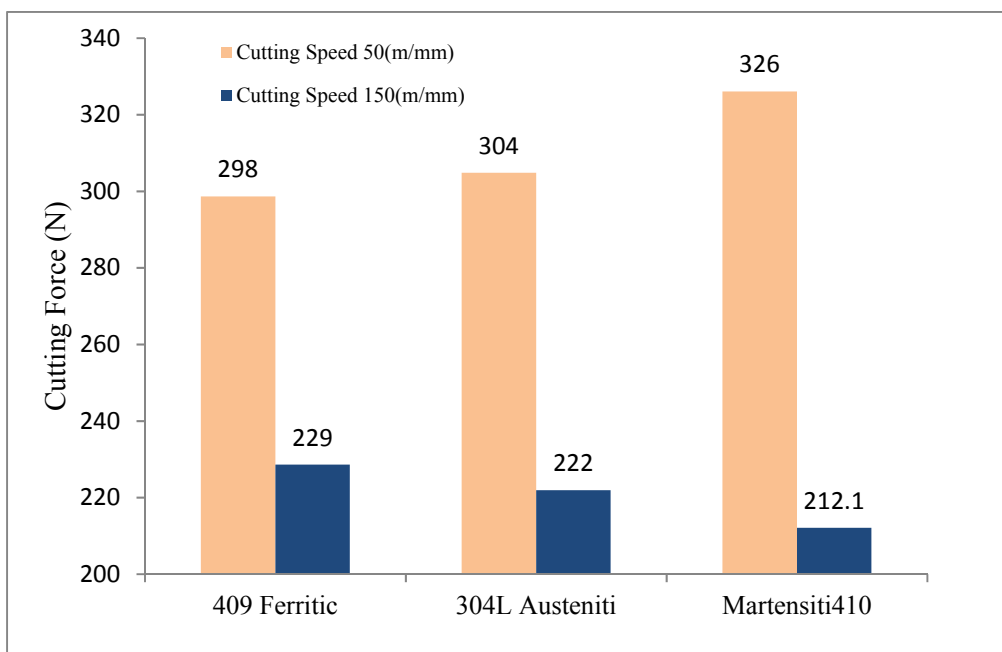


Figure 3.22 Cutting Forces of three different grades of stainless steel as a function of cutting speeds

3.4 Chip forming analysis

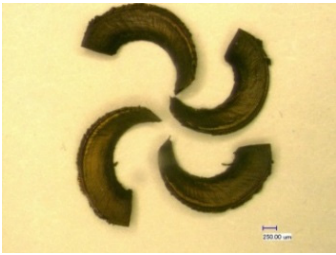
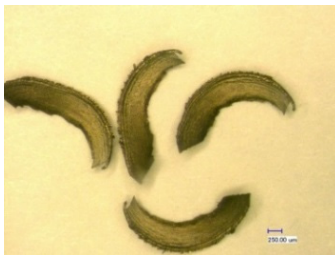
The relationship between the cutting parameters and the chip form is based on many features. The shape of each chip is successfully examined. It is possibly obtained using of distinct ways. A macroscopic study compared the chips with one after another has been done. To make comparison of each chip perfectly, several characteristics have been employed: the analysis of chip volume, thickness, and the chip length. The chip type and size obtained provides some data on the chip development. A study that employed chip length is to explain partially the loss of material during phase of machining. (Oxley, 1989; Wagner et al., 2016).

3.4.1 The chip forming of stainless steel materials 409 Ferritic

Table 3.16 shows the effect of feed rate and cutting speed on the chip Formation, for 9 tests of the 409 Ferritic stainless steel with a depth of cut 1 mm for all different parameters. As shown in Table 3.16, by testing at feed rate of 0.1 mm/tooth, cutting speed of 50 m/min and milling level of 15 mm, and the results found that chip form of 409 Ferritic were most of the arc-shaped chips are shorter than a semicircle and sometimes the fractured chips would be connected with each other. Sometimes, these two types of the chip would be intertwined with the carbide inserts and would probably collide with the machined surface which leads to increase of the workpiece's surface roughness. In the same feed rate 0.1 mm/tooth, with increasing cutting speed to 100 m/min, we found that leads to increasing the length and size of chip formation. However, when increasing the cutting speed to 150 m/min we found that the change in the form of chip formation to form a spiral. Furthermore, increasing cutting speed leads to an increase in the length of chip formation.

On the other hand, the increase in feed rate didn't have the big effect on the form of chip formation as much as cutting speed, when increasing feed rate from 0.1 mm/tooth to 0.2 mm/tooth It has been found the length of chip formation is clearly shorter than the feed rate 0.1 mm/tooth and with feed rate 0.3 mm/tooth the length of chip formation is decreased,

Table 3.16 Comparison of the chip form for the tests of 409 Ferritic

Cutting speed (m/min)	Feed rates (mm/tooth)		
	0.1	0.2	0.3
50			
100			
150			

but it has been found that increasing cutting speed 100 m/min with feed rate 0.2 mm/tooth It has been found the length of chip formation is clearly longer than the feed rate 0.1 in the same cutting speed, also in feed rate 0.3 mm/tooth and the same cutting speed, the chip formation leads to form more a spiral higher low feed rate, in additional increases the cutting speed 150 n/min with the highest feed rate 0.3mm/tooth. It has been found that the chip formation is the longest and more spiral.

3.4.1 The chip forming of stainless steel materials 304L Austenitic

Table 3.17 shows the effect of feed rate and cutting speed on the chip formation, for 9 tests of the 304L Austenitic with a depth of cut 1 mm for all different parameters.

Table 3.17 Comparison of the chip form for the tests of 304L Austenitic

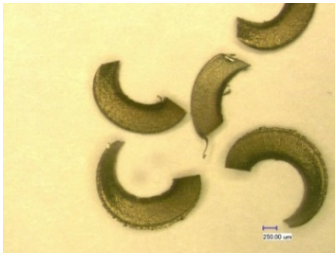
Cutting speed (m/min)	Feed rates (mm/tooth)		
	0.1	0.1	0.1
50			
100			
150			

Table 3.17 shows the evolution of the chips forms according to the cutting conditions for the tool. There is a combined effect of cutting speed and feed rate. When cutting speed is equal to 50m/mm and feed rate to 0.1 mm/ tooth, the chips were the in crescent form. Indeed, the

form evolves from crescent to spiral with increases in length, when the cutting speed 100m/mm and feed rate 0.1 mm/ tooth. When cutting speed is equal to 150 m/mm, the chips are longer with have a higher spiral. Two types of chips are denoted in Table 23 when increased feed rate. The first type is computed for the lowest cutting situations. These formed chips likely are crescent wrapped throughout a vertical axis which corresponds to the spindle axis. Some marks can seem at the chip bottom. These are mainly caused through inserting the radius of corner where the strains are visualizing higher and further, where the thickness of uncut chip is the smallest.

The chips of second type appear for the highest cutting situations and these are very serrated and spindle. The given figures illustrated the primary difference between the chips in term of their size and length. When the highest cutting speeds 150m/mm and feed rate 0.3 mm/ tooth generate some smallest chips

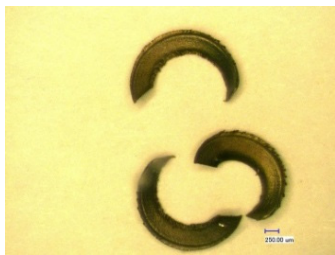
3.4.2 The chip forming of stainless steel materials 410 Martensitic

Table 3.18 shows the effect of feed rate and cutting speed on the chip formation, for 9 tests of the 410 Martensitic with a depth of cut 1 mm for all different parameters.

The Table3.18 shows the evolution of the chips form according to the cutting speed 50m/min, 100 m/min, and 150m/min, and the feed rate from 0.1mm/ tooth, 0.2, mm/tooth, and 0.3mm/ tooth. There is a combined effect of cutting speed and feed rate. When cutting speed 50 m/mm and feed rate 0.1 mm/ tooth, we got all the arc-shaped chips are shorter than a semicircle. With increased in the cutting speed it has been found the chips increased in the long and the size but the same form. In addition, when increasing the cutting speed to 150 m/min we found that the change in the form of chip formation is near to become half circle. Furthermore, increasing cutting speed leads to increase the length of ship formation.

On the other hand, the increase in feed rate to 0.2mm/tooth didn't have the big effect on the form of chip formation. Except with increased cutting speed, it has been found that the length of chip formation is little longer than the feed rate 0.1 mm/tooth and with increased in thickness.

Table 3.18 Comparison of the chip form for the tests of 410 Martensitic

Cutting speed (m/min)	Feed rates (mm/tooth)		
	0.1	0.1	0.1
50			
100			
150			

However, when increased the feed rate to 0.3 mm/tooth observes the length of chip formation is increased, and we found that increasing cutting speed 100 m/ min, also we found the length of chip formation is clearly longer and have changed the chip form, from crescent to spiral. In additional when increasing the cutting speed 150 m/min, it has been found the chip formation is the longest and more spiral, with increased in the thickness of the chip formation.

3.4.3 The Comparison of chip geometry for three different grades of stainless steel

Table 3.19 compares the experimental chip form geometry for the three tests of three materials on slot milling for the previously described materials machined under the same parameters; feed rate of 0.1 mm/tooth, cutting speed of 150 m/min, and depth of cut of 1 mm. Figure (a) shows the 409 Ferritic which also exhibited the lowest hardness while the best values of these parameters were obtained and a serrated chip is found in test no. 3 and the chip-form is observed spiral and the length of chip is the longest.

Table 3.19 Comparison of the from chip geometry for three tests of three materials

Tested materials		
a)409 Ferritic	b) 304L Austenitic	c) 410 Martensitic
		

As shown Figures (a) and (b), under the cutting conditions selected in this work, a slight chip undulation is observed in tests (a) for 409 Ferritic, and (b) for 304L Austenitic, respectively. Figure (c) shows the 410 Martensitic material which also exhibited highest hardness and the chip form is observed half-circle and the length of chip shorter than the chips illustrate in Figures (a) and (b). It is mentioned that the formation of chip mechanism can changes from continuous to serrate corresponding changes of rake angle, thus given two mechanisms direct to distinct thermo-mechanical fills in the cutting zone. In fact, in case of some indubitable cutting situations, the rates of plastic strain therefore high enough to produce required heat in the main shear zone which cannot extensively be dissolute to the remain of work piece material. This measurement in a quasi-adiabatic situation causes the material thermal softening (Xie et al., 1996).

The factors which had the greatest impact on roughness and quality of milling surfaces when milling both plastic stainless steels were cutting speed, feed rate, and milling cut depth of cut. They were the main factors of the experiment and resulted in both good quality milling surfaces and chip. As Table 3.11 shown chip from of 410 Martensitic was the shorter and slight spiral, so it differed from the chip form of 409 Ferritic which had much more chip roll. This demonstrated that lower spindle speeds and higher feed rates result in material shear of the tool cutter being greater, but causing less chip roll due to the speed of shear from feed rate.

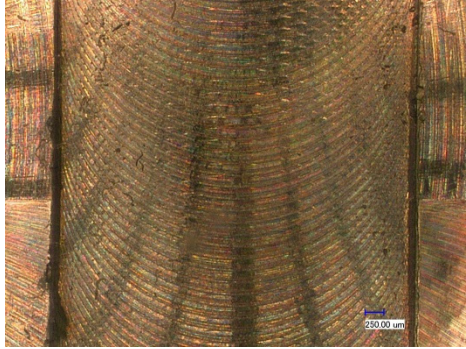
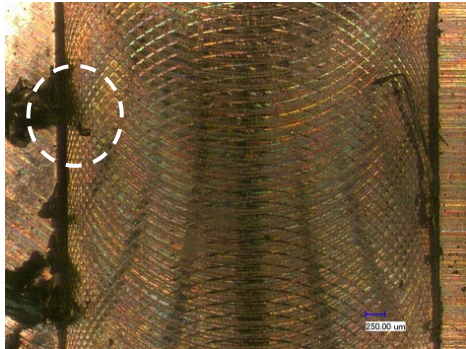
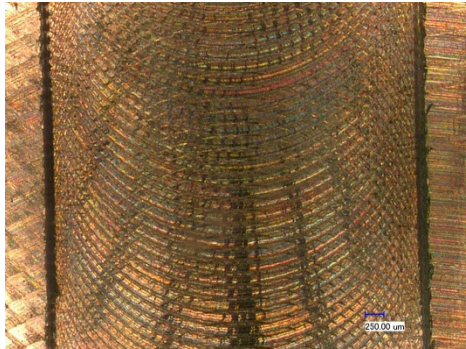
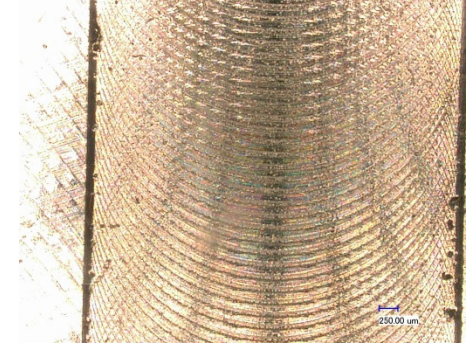
3.4.4 The burr:

Table 3.20 shows that for the three different types of stainless steel materials burr can be produced on the exit edge burn. The tool nose geometry has a significant influence on the formation and characteristics of the formed burr on the exit edge. Under finishing conditions, also the hardness of materials, cutting speed and feed rate affect (Chern, 2006; Lee et Dornfeld, 2005; Lin, 2000) (Lee et Dornfeld, 2005).

While increasing the cutting speed, therefore reduced the contact between the chip and the tool, the burr size will decrease. Meanwhile, the decreasing of the tool face friction, there is an equally increase in the shear angle and at the same time, an accompanying decrease in the chip thickness. The plastic strain linked with chip formation therefore is successfully reduced. This reduction affects the size of the burrs produced. It has been found that a low cutting speed of 50 m/mm leads to increased burr due to a larger chip load as shown in Figures A, B, and C illustrating the different types of burrs.

The burr is made by the push out of the uncut part when the tool chipping has not occurred. The burr is observed when a fracture effecting the separation of the burr that present close to the middle position of the burr. In this case, the burr is because of the stretching that the material considered when the burr is truly formed, which therefore result in the burr length at the top being larger compared to original length of the edge machine, and thus the burr is pushed to keep a wavy shape that able to hold itself.

Table 3. 20 Comparison of burr formation for the three stainless steel materials tested (feed rate 0.1mm/ tooth)

Materials	cutting speed : 50 m/min	cutting speed : 150 m/min
409		
304 L		
410		

However, the burr appeared clearly in low cutting speed meanwhile almost disappear in high cutting speed for all the three materials in milling operation. There is a good agreement between these results and other reported results (Niknam, 2013) (Lin, 2000) under the same parameters, i.e. feed rate of 0.1 mm/tooth, cutting speed of 150 m/min, and depth of cut of 1 mm. Figure (a) test 3 shows the grade 409 which simultaneously exhibited the lowest hardness and the best values of roughness. But, a serrated burr is found, and the length of the

burr is the longest. As shown in figures (a) test 3, and (b), under the cutting conditions selected in this work, a slight burr undulation is observed in tests (a) for 409, and (b) for AISI304L, respectively. Figure (c) shows the AISI 410 grade Martensitic stainless steel material which also exhibited the highest hardness and chip formation. It can be observed that the length of the burr is shorter and minimal compared to figures (a) and (b). This means that the hardness have a great effect on the burr. In fact, an increase of the hardness leads to a decrease of the burr. There is a good agreement between the obtained results and other reported results, (Chern, 2006).

3.5 Machinability Comparaison

The 409 ferritic stainless steel exhibited better machinability, especially at higher cutting speed:

- Better surface finish;
- Less burr;
- Good chip formation;
- Comparable forces
-

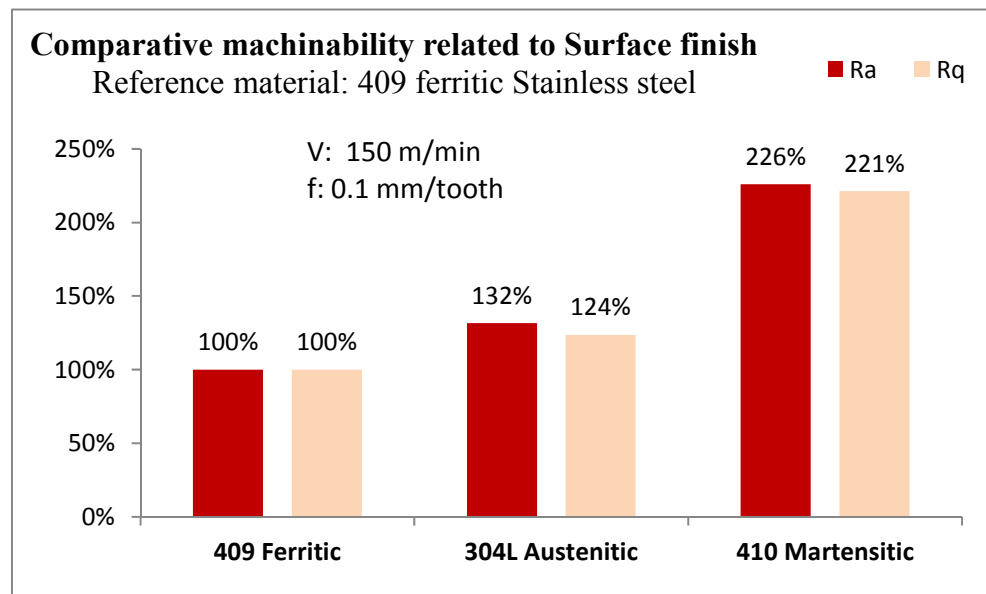


Figure 3.23 comparative machinability related to Surface finish

This performance of 409 ferritic stainless steel can be explained by its low mechanical properties as compared to 304L and 410 SS:

- Lower yield strength;
- Lower mechanical strength;
- Low toughness.

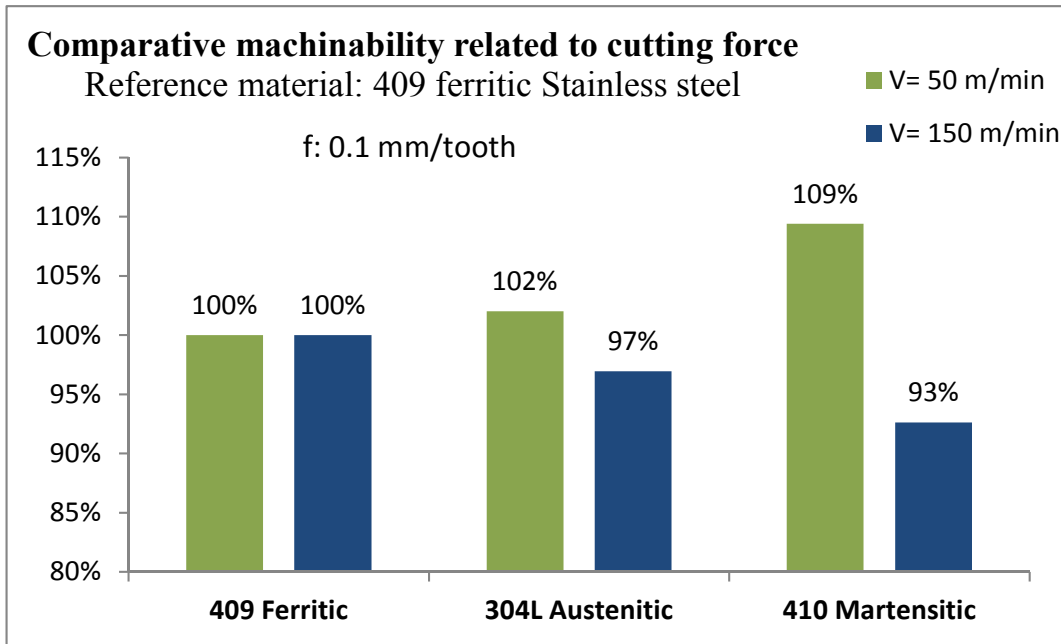


Figure 3.24 comparative machinability related to cutting force

CONCLUSION

The significant findings of this research are summarized as following:

In this machining process, the surface profile was strongly impacted by the feed rate. When examining the surface quality during the machining of stainless steel alloys, most of the previous studies that have taken into account the height parameters, such as the arithmetic mean (Ra and Rq), which may not fully describe the machined surface texture. Although little studies have been performed on the effect of the surface during orthogonal machining, there is not enough study on the effect of the surface finishes induced by the orthogonal dry machining of stainless steel alloys. In fact, restrictions concerning the hardness of the workpiece, have an impact on cutting conditions, which is reflected on surface roughness.

It was found that the feed rate has more effect than the cutting speed on the surface roughness and surface integrity. In particular, all the three materials exhibited significant tool wear when Milling at a feed rate equal to 0.3 mm/tooth. However, for 410 alloy when the feed rate is 0.1 mm/tooth and the speed is 150 mm/min, the tool exhibit noticeable wear, which may be related to the fact that it had the highest strength compared to other materials. This wear could be reduced by selecting appropriate cutting tool materials or coatings. In terms of the surface finishing, 410 performed poorly compared to the other alloys tested (409 and 304L). In this study, two of the machining parameters (namely cutting speed, feed rate) were positively correlated with surface roughness. The study showed that with increasing feed rate, the roughness response value also increased.

The examining of the variance (ANOVA) was employed to satisfy these interpretations. It was concluded that main impacts were important in observing the average roughness that feedback. For the 409 grade, the feed rate was found to be the most important parameter for Ra and Rq with a percent contribution of 92.4% in bringing down the average roughness values and 92.7% in the case of Rq. The contribution of cutting speed was observed to be 6.9% and 11.4% for Ra and Rq, respectively. Secondly, for the 304L grade, the feed rate was found to be the most important parameter affecting Ra and Rq with a percentage contribution

of 87.3% in bringing down the average roughness values to 80.9% in the R_q . The contribution of cutting speed was observed to be 0.06% and 0.85% for R_a and R_q , respectively. For the 410 grade, the feed rate was found to be the important parameter affecting R_a and R_q with a percent contribution of 76.7% in bringing down the average roughness values 71.4% for R_q . The contribution of cutting speed was observed to be 0.02% and 2.3% for R_a and R_q , respectively

The concluded results for surface roughness were examined when the cutting speed was 150 m/min and the feed rate at 0.1 mm/tooth. The cutting speed has low impact on surface roughness and hence can be set at the most convenient/suitable level. This research consequently concluded that an increase of the feed rate leads to the increase of surface roughness.

The most intense influence on forces was observed for the feed rate equal to 0.1 teeth/ mm. In this range, cutting force absolute values are significantly decreased with the growth of the cutting speed. Therefore, during end milling of the workpiece, the reduction of cutting forces can be obtained by the selection of the appropriate parameters in order to maintain the surface finish in the acceptable range. Generally, a high hardness induces an increase of cutting force values, during the low cutting speed .Furthermore, independently of the feed tooth, the high cutting speed leads to a decrease of the cutting force values. Furthermore, it has been found that a high hardness coupled with a high cutting speed induces a decrease of cutting force values more than allow hardness.

In addition, it was found that chip formation depends mainly on the machining of the workpiece and the properties of each stainless steel grade. It can be concluded that:

- 1) By elevating the cutting speed from low to high level, the form of the chip changed from arc and crescent to spindle with an increase in the length.
- 2) The formed chips accumulated when the used cutting speed was the lowest (equal to 50 m/min), leading to some problems of surface roughness. Nevertheless, at high enough cutting speed the formed chips are spread.

- 3) The length of the chip is mainly affected by the cutting speed and the hardness. In particular, the cutting speed increases the length of chip. On the other hand, when the hardness is the highest, the length of chip is the shortest. However, the actual chip length is always smaller than the theoretical chip length value.

As far as the results of the burr analysis are concerned, the following conclusions were reached:

- 1) The hardness of materials strongly influences the geometry of the burrs in end milling.
- 2) The burr is created when the cutting speed is low, approximately equal to 50m/min.
- 3) The machining guideline in end milling is to choose a large in-plane cutting speed about 150 m/min in order to reduce the burr size effectively.

Finally, the machining characteristics and surface integrity (surface finish, cutting force, chip form, and burr size) are concerned. Only the 409 Ferritic outperformed the benchmark 304L. While 410 Martensitic showed low Machinability compared to the 409 Ferritic. All the materials exhibited insignificant tool wear after Milling at 0.3mm/tooth feed rate. In terms of cutting force, the 409 Ferritic and the 304L Austenitic were comparable evenness, but upper from the 410. Whereas the 410 Martensitic generated higher force at low speed compared to others tested steels. This may be due to the microstructural alternations.

RECOMMENDATIONS

Our recommendations for future research and related to what has been addressed in this study are:

1. Investigate more accurately measurements of tool wear due to changes in cutting parameters and lubrication mode, tool geometry (number of teeth, radius of the cutting wedge and radius of the cutting edge).
2. Study the thermal phenomenon (heat generation) in the cutting area and its effect on hardness and surface condition.

BIBLIOGRAPHY

- Aidibe, Ali, Mojtaba Kamali Nejad, Antoine Tahan, Mohammad Jahazi et Sylvain G. Cloutier. 2016. « A Proposition for New Quality 3D Indexes to Measure Surface Roughness ». *Procedia CIRP*, vol. 46, p. 327-330.
- Akin, Ilna V. 2012. « a thesis submitted to the graduate school of natural and applied sciences of middle east technical university ».
- Altintas, Yusuf. 2012. *Manufacturing automation: metal cutting mechanics, machine tool vibrations, and CNC design*. Cambridge university press.
- Aslantas, K, HE Hopa, M Percin, I Ucu et A Çicek. 2016. « Cutting performance of nano-crystalline diamond (NCD) coating in micro-milling of Ti6Al4V alloy ». *Precision Engineering*, vol. 45, p. 55-66.
- Aurich, J. C., D. Dornfeld, P. J. Arrazola, V. Franke, L. Leitz et S. Min. 2009. « Burrs—Analysis, control and removal ». *CIRP Annals*, vol. 58, n° 2, p. 519-542.
- Axinte, D. A., et R. C. Dewes. 2002. « Surface integrity of hot work tool steel after high speed milling-experimental data and empirical models ». *Journal of Materials Processing Technology*, vol. 127, n° 3, p. 325-335.
- Benardos, P. G., et G. C. Vosniakos. 2002. « Prediction of surface roughness in CNC face milling using neural networks and Taguchi's design of experiments ». *Robotics and Computer-Integrated Manufacturing*, vol. 18, n° 5, p. 343-354.
- Bh, Varaprasad, Srinivasa Rao Ch et PV Vinay. 2014. « Effect of machining parameters on tool wear in hard turning of AISI D3 steel ». *Procedia Engineering*, vol. 97, p. 338-345.
- Black, Stewart C., Vic Chiles, A. J. Lissaman et S. J. Martin. 1996. « 8 - Introduction to Cutting ». In *Principles of Engineering Manufacture (Third Edition)*, sous la dir. de Black, Stewart C., Vic Chiles, A. J. Lissaman et S. J. Martin. p. 227-245. Oxford: Butterworth-Heinemann.
- Callister Jr, William D, et David G Rethwisch. 2012. *Fundamentals of materials science and engineering: an integrated approach*. John Wiley & Sons.
- Chern, Gwo-Lianq. 2006. « Experimental observation and analysis of burr formation mechanisms in face milling of aluminum alloys ». *International Journal of Machine Tools and Manufacture*, vol. 46, n° 12, p. 1517-1525.

- Chien, Wen-Tung, et Chung-Yi Chou. 2001. « The predictive model for machinability of 304 stainless steel ». *Journal of Materials Processing Technology*, vol. 118, n° 1, p. 442-447.
- Coelho, R. T., L. R. Silva, A. Braghini et A. A. Bezerra. 2004. « Some effects of cutting edge preparation and geometric modifications when turning INCONEL 718™ at high cutting speeds ». *Journal of Materials Processing Technology*, vol. 148, n° 1, p. 147-153.
- Coromant, Sandvik. 1996. *Modern metal cutting : a practical handbook* (1996). Fair Lawn N. J.: Sandvik Coromant, 1 v.
- Dhar, NR, M Kamruzzaman et Mahiuddin Ahmed. 2006. « Effect of minimum quantity lubrication (MQL) on tool wear and surface roughness in turning AISI-4340 steel ». *Journal of materials processing technology*, vol. 172, n° 2, p. 299-304.
- El-Sonbaty, I., U. A. Khashaba et T. Machaly. 2004. « Factors affecting the machinability of GFR/epoxy composites ». *Composite Structures*, vol. 63, n° 3, p. 329-338.
- Elgnemi, Tarek, Keivan Ahmadi, Victor Songmene, Jungsoo Nam et Martin BG Jun. 2017. « Effects of atomization-based cutting fluid sprays in milling of carbon fiber reinforced polymer composite ». *Journal of Manufacturing Processes*, vol. 30, p. 133-140.
- Ezugwu, E. O., et S. H. Tang. 1995. « Surface abuse when machining cast iron (G-17) and nickel-base superalloy (Inconel 718) with ceramic tools ». *Journal of Materials Processing Technology*, vol. 55, n° 2, p. 63-69.
- Faraz, Ali, Dirk Biermann et Klaus Weinert. 2009. « Cutting edge rounding: An innovative tool wear criterion in drilling CFRP composite laminates ». *International Journal of Machine Tools and Manufacture*, vol. 49, n° 15, p. 1185-1196.
- Gadelmawla, ES, MM Koura, TMA Maksoud, IM Elewa et HH Soliman. 2002. « Roughness parameters ». *Journal of Materials Processing Technology*, vol. 123, n° 1, p. 133-145.
- Gillespie, LaRoux K. 1999. *Deburring and edge finishing handbook*. Society of Manufacturing Engineers.
- Gómez-Parra, A., M. Álvarez-Alcón, J. Salguero, M. Batista et M. Marcos. 2013. « Analysis of the evolution of the Built-Up Edge and Built-Up Layer formation mechanisms in the dry turning of aeronautical aluminium alloys ». *Wear*, vol. 302, n° 1, p. 1209-1218.
- Jackson, Mark J, Grant M Robinson, Michael D Whitfield, Rodney G Handy et Jonathan S Morrell. 2013. « Machining of Uranium and Uranium Alloys with Coated Cutting Tools ». In *Uranium Processing and Properties*. p. 71-93. Springer.

- Jasni, Nur Akmal Hakim. 2013. « Cutting performance of advanced multilayer coated (TiAlN/AlCrN) in machining of aisi d2 hardened steel ». Universiti Tun Hussein Onn Malaysia.
- Jomaa, Walid, Victor Songmene et Philippe Bocher. 2014. « Surface finish and residual stresses induced by orthogonal dry machining of AA7075-T651 ». *Materials*, vol. 7, n° 3, p. 1603-1624.
- Kabakli, Evren. 2009. « Msc Thesis: Optimization Of Process Parameters Of Drilling Using The Taguchi Method ». N° Msc Thesis, P. 102.
- Kaplonek, Wojciech, et Krzysztof Nadolny. 2012. « Advanced 3D laser microscopy for measurements and analysis of vitrified bonded abrasive tools ». *Journal of Engineering Science & Technology*, vol. 7, n° 6, p. 714-732.
- Korkut, I., et M. A. Donertas. 2007. « The influence of feed rate and cutting speed on the cutting forces, surface roughness and tool–chip contact length during face milling ». *Materials & Design*, vol. 28, n° 1, p. 308-312.
- Krolczyk, Grzegorz, Maksymilian Gajek et Stanisław Legutko. 2013. « Predicting the tool life in the dry machining of duplex stainless steel ». *Eksploatacja i Niezawodność*, vol. 15, n° 1, p. 62-65.
- Li, Chuanwei, Zhanwei Liu, Huimin Xie et Dan Wu. 2013. « Novel 3D SEM Moiré method for micro height measurement ». *Optics express*, vol. 21, n° 13, p. 15734-15746.
- Lin, Tsann-Rong. 2000. « Experimental study of burr formation and tool chipping in the face milling of stainless steel ». *Journal of Materials Processing Technology*, vol. 108, n° 1, p. 12-20.
- Lin, WS, BY Lee et CL Wu. 2001. « Modeling the surface roughness and cutting force for turning ». *Journal of Materials Processing Technology*, vol. 108, n° 3, p. 286-293.
- Mantle, A. L., et D. K. Aspinwall. 2001. « Surface integrity of a high speed milled gamma titanium aluminide ». *Journal of Materials Processing Technology*, vol. 118, n° 1, p. 143-150.
- Nalbant, M, H Gökkaya et G Sur. 2007. « Application of Taguchi method in the optimization of cutting parameters for surface roughness in turning ». *Materials & design*, vol. 28, n° 4, p. 1379-1385.
- Oxley, Peter Louis Brennan. 1989. *The Mechanics of Machining: An Analytical Approach to Assessing Machinability*. Ellis Horwood.

- Philip Selvaraj, D., P. Chandramohan et M. Mohanraj. 2014. « Optimization of surface roughness, cutting force and tool wear of nitrogen alloyed duplex stainless steel in a dry turning process using Taguchi method ». *Measurement*, vol. 49, p. 205-215.
- Risbood, K. A., U. S. Dixit et A. D. Sahasrabudhe. 2003. « Prediction of surface roughness and dimensional deviation by measuring cutting forces and vibrations in turning process ». *Journal of Materials Processing Technology*, vol. 132, n° 1, p. 203-214.
- Saglam, Haci, Faruk Unsacar et Suleyman Yaldiz. 2006. « Investigation of the effect of rake angle and approaching angle on main cutting force and tool tip temperature ». *International Journal of Machine Tools and Manufacture*, vol. 46, n° 2, p. 132-141.
- Schäfer, Friedrich, Fritz Breuninger, Harro Sauer, Bernhard Schuh, Wolfgang Seyderhelm, Hans-Jochen Winter, Hans-Jürgen Warnecke et Hans U Brauner. 1975. *Entgraten: Theorie, Verfahren, Anlagen*. Krausskopf.
- Selvaraj, D Philip, P Chandramohan et M Mohanraj. 2014. « Optimization of surface roughness, cutting force and tool wear of nitrogen alloyed duplex stainless steel in a dry turning process using Taguchi method ». *Measurement*, vol. 49, p. 205-215.
- Senthil Kumar, A., A. Raja Durai et T. Sornakumar. 2006. « The effect of tool wear on tool life of alumina-based ceramic cutting tools while machining hardened martensitic stainless steel ». *Journal of Materials Processing Technology*, vol. 173, n° 2, p. 151-156.
- Stephenson, David A, et John S Agapiou. 2005. *Metal cutting theory and practice*, CRC Press, Taylor and Francis, 2 déc. 2005 - 864 pages.
- Stephenson, David A, et John S Agapiou. 2016. *Metal cutting theory and practice*. CRC Press, Taylor and Francis , 6 avr. 2016 - 947 pages.
- Sun, S., M. Brandt et M. S. Dargusch. 2009. « Characteristics of cutting forces and chip formation in machining of titanium alloys ». *International Journal of Machine Tools and Manufacture*, vol. 49, n° 7, p. 561-568.
- Suresh Kumar Reddy, N., et P. Venkateswara Rao. 2006. « Experimental investigation to study the effect of solid lubricants on cutting forces and surface quality in end milling ». *International Journal of Machine Tools and Manufacture*, vol. 46, n° 2, p. 189-198.
- Suresh, R, et S Basavarajappa. 2014. « Effect of process parameters on tool wear and surface roughness during turning of hardened steel with coated ceramic tool ». *Procedia Materials Science*, vol. 5, p. 1450-1459.
- Trent, Edward Moor, et Paul Kenneth Wright. 2000. *Metal cutting*. Butterworth-Heinemann.

- Ucun, İrfan, Kubilay Aslantas et Fevzi Bedir. 2015a. « The performance of DLC-coated and uncoated ultra-fine carbide tools in micromilling of Inconel 718 ». *Precision Engineering*, vol. 41, p. 135-144.
- Ucun, İrfan, Kubilay Aslantas et Fevzi Bedir. 2015b. « The performance Of DLC-coated and uncoated ultra-fine carbide tools in micromilling of Inconel 718 ». *Precision Engineering*, vol. 41, p. 135-144.
- Wagner, Vincent, Arnaud Vissio, Emmanuel Duc et Michele Pijolat. 2016. « Relationship between cutting conditions and chips morphology during milling of aluminium Al-2050 ». *The International Journal of Advanced Manufacturing Technology*, vol. 82, n° 9-12, p. 1881-1897.
- Wang, Ming-Yung, et Hung-Yen Chang. 2004. « Experimental study of surface roughness in slot end milling AL2014-T6 ». *International Journal of Machine Tools and Manufacture*, vol. 44, n° 1, p. 51-57.
- Wojciechowski, Szymon. 2015. « The estimation of cutting forces and specific force coefficients during finishing ball end milling of inclined surfaces ». *International Journal of Machine Tools and Manufacture*, vol. 89, p. 110-123.
- Wu, Baohai, Xue Yan, Ming Luo et Ge Gao. 2013. « Cutting force prediction for circular end milling process ». *Chinese Journal of Aeronautics*, vol. 26, n° 4, p. 1057-1063.
- Xavior, M. Anthony, et M. Adithan. 2009. « Determining the influence of cutting fluids on tool wear and surface roughness during turning of AISI 304 austenitic stainless steel ». *Journal of Materials Processing Technology*, vol. 209, n° 2, p. 900-909.
- Zhang, Julie Z., Joseph C. Chen et E. Daniel Kirby. 2007. « Surface roughness optimization in an end-milling operation using the Taguchi design method ». *Journal of Materials Processing Technology*, vol. 184, n° 1, p. 233-239.
- Zucuni, CP, LF Guilardi, S Fraga, LG May, GKR Pereira et LF Valandro. 2017. « CAD/CAM machining Vs pre-sintering in-lab fabrication techniques of Y-TZP ceramic specimens: Effects on their mechanical fatigue behavior ». *Journal of the mechanical behavior of biomedical materials*, vol. 71, p. 201-208.